DISCOVERY OF UNIQUE ANTIVIRAL PATHWAYS IN A BAT VIRAL RESERVOIR,

THE BLACK FLYING FOX

APPROVED BY SUPERVISORY COMMITTEE

John W. Schoggins, Ph.D.

Neal Alto, Ph.D.

Julie Pfeiifer, Ph.D.

David Russell, Ph.D

DEDICATION

I would like to thank my parents for their support and encouragement throughout my studies.

I would like to thank my significant other for his unrelenting support, enthusiasm, and surprises throughout the years, which were so important for keeping me motivated.

I would like to thank John for his guidance, encouragement, and willingness to allow me some independence during my graduate years.

I would like to thank my friends and lab members for their support, suggestions, and distractions, which kept me sane throughout grad school.

I would like to thank the members of my graduate committee, who followed my progress throughout these projects and provided invaluable feedback and encouragement.

Finally, I would like to thank Nancy Street, who has always been a positive and enthusiastic presence, particularly through difficult moments.

DISCOVERY OF UNIQUE ANTIVIRAL PATHWAYS IN A BAT VIRAL RESERVOIR, THE BLACK FLYING FOX

by

PAMELA CRISTINA DE LA CRUZ RIVERA

DISSERTATION/THESIS

Presented to the Faculty of the Graduate School of Biomedical Sciences

The University of Texas Southwestern Medical Center at Dallas

In Partial Fulfillment of the Requirements

For the Degree of

DOCTOR OF PHILOSOPHY

The University of Texas Southwestern Medical Center at Dallas

Dallas, Texas

Degree Conferral May, 2018

DISCOVERY OF UNIQUE ANTIVIRAL PATHWAYS IN A BAT VIRAL RESERVOIR, THE BLACK FLYING FOX

Publication No. _____

Pamela Cristina De La Cruz Rivera, Ph.D.

The University of Texas Southwestern Medical Center at Dallas, 2018

Supervising Professor: John W. Schoggins, Ph.D.

Bats are asymptomatic reservoirs for a number of viral pathogens. How they manage to host highly pathogenic viruses such a Nipah and Marburg without showing clinical symptoms remains unclear. One of the earliest defenses vertebrates use to control viral infections is the interferon response. Upon viral infection, cells produce interferon which inhibits viral infection through downstream effectors called interferon stimulated genes. I questioned whether bat interferon stimulated genes contained unique properties that would make bats less susceptible to damage from viral infection. To address this, I used genetic tools to identify which interferon

stimulated genes were expressed in cells from the black flying fox (*Pteropus alecto*). I found that RNASEL is uniquely induced in cells from the black flying fox, and that its activation is important for preventing viral infection. To determine if any bat interferon stimulated genes had evolved especially potent antiviral properties, I compared a group of bat and human interferon stimulated genes in a high-throughput format and discovered that bat IRF7 is more antiviral than human IRF7. Further studies demonstrated that bat IRF7 is active even in uninfected cells, and can induce a subset of protective antiviral genes without signaling through interferon. This function was in part due to unique serine residues at the C-terminal regulatory region of the protein that confer constitutive activity to bat IRF7. This work has uncovered two different mechanisms by which antiviral responses between bat and human hosts differ, and provides insight regarding how bats manage to keep numerous viral infections under control.

TABLE OF CONTENTS

PRIOR PUBLICATIONS

De La Cruz-Rivera, P. C., M. Kanchwala, H. Liang, A. Kumar, L. F. Wang, C. Xing and J. W. Schoggins (2017). "The IFN Response in Bats Displays Distinctive IFN-Stimulated Gene Expression Kinetics with Atypical RNASEL Induction." J Immunol.

LIST OF FIGURES

LIST OF TABLES

LIST OF DEFINITIONS

BP – Base pairs

CBP – CREB-binding protein

cGAS – Cyclic GMP-AMP synthase

Co-IP/MS – Co-immunoprecipitation/mass spectroscopy

DBD – DNA-binding domain

dsRNA – Double-stranded RNA

HeV – Hendra virus

Hr – Hour(s)

HSV-1 – Herpes simplex virus 1

IAD – IRF association domain

IAV – Influenza A virus

IFN – Interferon

IKKε – Inhibitor of nuclear factor kappa-B kinase subunit epsilon

IRF – Interferon regulatory factor

ISG – Interferon stimulated gene

ISRE – Interferon sensitive response element

JAK – Janus kinase

KIR – killer cell immunoglobulin-like receptors

KLR – killer cell lectin-like receptor

KSHV – Kaposi's sarcoma-associated herpesvirus

MAVS – mitochondrial antiviral signaling protein

MDA-5 – Melanoma differentiation-associated protein 5

MHC-I – Major histocompatibility complex class I

Min – Minute(s)

MyD88 – Myeloid differentiation primary response 88

NiV – Nipah virus

NK – natural killer

NLR – NOD-like receptor

ONNV – O'nyong'nyong virus

PAMP – Pattern-associated molecular pattern

pDCs – Plasmacytoid dendritic cells

Poly (I:C) – Polyinosinic:polycytidylic acid

PRD – Positive regulatory domain

PRD-LE – PRD-like element

PRR – Pattern recognition receptor

PTP – Protein tyrosine phosphatase

RIG-I – Retinoic acid-inducible gene I

SARS – Severe acute respiratory syndome

SC – Subclusters

Sec – Second(s)

SOCS – Suppressor of cytokine signaling

STAT – Signal transducer and activator of transcription

STING – Stimulator of interferon genes

TBK1 – Tank-binding kinase 1

TIRAP – TIR-associated protein

TLR – Toll-like receptor

TRAM – TRIF-related adaptor molecule

TRIF – TIR-domain-containing adaptor protein-inducing IFN-β

Tyk2 – Tyrosine kinase 2

USP18 – Ubiquitin specific peptidase

VEEV – Venezuelan equine encephalitis virus

vIRF – Viral IRF

VSV – Vesicular stomatitis virus

wHTH – Winged helix-turn-helix

YFV – Yellow fever virus

LIST OF APPENDICES

CHAPTER ONE
Review of the Literature

BATS ARE UNIQUE VIRAL RESERVOIRS

Overview

Bats have been singled out as unique viral hosts due to their ability to harbor pathogenic viruses without succumbing to disease symptoms. It is currently believed that bats are reservoirs for Nipah (Chua, Koh et al. 2002), Hendra (Halpin, Young et al. 2000), SARS-like coronaviruses (Li, Shi et al. 2005), and Ebola (Leroy, Kumulungui et al. 2005). Bats are a widespread host and can be found in all continents with the exception of Antarctica (Hayman 2016). To date, over 60 viruses have been identified in bats from all over the world (Calisher, Childs et al. 2006). Recently, bats were identified as mammals with the most viral diversity per species (Olival, Hosseini et al. 2017), further supporting the idea that viral responses in these animals deserve further study.

General Bat Facts

Bats comprise 20% of all mammalian species, with over 1100 species of bats identified worldwide (Teeling, Springer et al. 2005). Bats belong to the order Chiroptera and can be classified as megabats (Megachiroptera suborder) or microbats (microchiroptera suborder). Megachiroptera only contains a single family, Pteropodidae. Megabats, due to their large size and use of fruit as a main food source, are commonly called fruit bats, Old World fruit bats, or flying foxes. Megabats do not rely on echolocation to feed; their large eyes and keen sense of

smell are sufficient to find food sources (Muller, Goodman et al. 2007). There are over a dozen families belonging to the microchiptera (Calisher, Childs et al. 2006). Microbats, which include vampire bats and horseshoe bats, use mammals or insects as a food source. Both megabats and microbats can harbor zoonoses (Calisher, Childs et al. 2006).

Bats are the only mammals capable of sustained flight and frequently travel long distances to migrate or feed, which may have implications regarding immunity (Zhang, Cowled et al. 2013). Bats provide many benefits to an ecosystem, including seed dispersion, insect control, pollination, and fertilization.

Viruses in Bats

Over 60 viruses have been identified in bats tissues, with many more identified through serological studies (Calisher, Childs et al. 2006). Bats are recognized as important viral reservoirs, and many highly pathogenic viruses including Nipah virus (NiV) (Chua, Koh et al. 2002), Hendra virus (HeV) (Halpin, Young et al. 2000), Marburg virus (Towner, Pourrut et al. 2007), SARS-like coronaviruses (Li, Shi et al. 2005), and Ebolavirus (Leroy, Kumulungui et al. 2005) have been detected in various bat species. A recent study identified bats as hosts for a greater proportion of zoonotic viruses than all other mammalian orders tested, including rodents, with the highest viral richness found in flavi-, bunya- and rhabdoviruses (Olival, Hosseini et al. 2017). In experimental infection studies, certain bats can be productively infected with pathogenic viruses without obvious disease symptoms (Williamson, Hooper et al. 2000, Calisher, Childs et al. 2006, Lau, Li et al. 2010, Brook and Dobson 2015).

The most clinically important zoonotic virus spread by bats is rabies virus, which causes a fatal encephalitis if untreated. Rabies is a negative strand RNA virus that belongs to the *lyssavirus* genus and *Rhabdoviridae* family. It is believed that African bats are the original reservoirs of lyssaviruses and that they have been coevolving since (Nel and Rupprecht 2007). Although bats in the wild may succumb to neurological symptoms if infected, controlled studies have shown that bats are less susceptible to disease from aerosolized rabies virus than mice (Davis, Rudd et al. 2007).

Unique Genomic Features in Bats

Over the past few years, considerable progress has been made regarding bat genetics. To date, partial or complete genomes of three megabats (black flying fox/*Pteropus alecto*, large flying fox/*Pteropus vampyrus*, and straw-coloured fruit bat *Eidolon helvum*) and six microbats (greater horseshoe bat/*Rhinolophus ferrumequinum*, greater false vampire bat *Megaderma lyra*, Brandt's bat/*Myotis brandtii*, Parnell's moustached bat *Pteronotus parnellii*, David's myotis/*myotis davidii*, and little brown bat/ *Myotis lucifugus*) have been published (Parker, Tsagkogeorga et al. 2013, Seim, Fang et al. 2013, Zhang, Cowled et al. 2013). Studies of the recently sequenced black flying fox genome revealed that genes for key components of antiviral immunity are conserved in bats, such as pathogen sensors including toll-like receptors (TLRs) (Cowled, Baker et al. 2011), Retinoic acid Inducible Gene 1 (RIG-I)-like helicases, and NOD-like receptors (NLRs); interferons (IFNs) and their receptors; and interferon stimulated genes (ISGs) (Papenfuss, Baker et al. 2012, Zhang, Cowled et al. 2013). Nevertheless, certain differences between bats and other mammals have been reported.

Analysis of bat ancestor genomes suggest that DNA damage genes are under positive selection (Zhang, Cowled et al. 2013). The authors hypothesize that DNA repair may have been selected for due to increased reactive oxygen species generated as a result of the high metabolic rate required during flight.

Changes in immune genes were also observed. Both black flying fox and David's myotis genomes were missing the PYHIN gene family (Zhang, Cowled et al. 2013). This gene family encodes immune sensors, such as absent in melanoma 2 (*AIM2)* ,that are used to activate inflammasome and IFN pathways (Brunette, Young et al. 2012). Later studies confirmed loss of the PYHIN gene family in 10 different bat species (Ahn, Cui et al. 2016).

Another difference found between bat genomes and those of other mammals was the lack of the two known natural killer cell receptors: killer cell immunoglobulin-like receptors (KIRs) and killer cell lectin-like receptors (KLRs, also known as Ly49 receptors) (Zhang, Cowled et al. 2013). KIR orthologs from other species are also absent. As these receptors are used for natural killer (NK) cell sensing of major histocompatibility complex class I (MHC-I), the implication is that bats may have unusual strategies for differentiating self from non-self. The authors postulate that bats may use a novel receptor class for interactions between NK cells and MCH-I.

These studies suggest bats have unique immune features, although it is unclear if these are an evolutionary consequence of flight, host-pathogen interactions, or an undiscovered cause. Characterization of how these differences contribute to the antiviral and inflammatory response in bats could be of great interest.

Interferon Studies in Bats

There have been relatively few studies done on transcriptional responses to IFN or viral infection using bat cells (Biesold, Ritz et al. 2011, Zhou, Cowled et al. 2013, Glennon, Jabado et al. 2015, Holzer, Krahling et al. 2016, Zhang, Zeng et al. 2017). Although they report a conserved ISG signature, experiments investigating individual effector functions have not been reported. Studies regarding IFN expression have been inconsistent between species. Genomic analysis of the black flying fox genome revealed that IFNs and their receptors were present in the genome, but further analysis uncovered that the IFNα locus is contracted from 13 genes to 10 genes and that IFN may be expressed in uninfected tissues (Zhang, Cowled et al. 2013, Zhou, Tachedjian et al. 2016). In contrast, genes from the little brown bat and the large flying fox seemed to expand to around 60 type I IFN genes (Kepler, Sample et al. 2010). Thus, more data is needed to make general claims regarding the IFN response in bats versus other animals.

THE INTERFERON RESPONSE

Overview

IFNs were the first type of cytokine to be discovered; until then, it was not known that a substance created in one cell could provide antiviral protection to another. Interferon was first reported in 1957, when Isaacs and Lindenmann discovered that chick tissues exposed to heat-inactivated influenza virus secreted a factor that prevented infection in fresh tissues (Isaacs and Lindenmann 1957). They termed the factor "interferon" due to its ability to interfere with viral infection. Since then, the study of IFNs and other cytokines has increased our understanding of innate and adaptive immunity and served to develop treatments against a wide range of microbial infections.

The IFN response is the first line of defense against viral pathogens in vertebrates. When viral or bacterial pathogens are detected, a signaling cascade results in the production and secretion of IFNs. These IFNs travel to neighboring cells, where they serve as a warning against a potential pathogen. This warning signal induces the expression of hundreds of antimicrobial effectors called IFN-stimulated genes (ISGs), which work through several different mechanisms to protect cells against an invading pathogen.

Types of Interferons

Human IFNs

Currently, there are three known IFN families, named type I, type II, and type III IFNs. Within each family, IFNs signal through a common receptor composed of heterodimeric chains.

Type I IFNs were the first discovered and the most well-studied. Their genes are located in human chromosome 9. Type I IFNs include IFNα, of which there are 13 subtypes (IFNA1, IFNA2, IFNA4, IFNA5, IFNA6, IFNA7, IFNA8, IFNA10, IFNA13, IFNA14, IFNA16, IFNA17, IFNA21); IFNβ, with a single subtype (IFNB1); IFNε, encoded by IFNE; IFNκ, encoded by IFNK; and IFNω, which includes a single functional gene (IFNW1), but several pseudogenes (IFNWP2, IFNWP4, IFNWP9, IFNP15, IFNP18, IFNP19) (Pestka, Krause et al. 2004). Type I IFNs signal through the IFNα Receptor (IFNAR), which consists of IFNAR1 and IFNAR2 heterodimers (Aguet, Grobke et al. 1984).

Type II IFNs have only a single member, IFNγ, which is encoded by the IFNG gene on chromosome 12. Type II IFNs signal though the IFNγ receptor (IFNGR) complex, composed of IFNGR1 (also known as CDw119) and IFNGR2 (also known as AF-1) subunits (Bach, Aguet et al. 1997).

Type III IFNs, found on chromosome 19, include IFNλ1 (also known as IL29); IFNγ2 (also known as IL28A); and IFNλ3 (also known as IL28B). Type III IFNs signal through IL10R2 (also called CRF2-4) and IL28RA (also called IFNLR1, CRF2-12) (Kotenko, Gallagher et al. 2003, Sheppard, Kindsvogel et al. 2003, Vilcek 2003).

IFNs found in other vertebrates

Although most vertebrates share a conserved set of IFNs, there are a few that have only been detected in certain species. Mice encode an additional subtype of IFNα (IFNA11), as well as an additional type I IFN termed IFNζ (also known as limitin)(Oritani, Medina et al. 2000). IFNδ was originally discovered in pigs (Lefevre, Guillomot et al. 1998), but since then has also

been found in horse and sheep (Cochet, Vaiman et al. 2009). IFNτ is expressed in ruminants such as cows and sheep (Roberts, Liu et al. 1997).

IFN Signaling Cascade

IFNs are transcriptionally regulated and are secreted in response to viral or bacterial invasion of the host cell. Depending on cell type, different IFNs can be produced in response to specific stimuli. This section will focus on the signaling cascade of type I IFNs (Figure 1).

The canonical Type I IFN signaling cascade begins with the detection of viral or bacterial components known as Pathogen-Associated Molecular Patterns (PAMPS), which usually consist of nucleic acids in the case of viral infection. PAMPS are detected by

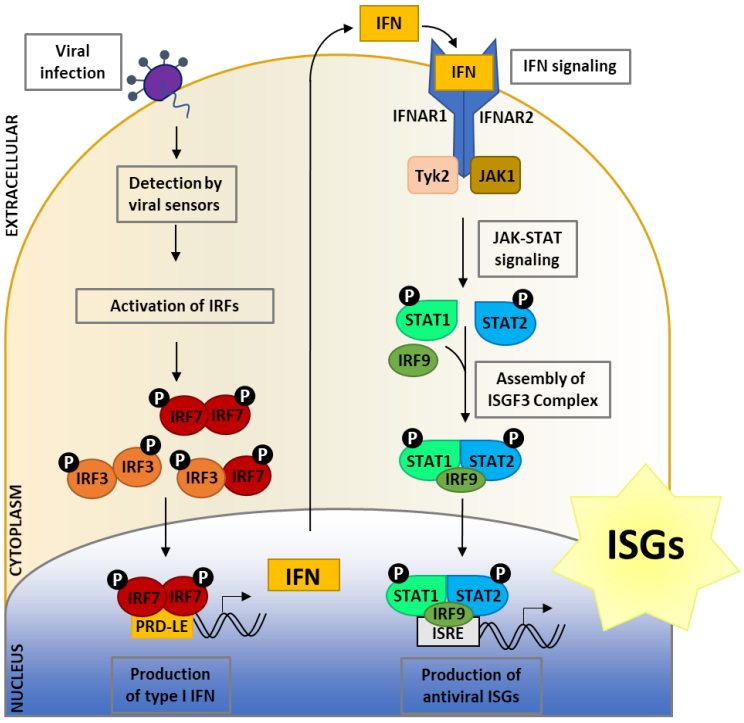

Figure 1: IFN Signaling Cascade
Invading viruses are detected by cytoplasmic and membrane-bound sensors that signal through adaptor proteins. Signaling cascades converge on the phosphorylation and dimerization of the transcription factors IRF3/7. Dimeric IRF7 translocates to the nucleus and binds the PRD-LE region of the IFNα promoter, inducing expression and secretion of IFNα. IFN then signals in a paracrine or autocrine manner through its cognate receptor. Receptor binding activates the kinases JAK1 and Tyk2, which phosphorylate STAT1 and STAT2. The ISGF3 transcription factor complex (STAT1/STAT2/IRF9) translocates to the nucleus and binds ISRE sequences on the promoters of ISGs, inducing transcriptional signature of over 100 protective effectors.

Pattern Recognition Receptors (PRRs), which include cytoplasmic RNA sensors Retinoic Acid-Inducible gene I (RIG-I) and Melanoma Differentiation-Associated Protein 5 (MDA-5), the cytoplasmic DNA sensor Cyclic GMP-AMP synthase (cGAS), and membrane-bound DNA or RNA-sensing Toll-Like Receptors (TLRs) (Saito and Gale 2007, Jensen and Thomsen 2012). PRRs then signal through adaptor proteins to induce the phosphorylation of Interferon Regulatory Factors -3 and/or -7 (IRF3, IRF7). Phosphorylation causes IRF3 and IRF7 to dimerize and translocate to the nucleus, where they induce the expression and secretion of type I IFN.

Secreted type I IFNs bind their cognate receptors on the cell surface in an autocrine or paracrine manner and activate receptor-associated kinases Janus Kinase 1 (JAK1) and Tyrosine Kinase 2 (Tyk2). These kinases phosphorylate Signal Transducers and Activators of Transcription 1 and 2 (STAT1/2) (Darnell, Kerr et al. 1994). Activated STAT1, STAT2, and constitutively-expressed IRF9 form a trimeric transcription factor complex that moves into the nucleus and binds to Interferon Stimulated Response Elements (ISREs) on the promoters of ISGs, leading to expression of hundreds of effector molecules, some of which have been shown to have antiviral activity (Schoggins, Wilson et al. 2011).

Interferon Regulatory Factors

IRFs are a group of DNA-binding proteins that play essential roles during innate immune signaling. There are nine members of the IRF transcription factor family: IRF1, IRF2, IRF3,

IRF4 (also called PIP or ICSAT), IRF5, IRF6, IRF7, IRF8 (also called ICSBP), and IRF9 (also called ISGF3γ) (Honda, Takaoka et al. 2006).

IRFs are modular proteins that share several sequence features. The first is an N-terminal DNA-binding domain (DBD) which contains a conserved tryptophan pentad. This sequence forms a winged helix-turn-helix (wHTH) motif that binds DNA, as revealed by crystal structures of IRF3 and IRF7 (Qin, Liu et al. 2003, De Ioannes, Escalante et al. 2011). The putative binding sequences for IRF3, IRF5, and IRF7 have been solved (Morin, Braganca et al. 2002, Andrilenas, Ramlall et al. 2018). Kaposi's sarcoma-associated herpesvirus (KSHV) encodes viral IRF (vIRF) homologs that lack essential tryptophan residues in the DBD, rendering dominant negative regulators of IFN signaling (Lee, Kim et al. 2009).

The second shared feature between IRFs is an IRF association domain (IAD) which mediates protein-protein interaction between IRFs and other IRFs or their cofactors, such as IRF9 interactions with STAT protein (Taniguchi, Ogasawara et al. 2001). IRF1 and IRF2 appear to lack this domain (Honda, Takaoka et al. 2006). IRF1 has a constitutively active domain and has been shown to induce ISGs independently of IFN signaling (Pine 1992, Rani, Croze et al. 2010).

IRF3, IRF7, IRF5 and IRF9 are all positive regulators of type I IFN transcription (Honda, Takaoka et al. 2006), but only IRF3 and IRF7 are essential. IFNβ transcription is dependent on IRF3, and IFNα transcription requires type IRF7 (Nakaya, Sato et al. 2001). IRF3 and IRF7 are the most closely related in the IRF family and are similarly activated. The autoinhibitory model, proposed for IRF3 upon analysis of the crystal structure, predicts that N- and C-terminal α-

helices flank and shield a β-sandwich IAD (Qin, Liu et al. 2003). The negative charges imposed by phosphorylation of specific serine or threonine residues on the C-terminal regulatory domain force the structure open, relieving steric hindrance and permitting dimerization (Qin, Liu et al. 2003). Studies in IRF7 have shown that dimerization is sufficient for transcription of IFN (Marie, Smith et al. 2000).

IRF3 is expressed constitutively in the cell, allowing a rapid response to pathogenic invasion. When IRF3 is phosphorylated by the kinases Tank Binding Kinase 1 (TBK1) or Inhibitor of nuclear factor Kappa-B Kinase subunit Epsilon (IKKε) downstream of pathogen recognition, it moves into the nucleus and activates transcription of IFNβ by recruiting transcriptional co-activators P300 and CREB-Binding Protein (CBP) and binding to the Positive Regulatory Domains (PRDs) PRD I and PRD III of the IFNβ promoter (Lin, Heylbroeck et al. 1998, Hiscott, Pitha et al. 1999, Suhara, Yoneyama et al. 2002, Honda, Takaoka et al. 2006).

IRF7 is expressed at low to undetectable levels in most cell types, but is highly IFN-inducible (Marie, Durbin et al. 1998, Sato, Suemori et al. 2000). IRF7 is expressed constitutively only in cells specialized for IFN production, such as plasmacytoid dendritic cells (pDCs). IRF7 binds PRD I- and PRD III-like elements (PRD-LE) in the IFNα promoter to induce its expression (Honda, Takaoka et al. 2006). Due to its IFN-inducibility and IFN transcriptional activity, IRF7 is essential for maintaining a positive feedback loop of type I IFN signaling. During early infection, IFN is produced mainly due to the activation of IRF3 downstream of viral sensing. This “first wave” of IFN leads to potent induction of IRF7, which induces the expression of additional IFN (“second wave”) to maintain an effective antiviral response over time (Marie,

Durbin et al. 1998). There is evidence supporting the differential induction of specific IFN subtypes during early and late phases of IFN production, indicating that the IFN response is carefully orchestrated by IRF7 (Marie, Durbin et al. 1998).

Viral Sensing

Detection of RNA viruses by the cytoplasmic RNA sensors RIG-I and Melanoma Differentiation-Associated Protein 5 (MDA-5) leads to downstream signaling though the adaptor protein Mitochondrial Antiviral Signaling Protein (MAVS; also called VISA, IPS-1, and Cardif). Activated MAVS then forms prion-like aggregates that induce activation and dimerization of cytoplasmic IRF3 (Hou, Sun et al. 2011). IRF3 homodimers translocate into the nucleus, where they can induce expression of type I IFNs and some ISGs (Schafer, Lin et al. 1998, Nakaya, Sato et al. 2001).

DNA viruses in the cytoplasm are mainly sensed by the cytosolic DNA sensor cGAS (Tao, Zhou et al. 2016). DNA binds to cGAS, which then produces the dinucleotide 2’3’-cGAMP (Sun, Wu et al. 2013). This molecule binds the adaptor protein Stimulator of Interferon Genes (STING), leading to its activation (Wu, Sun et al. 2013). Activated STING aggregates and translocates from the ER to the Golgi, recruiting TBK1 in the process. TBK1 phosphorylates and activates IRF3, and downstream signaling leads to IFN production.

Viruses can also be sensed by membrane-bound TLRs. There are 10 known TLRs in humans which can detect bacterial, fungal, and viral PAMPs. Viral sensing by TLRs is dependent on cell type, as not all cells express the same TLRs. TLR9 detects viral DNA that contains CpG-DNA motifs, mainly in immune pDCs (Akira, Uematsu et al. 2006). Single

stranded RNA viruses are sensed by endosomal TLR7/8. Double-stranded RNA (dsRNA) and the dsRNA structural analog Polyinosinic:polycytidylic acid (poly(I:C)) are sensed by TLR3. dsRNA can be a product of viral replication of both RNA and DNA viruses. Viral glycoproteins proteins can be sensed by TLR2/4 (Kurt-Jones, Popova et al. 2000, Akira, Uematsu et al. 2006). Upon sensing, TLRs signal through adaptor proteins Myeloid Differentiation primary response 88 (MyD88), TIR-associated protein (TIRAP), TIR-domain-containing adaptor protein-inducing IFN-β (TRIF), and TRIF-related Adaptor Molecule (TRAM) (Oshiumi, Matsumoto et al. 2003, Akira, Uematsu et al. 2006). MyD88 activation leads to the activation of TBK1 and IKKε, which trigger the inflammatory response through IRF3 and/or IRF7 (Deguine and Barton 2014).

Negative Regulators of IFN Signaling

Cell-Intrinsic IFN Inhibition

The protective effects of IFN have a cost. Namely, overactivation of IFN signaling cascades can result in uncontrolled inflammation. The IFN response is carefully regulated by the cell to maintain homeostasis in a variety of ways. Two well-described mechanisms of cell-intrinsic negative IFN regulation involve post-translational inhibition of major players in the IFN pathway by using protein-protein interactions to block steps of the IFN cascade.

The Suppressor of Cytokine Signaling (SOCS) family of proteins contains eight members (SOCS1-7 and CIS). These proteins contain a C-terminal “SOCS box” and an N-terminal SH2 domain. The SH2 domain binds JAK proteins, preventing them from carrying out their kinase function and consequently halting signal transduction (Endo, Masuhara et al. 1997, Starr, Willson et al. 1997). The SOCS box increases proteasomal-mediated degradation of JAK and

other proteins, but this effect is minor compared to the effect on signal transduction (Kamizono, Hanada et al. 2001).

Ubiquitin Specific Peptidase 18 (USP18, also known as ISG43) is a negative regulator of type I IFN signaling with several reported mechanisms of IFN inhibition. Its most well-understood function is cleavage of ubiquitin-like chains attached to proteins by ISG15, a process termed ISGylation. ISGylation protects IRF3 from degradation to maintain transcription of IFN genes during viral infection (Lu, Reinert et al. 2006). Thus, USP18 can serve as a negative regulator of IFN signaling by preventing IFN transcription. Furthermore, USP18 has been reported to use STAT2 to interact with IFNAR2 (Arimoto, Lochte et al. 2017). Binding of USP18 to IFNAR2 is independent of its deconjugating function and serves to prevent IFNAR2-JAK1 interactions, thereby blocking canonical type I IFN signaling (Malakhova, Kim et al. 2006). It also plays a role in maintaining STING protein stability via interactions with USP20, which deconjugates ubiquitin chains from STING during DNA virus infection (Zhang, Zhang et al. 2016). Patients lacking functional USP18 suffer from a type I interferonopathy that leads to a pseudo-TORCH syndrome characterized by microcephaly, enlarged ventricles, calcification of the cerebrum, and sometimes features resembling a congenital infection (Meuwissen, Schot et al. 2016). Interestingly, expression of a deconjugation-deficient USP18 in mice renders the mice more resistant to viral infection without the interferonopathy symptoms reported for *USP18*$^{-/-}$ mice (Ketscher, Hannss et al. 2015).

There is evidence for other negative regulators apart from SOCS and USP18, but they are not as well understood. Protein tyrosine phosphatases (PTPs), which include CD45, contain SH2

domains necessary for their inhibitory function. CD45 and some other PTPs can not only block JAK kinase activity, but reverse its phosphorylation, rendering it inactive(Shuai and Liu 2003). Protein Inhibitors of Activated STAT (PIASs) negatively affect the transcriptional efficiency of STAT proteins, leading to decreased cytokine expression (Seif, Khoshmirsafa et al. 2017).

Carefully orchestrated negative regulation of IFN signaling ensures effective antimicrobial protection while minimizing damage to the host. In fact, pathways that inhibit IFN signaling have been targeted to develop therapeutics against autoimmune diseases. The use of JAK inhibitors for rheumatoid arthritis and other inflammatory diseases is currently being evaluated in clinical trials (Winthrop 2017).

Virally-Mediated IFN Inhibition

Due to IFN being a central component of the antiviral response, viruses have evolved numerous different strategies to overcome or inhibit IFN signaling. Viruses can block the effects of IFNs by downregulating IFNs or their receptors, preventing IFNs from interacting with their receptors, interfering with the JAK-STAT signaling cascade, or causing upregulation or activation of cell intrinsic negative regulators (Fleming 2016).

Flaviviruses are well-known for their ability to block JAK-STAT signaling. Japanese encephalitis virus inhibits phosphorylation of STAT proteins and the Tyk2 kinase (Lin, Liao et al. 2004). The NS5 protein of Langat virus was sufficient to prevent STAT1 phosphorylation (Best, Morris et al. 2005). West Nile virus has also been shown to prevent STAT phosphorylation (Guo, Hayashi et al. 2005).

Blocking IFN-receptor interactions is another strategy employed by viruses. For example, measles virus accessory protein C and V can bind to the IFNAR1 chain of the type I IFN receptor and hinder its mobility to prevent downstream signaling through JAK1 (Yokota, Saito et al. 2003). Influenza NS1 protein prevents IFN signaling using two methods: preventing production of IFNAR1 and inhibiting STAT phosphorylation (Jia, Rahbar et al. 2010).

Some viruses encode soluble IFN inhibitors that interfere with IFN signaling in both infected cells as well as neighboring uninfected cells. For example, expression of ICP27 during Herpes simplex 1 (HSV-1) infection results in secretion of a heat-stable molecule that inhibits STAT1 nuclear accumulation (Johnson, Song et al. 2008). Myxoma virus expresses an IFNγ receptor-like protein called T7 (Upton, Mossman et al. 1992) and vaccinia virus expresses a protein called B18R (sometimes called B19R) that acts as a type I IFN decoy receptor (Colamonici, Domanski et al. 1995). These decoy receptors bind and sequester secreted IFNs, preventing them from signaling through their receptors.

Viruses can also inhibit IFN signaling by taking advantage of cell-intrinsic negative regulators. HSV-1 promotes the upregulation of SOCS1 and SOCS3 in a cell type-dependent manner (Yokota, Yokosawa et al. 2005, Frey, Ahmed et al. 2009). Varicella and influenza A also inhibit IFN signaling by increasing cellular levels of SOCS3 (Pauli, Schmolke et al. 2008, Choi, Lee et al. 2015). Although viral SOCS mimics have not yet been discovered in human viruses, infectious spleen and kidney necrosis virus, which infects fish, encodes a SOCS1 analog which prevents JAK1 phosphorylation (Guo, Yang et al. 2012).

IFNs as Therapeutics

Interferons were the first cytokines to be used in therapy (Pestka, Langer et al. 1987). By the 1980's, despite lack of large sequence databases, IFNs were being purified and characterized (McCandliss, Sloma et al. 1981). In 1986, IFNα was approved by the Food and Drug Administration for treatment against hairy cell leukemia (Pestka 2007). IFN therapy was later approved for use treat to treat several infectious or cancer-related disease, including relapsing-remitting multiple sclerosis, malignant melanoma, herpes simplex, Kaposi's sarcoma, malignant osteoporosis, and chronic forms of hepatitis B and C (Pestka 2007).

Unfortunately, the use of IFN to treat disease results in significant side effects that affect virtually all organ systems and therefore hamper its use as a therapeutic. Common side effects include malaise, nausea, flu-like symptoms, and sensitivity at the injection site (Sleijfer, Bannink et al. 2005). More serious side effects are associated with chronic or high-dose treatment. These include liver damage, leukocytosis (decreased blood counts), autoimmune disease that may cause or exacerbate conditions such as diabetes mellitus and thyroid dysfunction, and neurological symptoms such as cognitive impairment and delirium (Sleijfer, Bannink et al. 2005).

Due to the toxicity profile associated with IFN treatment, new therapies have replaced the use of IFN for certain diseases. Despite unfavorable side effects, IFN has proved to be an efficacious medication and it continues to be used, frequently in combination with other medications, as a therapeutic for multiple sclerosis and some malignancies.

CHAPTER TWO
The Transcriptional Response to Type I Interferon in *P. alecto*-derived Immortalized Kidney Cells

ABSTRACT

Bats host a large number of zoonotic viruses, including several viruses that are highly pathogenic to other mammals. The mechanisms underlying this rich viral diversity are unknown, but they may be linked to unique immunological features that allow bats to act as asymptomatic viral reservoirs. Vertebrates respond to viral infection by inducing interferons (IFNs), which trigger antiviral defenses through interferon-stimulated gene (ISG) expression. While the IFN system of several bats is characterized at the genomic level, less is known about bat IFN-mediated transcriptional responses. Here, I show that IFN signaling in bat cells from the black flying fox (*Pteropus alecto*) consists of both conserved and unique ISG expression profiles. In IFN-stimulated cells, bat ISGs comprise two unique temporal subclusters with similar early induction kinetics but distinct late-phase declines. By contrast, human ISGs lack this decline phase and remained elevated for longer periods. Notably, in unstimulated cells, bat ISGs were expressed more highly than their human counterparts. I also found that the antiviral effector RNASEL, which is not an ISG in humans, is highly IFN-inducible in black flying fox cells and contributes to cell intrinsic control of viral infection. These studies reveal distinctive innate immune features that may underlie a unique virus-host relationship in bats.

INTRODUCTION

Bats are recognized as important viral reservoirs, and many highly pathogenic viruses including Nipah virus (NiV) (Chua, Koh et al. 2002), Hendra virus (HeV) (Halpin, Young et al. 2000), Marburg virus (Towner, Pourrut et al. 2007), SARS-like coronaviruses (Li, Shi et al. 2005), and Ebolavirus (Leroy, Kumulungui et al. 2005) have been detected in various bat species. In experimental infection studies, certain bats can be productively infected with pathogenic viruses without obvious disease symptoms (Williamson, Hooper et al. 2000, Calisher, Childs et al. 2006, Lau, Li et al. 2010, Brook and Dobson 2015). A recent study identified bats as hosts for a greater proportion of zoonotic viruses than all other mammalian orders tested, with the highest viral richness found in flavi-, bunya- and rhabdoviruses (Olival, Hosseini et al. 2017). While the mechanisms underlying disease resistance are not known, it has been speculated that bats possess unique immune features that confer innate antiviral protection (Zhang, Cowled et al. 2013, Brook and Dobson 2015).

In vertebrates, one of the first lines of defense against viral pathogens is the interferon (IFN) response. Upon viral infection, pattern-recognition receptors (PRRs) sense viral components and initiate a signaling cascade that results in the secretion of IFNs. These IFNs bind their cognate receptors to activate the JAK-STAT signaling pathway, leading to the transcriptional induction of hundreds of interferon-stimulated genes (ISGs), many of which have antiviral activity (Schoggins, Wilson et al. 2011).

The black flying fox (*Pteropus alecto*) is an asymptomatic natural reservoir for the highly lethal Hendra virus (Halpin, Young et al. 2000, Field, Young et al. 2001, Wang, Mackenzie et al.

2013). Studies of the recently sequenced black flying fox genome revealed that genes for key components of antiviral immunity are conserved in bats, such as pathogen sensors (including toll-like receptors (Cowled, Baker et al. 2011), RIG-I-like helicases, and NOD-like receptors), IFNs and their receptors, and ISGs (Papenfuss, Baker et al. 2012, Zhang, Cowled et al. 2013). Previous efforts to study bat-virus interactions have mainly focused on the host response to viral infection (Wu, Zhou et al. 2013, Wynne, Shiell et al. 2014, Glennon, Jabado et al. 2015, Holzer, Krahling et al. 2016), but global transcriptional responses to type I IFN remain uncharacterized.

Since the black flying fox harbors pathogenic human viruses and has an annotated genome, I sought to characterize the IFN-induced transcriptional response in this species. Gene expression analyses revealed that bat cells induce a pool of common ISGs. However, they also induced a small number of apparent novel ISGs, including 2-5A-dependent endoribonuclease (RNASEL). Kinetic analyses revealed that bat ISGs can be categorized into distinct groups depending on their temporal gene expression patterns. Additionally, maintenance of ISG expression over time differed between bat and human cells, suggesting distinct mechanisms of gene regulation.

METHODOLOGY

Cell Lines

Black flying fox-derived PaBr (brain), PaLu (lung), and PaKi (kidney) immortalized cell lines (Crameri, Todd et al. 2009) were grown at 37°C and 5% CO_2 and passaged in DMEM/F-12 media (GIBCO #11320033) supplemented with 10% FBS. Human A549 lung adenocarcinoma and HEK293 cells were grown at 37°C and 5% CO_2 and passaged in DMEM media (GIBCO #119995065) supplemented with 10% FBS and 1X non-essential amino acids (NEAA) (GIBCO #11140076).

Viruses

YFV-Venus (derived from YF17D-5C25Venus2AUbi) stocks were generated by electroporation of in vitro-transcribed RNA into *STAT1*$^{-/-}$ fibroblasts as previously described (Schoggins, Wilson et al. 2011). VSV-GFP, Indiana serotype (provided by Jack Rose) was generated by passage in BHK-J cells. For both viruses, virus-containing supernatant was centrifuged to remove cellular debris and stored at -80°C until use.

Viral Infection

Cells were seeded into 24-well plates at a density of $1x10^5$ cells per well. Viral stocks were diluted into DMEM/F-12 media supplemented with 1% FBS to make infection media. Media was aspirated and replaced with 200 µL of infection media. Infections were performed at 37°C for 1h, then 800 µL DMEM/F-12 media supplemented with 10% FBS was added back to

each well. After approximately one viral life cycle (5h for VSV, 25h for YFV), cells were harvested for flow cytometry.

Flow Cytometry

Cells were detached using Accumax, fixed in 1% PFA for 10 min at room temperature, and pelleted by centrifugation at 800 x g. Fixed cell pellets were resuspended in 200 µL FACS buffer (1X PBS supplemented with 3% FBS). Samples were run on a Stratedigm S1000 instrument using CellCapTure software and gated based on GFP fluorescence. Data analysis was done using FlowJo software (v9.7.6).

Interferon Treatment and RNA Isolation

Cells were seeded into 6-well plates at $3x10^5$ cells per well. The following day, cells were treated with 2 mL of DMEM/F-12 media supplemented with 10% FBS and 50 units/mL of Universal Type I IFN Alpha (PBL Assay Science Cat. #11200). The cells were harvested by aspirating the media, washing twice with 2 mL of sterile 1X PBS, then lysing with 350 µL RLT buffer from the RNeasy Mini kit (Qiagen). The cell lysate was stored at -80°C until RNA isolation was completed using the RNeasy kit following the manufacturer's protocol.

RNA-Sequencing

Total RNA samples for each time point were prepared in three independent experiments as described above. The Agilent 2100 Bioanalyzer was used to determine RNA quality; all samples had a RIN Score >9. A Qubit fluorometer was used to determine RNA concentration. Libraries were prepared using the TruSeq Stranded mRNA LT Library Prep Kit (Illumina)

following the manufacturer's instructions, summarized as follows. Four µg of DNAse-treated total RNA was used as input. Poly-A RNA was purified and fragmented before strand specific cDNA synthesis. cDNA was then A-tailed and ligated with indexed adapters. Samples were then PCR amplified using the following parameters: 5 ul of PCR Primer Cocktail was added to 20 ul of adapter ligated library, and then 25 µl of PCR Master Mix was added to each sample. Samples were mixed by pipet, the plate sealed and cycled on the thermal cycler with a 100°C heated lid under the following conditions: initial denaturing at 98°C for 30 sec; 15 cycles of 98°C for 10 sec, 60°C for 30 sec, and 72°C for 30 sec; final extension at 72°C for 5 min, hold at 4°C. Samples were then purified with AmpureXP beads, and re-validated on the Agilent 2100 Bioanalyzer and Qubit. Normalized and pooled samples were run on the Illumina HiSeq 2500 using SBS v3 reagents.

Paired-end 100 bp read length FASTQ files were checked for quality using fastqc (**http://www.bioinformatics.babraham.ac.uk/projects/fastqc**) and fastq_screen (**http://www.bioinformatics.babraham.ac.uk/projects/fastq_screen/**) and were quality trimmed using fastq-mcf (**https://github.com/ExpressionAnalysis/ea-utils/blob/wiki/FastqMcf.md**). Trimmed fastq files were mapped to black flying fox assembly ASM32557v1 (**ftp://ftp.ncbi.nih.gov/genomes/Pteropus_alecto**) using TopHat (Kim, Pertea et al. 2013). Duplicates were marked using picard-tools (**https://broadinstitute.github.io/picard/**). Reference annotation based transcript assembly was done using cufflinks (Roberts, Pimentel et al. 2011), and read counts were generated using featureCounts (Liao, Smyth et al. 2014). Pairwise differential expression analysis was performed using edgeR (Robinson, McCarthy et al. 2010), and longitudinal analysis was performed using time course (Tai 2006) after data

transformation by voom (Law, Chen et al. 2014). Differentially-expressed unannotated genes were manually annotated using a nucleotide BLAST (Altschul, Madden et al. 1997) search for homologous genes.

Data were deposited in the GEO database (https://www.ncbi.nlm.nih.gov/geo/) under accession number GSE102296.

Heatmaps

Heatmaps were constructed using GENE-E and Morpheus, both available at https://software.broadinstitute.org.

Nanostring Analysis

A customized panel targeting both black flying fox and human genes (Schoggins_1_C4066, NanoString Technologies, Seattle, WA, USA) was used to measure the expression of 50 genes per species. Probes were designed to target as many known transcript variants as possible (see dataset S2 for accession numbers of targeted genes). Total RNA was isolated from IFN-treated samples as described above. 100 ng of total RNA in 5 µL was used as input in each reaction for NanoString assay. RNA samples were processed according to the NanoString nCounter XT Codeset Gene Expression Assay manufacturer's protocol. Following hybridization, transcripts were quantitated using the nCounter Digital Analyzer.

Real Time Quantitative PCR

Total RNA was prepared as described above. Reactions were prepared with the QuantiFast SYBR Green RT-PCR kit (Qiagen #204154) as recommended by the manufacturer,

using 50 ng total RNA per reaction. Samples were run on the Applied Biosystems 7500 Fast Real-Time PCR System using 7500 Software v2.0.6. The program consisted of a reverse transcription step at 50°C for 10 min, a polymerase activation step at 95°C for 5 min, and cycling steps alternating between 95°C for 10 sec and 60°C for 30 sec (40 cycles). Melt curves were generated for all experiments by ramping up the temperature 1°C/minute from 60°C to 95°C. Only a single melt curve peak was observed for all primer sets. Primers used to amplify *RNASEL* (XM_006907762.2) are 5'-CCACCCTGGGGAAAATGTGA-3' and 5'-GGAGGATCCTGCTTGCTTGT-3'. Primers used to amplify reference gene *RPS11* (XM_006905029) are 5'-ATCCGCCGAGACTATCTCCA-3' and 5'-GGACATCTCTGAAGCAGGGT-3'. Relative expression in IFN-treated samples versus untreated samples was calculated using the comparative C_T method using *RPS11* as the reference gene.

DNA Constructs and Plasmid Propagation

lentiCRISPR v2 was a gift from Feng Zhang (Addgene plasmid # 52961). *RNASEL* targeting guides were generated by cloning annealed, complementary 20-bp oligos with *Esp3I*-compatible overhangs (5'-caccgAGACCCACACCCTCCAGCAG-3' and 5'-aaacCTGCTGGAGGGTGTGGGTCTc-3') targeting the black flying fox *RNASEL* gene into the lentiCRISPRv2 backbone as described in (Sanjana, Shalem et al. 2014). CRISPR guide oligos were designed using CRISPRdirect (Naito, Hino et al. 2015). Proper assembly was confirmed using Sanger sequencing.

Lentiviral Pseudoparticles

Lentiviral pseudoparticles were made as described in (Shalem, Sanjana et al. 2014), with some modifications. Briefly, $2x10^6$ HEK293T cells were seeded on a poly-lysine coated 10 cm plate. The following day, media was changed to 7.5 mL DMEM with 3% FBS and 1x NEAA. Cells were co-transfected with 5 µg lentiCRIPSRv2, 2.5 µg pCMV-VSVg and 3.5 µg pGag-pol. 4h post-transfection, media was changed to 7.5 mL fresh DMEM with 3% FBS and 1X NEAA. Supernatant was collected 48h post-transfection, filtered through 0.45 µm to remove debris, and stored at -80°C until use.

***RNASEL* KO bulk PaKi cell lines**

$3x10^5$ PaKi cells were seeded on 6-well plates. The following day, media was changed to DMEM/F-12 supplemented with 3% FBS, 4 µg/mL polybrene and 20 mM HEPES. LentiCRISPRv2 lentiviral pseudoparticles were added and cells were spinoculated at 800 x g for 45 min at 37°C. Media was changed to DMEM/F-12 with 10% FBS immediately following spinoculation. 48h after transduction, cells were pooled into a 10-cm dish and selected in DMEM/F-12 with 10% FBS and 5 µg/mL puromycin.

Genomic Characterization of PaKi *RNASEL* KO Bulk Cell Lines

Genomic DNA was isolated from wild-type or RNASEL KO bulk populations using the DNeasy Blood and Tissue Kit (Qiagen). The region flanking the CRISPR-targeted sequence was amplified via PCR using primers (5'-ATGGAGACCAAGAGCCACAACA-3') and (5’-CGTCCTCGTCCTGGAAATTGA-3’). PCR products were gel-purified using the QIAquick Gel Extraction Kit (Qiagen) and subsequently used in TOPO cloning reactions using the TOPO TA

Cloning Kit (Thermo Fisher). Several colonies were selected for each cell background and colony PCR was used to amplify the CRISPR-targeted region. Samples were then analyzed using Sanger sequencing.

Ribosomal RNA Degradation Assay

$3x10^5$ PaKi cells were seeded on 6-well plates. The following day, universal IFN (100 U/mL) was added to the media. After 24h, cells were transfected with 100 ng/mL poly(I:C) in Optimem using Lipofectamine 3000. After 4h, RNA was harvested using the RNeasy Mini Kit (Qiagen) and RNA integrity was measured on a Total RNA Nano chip using an Agilent 2100 Bioanalyzer.

RESULTS

Black Flying Fox-Derived Cell Lines Respond to Exogenous Type I Interferon

Previous studies have shown that exogenous IFNα and IFNγ treatment of cells from the black flying fox can suppress *Pteropine orthoreovirus* Pulau virus (Zhou, Tachedjian et al. 2016) and Hendra virus (Janardhana, Tachedjian et al. 2012), respectively. I treated immortalized black flying fox kidney-derived (PaKi) cells for 24h with universal IFNα, which is designed for activity across multiple species. I then infected the cells with two model GFP-expressing reporter viruses: a negative-sense RNA rhabdovirus, vesicular stomatitis virus (VSV), and a positive-sense RNA flavivirus, yellow fever virus (YFV). I observed a dose-dependent inhibition of both viruses with IFN treatment (Figure 2, B). VSV infection was maximally inhibited by only 50%, whereas YFV infection was suppressed completely at the highest IFN dose. In addition, I confirmed IFN-mediated dose-dependent and time-dependent induction of the canonical ISG MX1 (Figure 2, D) (Zhou, Cowled et al. 2013). These data confirm that PaKi cells are capable of mounting an antiviral response and highlight virus-specific sensitivities to IFN in this cellular background.

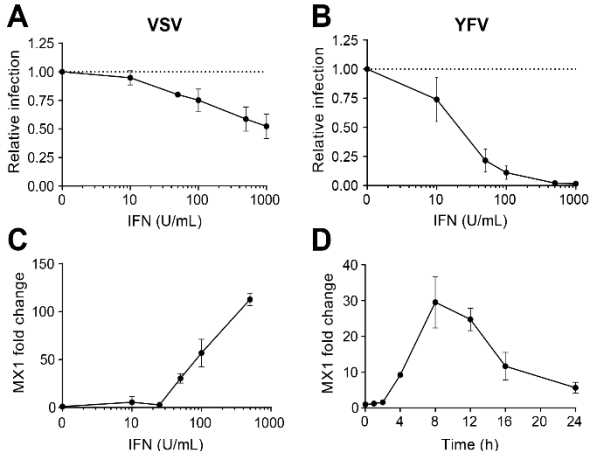

Figure 2: Bat-Derived Cells Respond to Type I IFN. ***(A)*** *PaKi cells were treated with increasing doses of IFNα for 24h and then infected with VSV-GFP at an MOI of 1. The percentage of infected cells was quantified using flow cytometry and normalized to a mock-treated control. Data are represented as mean ± SD for three independent experiments.* ***(B)*** *Same as (A), using YFV-17D Venus.* ***(C)*** *PaKi cells were treated with increasing doses of IFNα and RNA was harvested at 8h. MX1 mRNA levels were quantified using qRT-PCR and normalized to RPS11. Data are represented as mean ± SD for three independent experiments.* ***(D)*** *PaKi cells were treated with IFNα (50U/mL) and RNA was harvested at several time points. MX1 mRNA levels were measured using qRT-PCR and normalized to RPS11. Data are represented as mean ± SD for three independent experiments.*

IFN Induces a Classical ISG Signature in PaKi cells

I next used total RNA sequencing (RNA-Seq) to profile the global transcriptional response of PaKi cells treated with IFNα over time (Figure 3A). Transcriptome assembly analysis across all experimental conditions returned approximately 30,000 genes, of which 11,559 met a minimal read count threshold (mean $log_2CPM \geq 0$). Differential gene expression analysis revealed that IFN induced 93 genes at 4h, 104 at 8h, 103 at 12h, and 103 at 24h (fold change (FC)≥1.5, FDR≤0.05) (Figure 3B). There were no downregulated genes at 4h, 2 at 8h,

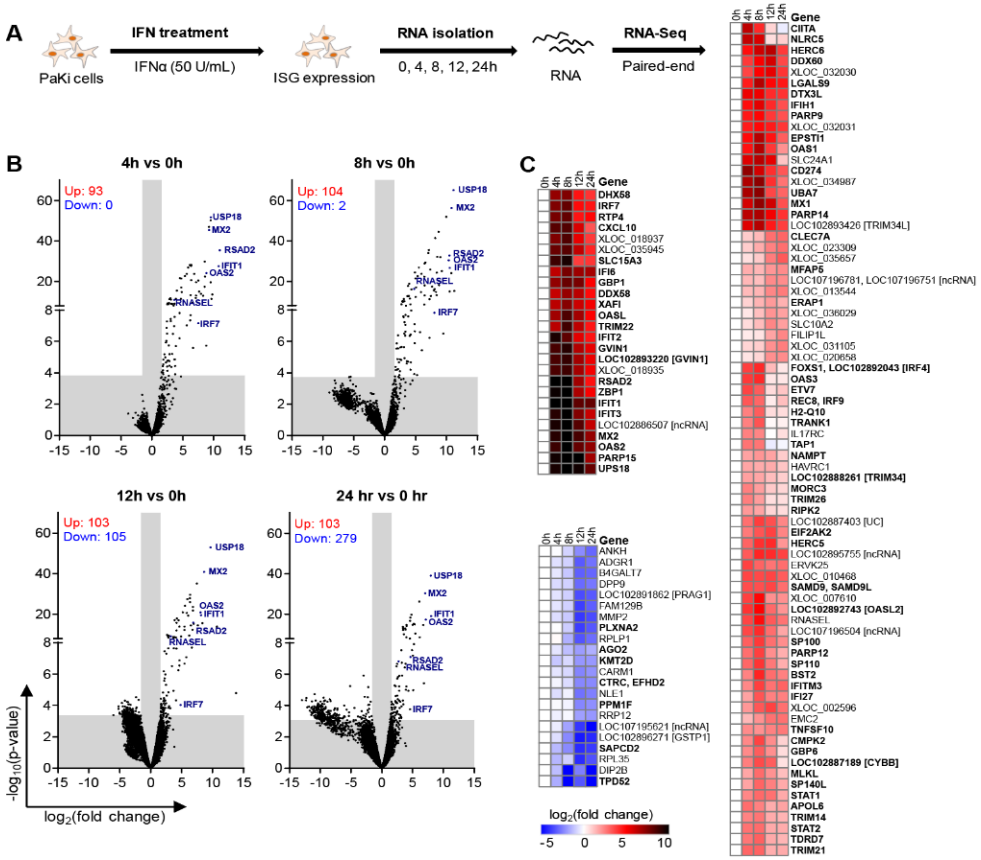

Figure 3: PaKi Transcriptome Response to IFN.
(A) *Experimental schematic.* ***(B)*** *Volcano plots for all time points. Differentially-expressed genes are quantified on the top left. Grey bars indicate $log_2FC \geq 1.5$ (vertical) or FDR≤0.05 (horizontal). Data is a result of three independent experiments* ***(C)*** *Heatmap including genes that meet the cutoffs mean $log_2CPM \geq 0$, $log_2FC \geq 2$, FDR≤0.05 for at least two time points. XLOC genes represent unannotated genes.*

105 at 12h, and 279 at 24h. However, statistical significance of upregulated genes was more robust than the statistical significance of the downregulated genes. Overall, IFN treatment of PaKi cells produced a positive gene induction signature.

Next, heat maps were generated to assess individual gene induction, using a cutoff of FDR≤0.05 and FC≥4 for at least two time points (Figure 3C). Many genes in this list have known roles in innate immunity, including well-known ISGs (*IFIT1*, *MX1*, *OAS2*, *RSAD2*/viperin, *USP18*), members of the JAK-STAT signaling cascade (*STAT1*, *STAT2*, *IRF9*), pattern recognition receptors (*DDX58*/RIG-I, *IFIH1*/MDA5, *ZBP1*) and transcription factors (*ETV7*, *IRF7*, *SP110*) (Mi, Poudel et al. 2016). Notably, I detected induction of *GVIN1* (interferon-induced very large GTPase), which is predicted to encode a protein in bats but is annotated as a pseudogene in humans. This list also included transcripts predicted to encode an endogenous retrovirus (*ERVK25*) and several transcripts predicted to be long non-coding RNAs.

Differentially-expressed genes were cross-referenced to the INTERFEROME v2.0 database (Rusinova, Forster et al. 2013) to determine if they had previously been reported as IFN-induced genes. At the 4h and 8h time points, more than 80% of the genes in our data set overlapped with INTERFEROME v2.0. Since the INTEFEROME database consists predominantly of human and mouse data sets, this result suggests that antiviral responses in bat cells include a conserved repertoire of IFN-inducible genes commonly found in other mammalian species.

Differential Temporal Regulation of Black Flying Fox ISGs

I, together with help from the McDermott Sequencing Core team, which included Mohammed Kanchwala, Hanquan Liang, and Ashwani Kumar and was led by Chao Xing, used a clustering algorithm to group genes in the RNA-Seq data set based on induction kinetics, without imposing fold change or FDR cutoffs (Tai 2006). This analysis revealed that genes were organized into eight subclusters (SC) based on changes in expression levels throughout the IFN time course (Figure 4A, Supplemental Table 1). Genes in SC1 and SC2 increased in expression after 8h. Genes in SC3 and SC4 were induced by 4h and peaked at 4-8h, with genes in SC3 returning close to baseline by 12h and SC4 genes remaining elevated for at least 24h. These two SCs were highly-enriched for genes found in the INTERFEROME v2.0 database. Genes in SC5 increased slightly and peaked at 8h, returning to baseline levels by 12h. Levels of SC6 genes either increased or decreased by 4h, followed by decreased levels at 12-24h. SC7 gene expression levels decreased sharply by 8h, followed

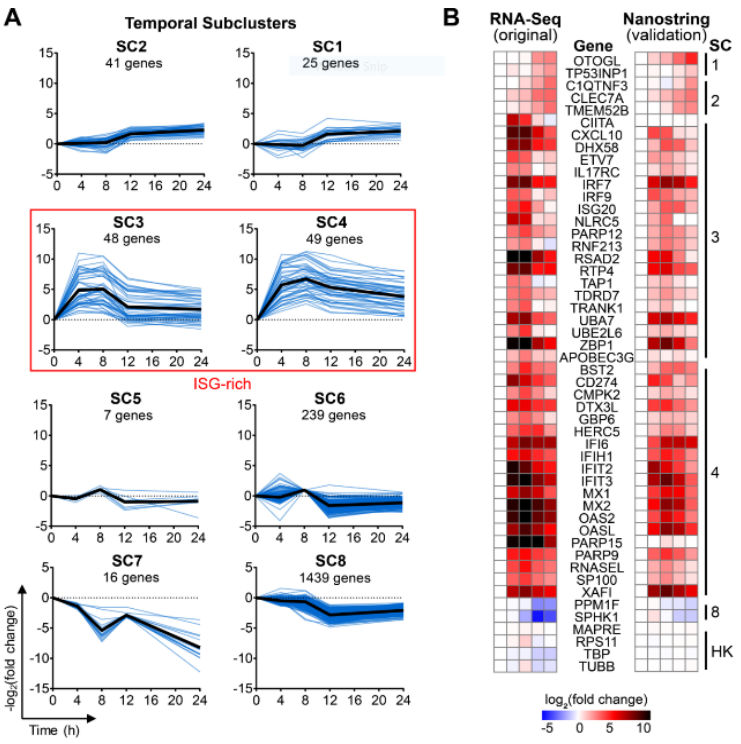

Figure 4: Temporal Clustering Analysis.
(A) *Temporal subclusters. The number of genes in each subcluster is indicated below the title. Blue lines represent mean log_2(fold change) over time for a single gene. Black lines represent median of all genes in the subcluster.* ***(B)*** *RNA-seq validation using Nanostring. RNA was isolated from PaKi cells and gene expression over time was compared between RNA-seq data (left) and Nanostring data (right). Data presented is the mean of three independent experiments. HK = housekeeping genes.*

by a partial recovery by 12h and further decrease in expression by 24h. Finally, genes in SC8 exhibited a sustained decrease in expression levels starting at 8-12h. These data demonstrate that interferon induces distinct subsets of genes which are characterized by differing temporal expression patterns.

Orthogonal Validation of RNA-Seq Data

To validate our RNA-seq results, I used Nanostring nCounter technology, which uses colorimetrically-barcoded DNA probes for direct detection of mRNA without the use of nucleic acid amplification. A customized nCounter codeset was designed containing 50 genes from several temporal SCs, with a focus on the ISG-rich SC3 and SC4 (Appendix A). Temporal expression profiles using Nanostring were generally similar to the RNA-Seq data (Figure 4B). SC1 and SC2 contained genes with increased expression levels at the later time points. SC3 and SC4 had genes with peak expression levels at 8h, with genes in SC4 exhibiting expression levels that remained elevated at 24h. Genes in SC8 decreased in expression over time, with the lowest expression levels observed at 24h.

Human vs. Bat Temporal ISG Regulation

I next used Nanostring to compare temporal regulation of ISGs between bat and human cell lines. I first compared gene expression between PaKi and HEK293 as both cell lines are kidney-derived, but HEK293 cells responded poorly to type I IFN (Appendix A). After screening for robust IFN responses in other human cell lines, I chose human A549 cells for comparative studies (Figure 5A). A striking difference was observed between expression profiles of SC1 and SC2 when comparing PaKi and A549 cells. Of the 5 selected genes in SC1 and SC2, none were

significantly upregulated in IFN-treated A549 cells. Similarly, the decreased expression levels observed for bat genes in SC8 were not observed in A549 cells.

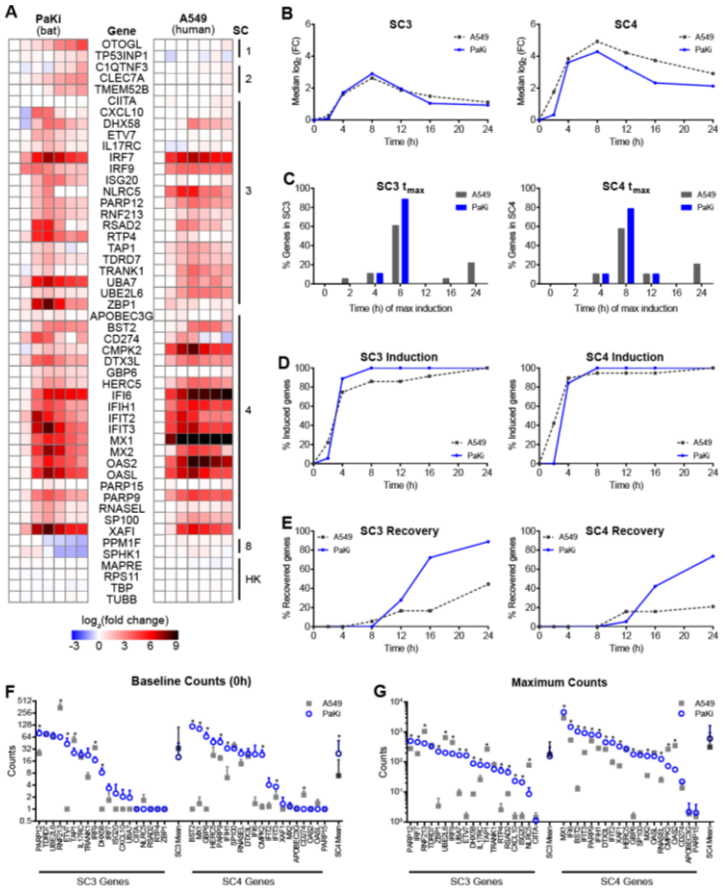

Figure 5: ISG Expression Over Time in Bat and Human Cells. ***(A)*** *Nanostring gene expression for PaKi (left) and A549 cells (right). PaKi data is the same shown in Fig 3B, with additional time points. Data presented is the mean of three independent experiments. HK = housekeeping genes.* ***(B)*** *Expression over time for PaKi and A549 genes in SC3 and SC4. Each line represents the median log_2(FC) for all genes in a SC.* ***(C)*** *Time at peak induction for PaKi and A549 genes in SC3 and SC4.* ***(D)*** *Percent genes induced to levels ≥50% of maximum induction at specified time points in SC3 and SC4.* ***(E)*** *Percent genes that recovered to levels ≤50% of maximum induction at specified time points in SC3 and SC4.* ***(F)*** *Baseline mRNA counts for PaKi and A549 genes in SC3 and SC4. Data are represented as mean + SD for three independent experiments. Darker symbols represent mean counts for each subcluster. * = p-value <0.05 using Student's t-test.* ***(G)*** *Maximum mRNA counts for PaKi and A549 genes in SC3 and SC4. Data are represented as mean + SD for three independent experiments. Darker symbols represent mean counts for each subcluster. * = p-value <0.05 using Student's t-test.*

For further analysis, I chose to focus on previously-reported ISGs, particularly those found in SC3 and SC4. When comparing changes in gene expression in SC3, the median fold-change of all genes in SC3 followed similar trends between bat and human cell lines (Figure 5B). In SC4, however, genes from A549 cells exhibited higher fold induction and remained elevated at later time points when compared to PaKi cells.

I next determined the time point at which I observed maximum gene induction (t_{max}). For both SC3 and SC4, approximately 80% of IFN-induced PaKi genes peaked at 8h (Figure 5C). However, A549

genes had a bimodal pattern within both SCs, with most genes peaking at 4-8h and a smaller subset peaking at 12h or later.

To identify potential differences in induction kinetics, I calculated the percentage of genes that were induced to at least 50% of maximum expression for each time point. Greater than 80% of PaKi genes in both SCs were induced by 4h (Figure 5D). A549 genes in SC3 behaved similarly, although a small subset of genes was induced by 2h. However, approximately 40% of A549 genes in SC4 were induced by 2h, indicating faster induction of this subset of genes. Genes in this list include *HERC5*, *IFI6*, *IFIH1*, *MX1*, *NLRC5*, *OAS2*, *OASL*, and *PARP12*. Notably, PaKi cells express higher baseline levels of ISGs such that by full induction at 8h, PaKi cells express similar or greater mRNA counts compared to A549 cells, despite faster induction in A549 cells (Figure 5D, Figure 5G, and Appendix A).

Next, I calculated the percentage of genes that had recovered to below 50% of maximum expression for each time point. In both SCs, recovery occurred earlier in PaKi cells, with most genes recovering by 16h (Figure 5E). In contrast, the expression levels for most A549 genes remained elevated throughout the time course. Together, these data suggest that the regulatory mechanisms governing IFN-mediated gene induction and maintenance of gene expression differs in each cell type, particularly with genes in SC4.

It was recently reported that black flying fox tissues have constitutive and ubiquitous expression of IFNα, suggesting that cells from this species may be primed to inhibit viral infection due to constitutive expression of certain ISGs (Zhou, Tachedjian et al. 2016). Indeed, I observed overall higher ISG mRNA levels in unstimulated PaKi cells, particularly the SC4 genes

(Figure 5F). In addition, I found that over half of SC4 PaKi ISGs were induced to higher maximum counts than corresponding A549 ISGs (Figure 5G).

Bat Cells Express Multiple Non-Canonical ISGs, Including an Active RNASEL

Our gene expression profiling revealed several genes not previously reported to be ISGs. These included *EMC2*, *FILIP1*, *IL17RC, OTOGL*, *SLC10A2*, and *SLC24A1* (**Figure** 3A). It is unclear whether the induction of these genes is cell type or species specific. In addition, I observed IFN-mediated induction of *RNASEL*, which encodes a 2'-5'-oligoadenylate synthetase-dependent ribonuclease. This protein exerts its antiviral effect by degrading viral RNA in response to 2'-5'-linked oligoadenylates, which are generated by the IFN-inducible oligoadenylate synthase (OAS) family of enzymes upon stimulation by dsRNA in the cytosol (Figure 6)(Silverman 2007).

In human cells, RNASEL is a constitutively-expressed latent enzyme and is not IFN-inducible (Figure 5A, Appendix A) (Zhou, Molinaro et al. 2005). Interestingly, I observed a dose-dependent induction of *RNASEL* in IFN-treated PaKi cells (Figure 7A). Of note, similar mRNA expression levels of *RNASEL* were observed in unstimulated human and bat cell lines (Figure 5F and Appendix A). In addition, I observed IFN-mediated *RNASEL* induction in brain-derived (PaBr) and lung-derived (PaLu) black flying fox cell lines (Figure 7B), suggesting IFN-mediated induction of RNASEL in the black flying fox is not cell type-specific.

Next, I constructed RNASEL-deficient PaKi cells using CRISPR (Mali, Yang et al. 2013). Due to lack of a bat-specific RNASEL antibody, I was not able to monitor RNASEL

protein levels. However, I detected modifications to the *RNASEL* gene in the PaKi knock-out bulk population (KO bulk) as compared to the parental wild-type (WT) population (Table 1).

Table 1: Genomic Characterization of RNASEL KO Bulk Cells. *Genomic DNA was isolated from parental PaKi cells (WT) or cells targeted for RNASEL deletion by CRISPR-Cas9 RNASEL (KO). The RNASEL gene was amplified using PCR and sequenced to identify changes to the coding region of RNASEL.*

Sample	Cas9 target *PAM*	Genotype	Amino Acid Sequence
Ref.	…GAG**AGACCCACACCCTCCAGCAG*TGG***GGAGACTTCTGGGCACGACAATCATTCGTTGATAAAAGCTGTTAAAGA…	N/A	…PTPSSSGETSGHDNHSLIKAVKEGDIK…
WT 1	…GAGAGACCCACACCCTCCAGCAGTGGGGAGACTTCTGGGCACGACAATCATTCGTTGATAAAAGCTGTTAAAGA…	WT	…PTPSSSGETSGHDNHSLIKAVKEGDIK…
WT 2	…GAGAGACCCACACCCTCCAGCAGTGGGGAGACTTCTGGGCACGACAATCATTCGTTGATAAAAGCTGTTAAAGA…	WT	…PTPSSSGETSGHDNHSLIKAVKEGDIK…
WT 3	…GAGAGACCCACACCCTCCAGCAGTGGGGAGACTTCTGGGCACGACAATCATTCGTTGATAAAAGCTGTTAAAGA…	WT	…PTPSSSGETSGHDNHSLIKAVKEGDIK…
WT 4	…GAGAGACCCACACCCTCCAGCAGTGGGGAGACTTCTGGGCACGACAATCATTCGTTGATAAAAGCTGTTAAAGA…	WT	…PTPSSSGETSGHDNHSLIKAVKEGDIK…
WT 5	…GAGAGACCCACACCCTCCAGCAGTGGGGAGACTTCTGGGCACGACAATCATTCGTTGATAAAAGCTGTTAAAGA…	WT	…PTPSSSGETSGHDNHSLIKAVKEGDIK…
KO 1	…GAGAGACCCACACCCTCCAGCAGTGGGGAGACTTCTGGGCACGACAATCATTCGTTGATAAAAGCTGTTAAAGA…	WT	…PTPSSSGETSGHDNHSLIKAVKEGDIK…
KO 2	…GAGAGACCCACACCCTCCAG---TGGGGAGACTTCTGGGCACGACAATCATTCGTTGATAAAAGCTGTTAAAGA…	Δ51-53	…PTPSS-GETSGHDNHSLIKAVKEGDIK…
KO 3	…GAGAGACCCACACCCTCCAGCAGTGGGGAGACTTCTGGGCACGACAATCATTCGTTGATAAAAGCTGTTAAAGA…	WT	…PTPSSSGETSGHDNHSLIKAVKEGDIK…
KO 4	…GAGAGACCCACACCCTCCAG----------ACTTCTGGGCACGACAATCATTCGTTGATAAAAGCTGTTAAAGA…	Δ51-60	…PTPS**RLLGTTIIR***
KO 5	…GAGAGACCCACACCCTCCAGCAGTGGGGAGACTTCTGGGCACGACAATCATTCGTTGATAAAAGCTGTTAAAGA…	WT	…PTPSSSGETSGHDNHSLIKAVKEGDIK…
KO 6	…GAGAGACCCACACCCTCCAGCAGTGGGGAGACTTCTGGGCACGACAATCATTCGTTGATAAAAGCTGTTAAAGA…	WT	…PTPSSSGETSGHDNHSLIKAVKEGDIK…
KO 7	…GAGAGACCCACACCCTCCAGCAGTGGGGAGACTTCTGGGCACGACAATCATTCGTTGATAAAAGCTGTTAAAGA…	WT	…PTPSSSGETSGHDNHSLIKAVKEGDIK…
KO 8	…GAGAGACCCACACCCTCCAGCAGTGGGGAGACTTCTGGGCACGACAATCATTCGTTGATAAAAGCTGTTAAAGA…	WT	…PTPSSSGETSGHDNHSLIKAVKEGDIK…
KO 9	…GAGAGACCCACACCCTCCAG---TGGGGAGACTTCTGGGCACGACAATCATTCGTTGATAAAAGCTGTTAAAGA…	Δ51-53	…PTPSS-GETSGHDNHSLIKAVKEGDIK…
KO 10	…GAGAGACCCACACCCTCCAGCAGTGGGGAGACTTCTGGGCACGACAATCATTCGTTGATAAAAGCTGTTAAAGA…	WT	…PTPSSSGETSGHDNHSLIKAVKEGDIK…
KO 11	…GAGAGACCCACACCCTCCAGCAGTGGGGAGACTTCTGGGCACGACAATCATTCGTTGATAAAAGCTGTTAAAGA…	WT	…PTPSSSGETSGHDNHSLIKAVKEGDIK…
KO 12	…GAGAGACCCACACCCTCCAGCAGTGGGGAGACTTCTGGGCACGACAATCATTCGTTGATAAAAGCTGTTAAAGA…	WT	…PTPSSSGETSGHDNHSLIKAVKEGDIK…
KO 13	…GAGAGACCCACACCCTCCAGCAGTGGGGAGACTTCTGGGCACGACAATCATTCGTTGATAAAAGCTGTTAAAGA…	WT	…PTPSSSGETSGHDNHSLIKAVKEGDIK…
KO 14	…GAGAGACCCACACCCTCCAGCAGTGGGGAGACTTCTGGGCACGACAATCATTCGTTGATAAAAGCTGTTAAAGA…	WT	…PTPSSSGETSGHDNHSLIKAVKEGDIK…
KO 15	…GAGAGACCCACACCCTCCAG---TGGGGAGACTTCTGGGCACGACAATCATTCGTTGATAAAAGCTGTTAAAGA…	Δ51-53	…PTPSS-GETSGHDNHSLIKAVKEGDIK…
KO 16	…GAGAGACCCACACCCTCCAG----------TGGGCACGACAATCATTCGTTGATAAAAGCTGTTAAAGA…	Δ51-65	…PTPSS-----GHDNHSLIKAVKEGDIK…
KO 17	…GAGAGACCCACACCCTCCAGCAGTGGGGAGACTTCTGGGCACGACAATCATTCGTTGATAAAAGCTGTTAAAGA…	WT	…PTPSSSGETSGHDNHSLIKAVKEGDIK…
KO 18	…GAGAGACCCACACCCTCCAGCAGTGGGGAGACTTCTGGGCACGACAATCATTCGTTGATAAAA**A**GA…	+A 102	…PTPSSSGETSGHDNHSLIKAVK**RRRH***
KO 19	…GAGAGACCCACACCCTCCAGCAGTGGGGAGACTTCTGGGCACGACAATCATTCGTTGATAAAAGCTGTTAAAGA…	WT	…PTPSSSGETSGHDNHSLIKAVKEGDIK…
KO 20	…GAGAGACCCACACCCTCCAGCAGTGGGGAGACTTCTGGGCACGACAATCATTCGTTGATAAAAGCTGTTAAAGA…	WT	…PTPSSSGETSGHDNHSLIKAVKEGDIK…
KO 21	…GAGAGACCCACACCCTCCAG---TGGGGAGACTTCTGGGCACGACAATCATTCGTTGATAAAAGCTGTTAAAGA…	Δ51-53	…PTPSS-GETSGHDNHSLIKAVKEGDIK…
KO 22	…GAGAGACCCACACCCTCCAGCAGTGGGGAGACTTCTGGGCACGACAATCATTCGTTGATAAAAGCTGTTAAAGA…	WT	…PTPSSSGETSGHDNHSLIKAVKEGDIK…
KO 23	…GAGAGACCCACACCCTCCAG---TGGGGAGACTTCTGGGCACGACAATCATTCGTTGATAAAAGCTGTTAAAGA…	Δ51-53	…PTPSS-GETSGHDNHSLIKAVKEGDIK…

To test if RNASEL protein was functional, I activated RNASEL with poly (I:C) transfection after IFN or mock treatment and monitored RNA integrity (Figure 7C) (Wreschner, James et al. 1981, Li, Banerjee et al. 2016). I observed ribosomal RNA (rRNA) degradation when cells were treated with poly(I:C), but not with IFN alone. Treating cells with IFN for 24h to induce RNASEL expression before poly (I:C) transfection resulted in increased RNA degradation and accumulation of smaller products, suggesting increased RNASEL activity. The RNA degradation observed in the WT cells was reduced in the bulk KO cells. Together, these data indicate that RNASEL is a functional ribonuclease that, unlike its human ortholog, is IFN-

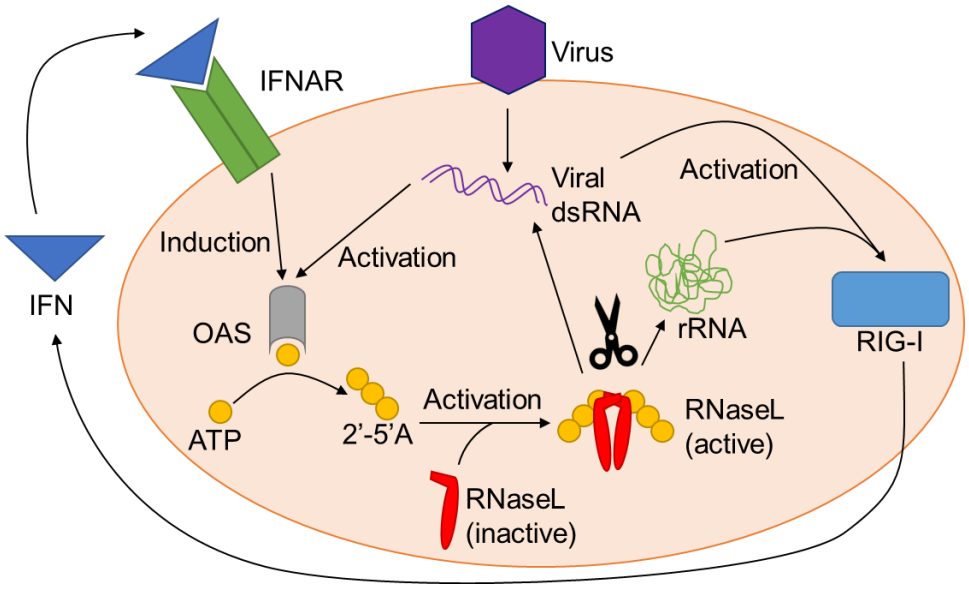

Figure 6: OAS/RNASEL Pathway
Viral sensing leads to induction and activation of OAS proteins. Activated OAS proteins produce 2'5'A products that activate latent RNASEL. Activated RNASEL cleaves viral and cellular RNA. Some cleaved RNA products serve as substrates for RIG-I, providing a positive feedback loop that results in stronger IFN signaling.

inducible.

To test if the presence of RNASEL is important in the context of viral infection, I infected both WT and bulk KO cells with YFV17D-Venus and quantified infectivity after one viral life cycle (Figure 7D). RNASEL KO cells were more permissive to infection at all doses

used, suggesting that RNASEL is important for suppression of initial viral infection. To test if RNASEL induction played a role in the protective effect of the IFN response, I treated PaKi WT and KO bulk cells with increasing doses of IFNα for 24h, then infected with YFV17D-Venus (Figure 7E). Consistent with previous results, KO bulk cells were more permissive to infection than WT cells. In addition, KO bulk cells were resistant to the protective activity of IFN. IFNα (100U/mL) pre-treatment resulted in 80% reduction of infection in WT cells, but only 50% reduction in bulk KO cells**.** Together, these data suggest RNASEL plays a significant role in the inhibition of viral infection, particularly in the context of the IFN response.

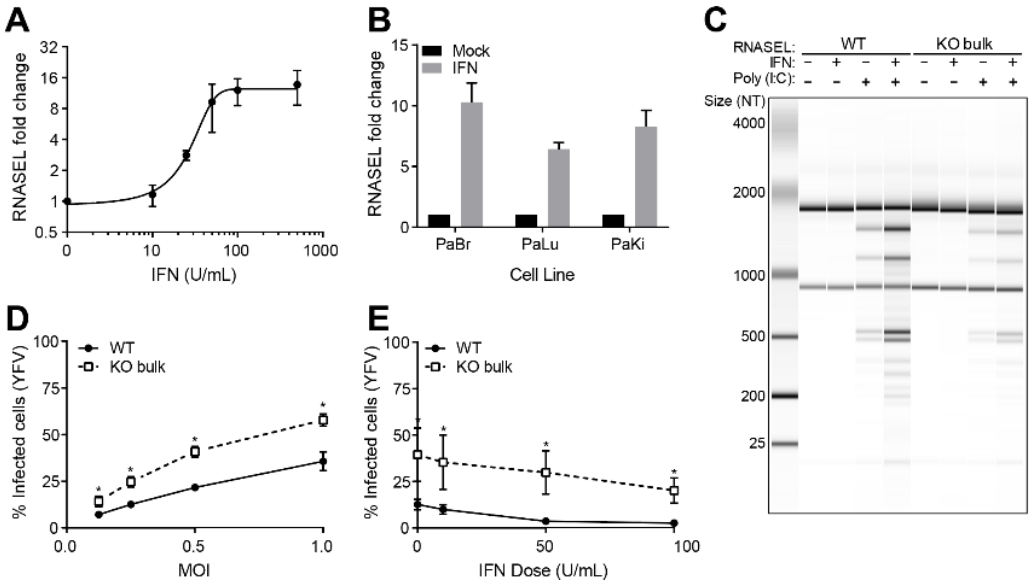

Figure 7: RNASEL is IFN-Inducible in P. alecto.
(A) *PaKi cells were treated with increasing doses of IFNα and RNA was harvested at 8h. RNASEL mRNA levels were measured using qRT-PCR and normalized to untreated control using RPS11 as a housekeeping control. Data are represented as mean ± SD for two independent experiments.* ***(B)*** *RNASEL induction in P. alecto brain, lung, and kidney cells. Cells were treated with IFNα (100U/mL) and RNA was harvested at 8h. RNASEL levels were quantified using qRT-PCR and normalized to untreated control using RPS11 as housekeeping control. Data are represented as mean ± SD for three independent experiments.* ***(C)*** *PaKi cells were treated with IFNα (100U/mL) or mock-treated for 24h, followed by transfection with poly(I:C) (100ng/mL) or mock-transfected for 4h and RNA integrity was monitored using a bionalyzer. 100 ng total RNA was run per lane. Data is representative of two independent experiments.* ***(D)*** *WT or RNASEL KO bulk PaKi cells were infected with YFV-17D Venus for 24h and viral infection was quantified using flow cytometry. Data are represented as mean ± SD for three independent experiments. * = p-value < 0.05 using Student's t-test.* ***(E)*** *WT or RNASEL KO bulk PaKi cells were treated with increasing doses of IFNα for 24h, then infected with YFV-17D Venus at an MOI of 0.5 for 24h. Viral infection was quantified using flow cytometry. Data are represented as mean ± SD for three independent experiments. * = p-value < 0.05 using Student's t-test.*

DISCUSSION

This study aimed to identify IFN-stimulated transcripts in a cell line from the black flying fox. Transcriptional analysis revealed over 100 genes induced in response to IFNα. Most of these genes have been previously described as ISGs, suggesting strong evolutionary conservation of the ISG pool, as would be predicted by previous genomic studies of immune genes in the black flying fox (Papenfuss, Baker et al. 2012, Zhang, Cowled et al. 2013).

I have provided a framework of black flying fox ISGs, organized by early, mid, and late responses to type I IFN. Temporal expression profiling delineated two separate ISG pools based on unique temporal induction profiles. While both SCs are characterized by similar peak mRNA levels and a subsequent decline by 12-24 hours, SC4 contained some genes that remained elevated. These genes may offer residual antiviral protection, even when IFN signaling has returned to basal levels. In addition, many genes in SC4 have both higher baseline and higher maximal induction levels in bat PaKi cells compared to human A549 cells, which could result in species-specific differences in susceptibility to viral infection. It remains unclear why only particular ISGs are differentially expressed in this context, but it would be interesting to identify unique features or functions of these ISGs that could explain their differing expression patterns. Compared to human A549 cells, bat PaKi cells have a more rapid decline in ISG levels, suggesting tightly-regulated expression kinetics. The reason for this strict transcriptional regulation remains unclear, but such a mechanism may exist to prevent excessive inflammation in a highly metabolically active host (Zhang, Cowled et al. 2013).

I also identified several previously unrecognized, or non-canonical ISGs, including RNASEL. Notably, while our manuscript was under review, another transcriptome study of IFN-treated black flying fox cells also uncovered RNASEL as an ISG (Zhang, Zeng et al. 2017).The OAS/RNASEL pathway, by which OAS proteins use viral dsRNA to create short oligonucleotides that act as second messengers to activate the constitutively-expressed latent enzyme RNASEL, is used to clear viral genetic material from the cell. Due to cleavage of both viral and cellular RNA, RNASEL activation can also lead to apoptosis of infected cells (Li, Xiang et al. 2004). In addition, the short RNA fragments created by RNASEL can potentiate the IFN response by activating the cytosolic RNA sensor RIG-I (Malathi, Dong et al. 2007). The induction of RNASEL in response to IFN in bats may provide an additional layer of antiviral protection. Indeed, knockout of RNASEL increased viral susceptibility of black flying fox-derived cells. Although induction itself does not result in significant nuclease activity, stimulation with poly (I:C) is sufficient to cause degradation of total RNA in the cell. Unlike in humans, where only the upstream OAS proteins are IFN-induced, bat cells co-induce both components of the OAS/RNASEL pathway, likely creating a more rapid and potent effect that would inhibit viral replication before extensive viral spread could occur. Induction of RNASEL could also be a way of attenuating the effect of viruses that affect RNASEL activity either by direct inhibition, as seen with the L* protein of murine Theiler's virus (Sorgeloos, Jha et al. 2013), or via increased expression of an RNASEL inhibitor as seen with HIV(Martinand, Montavon et al. 1999) and EMCV(Martinand, Salehzada et al. 1998).

There is some evidence of modest (~2-fold) RNASEL induction in certain mouse cell lines (Essers, Offner et al. 2009, Mostafavi, Yoshida et al. 2016). One mouse cell line with low

endogenous levels of RNASEL, however, has been shown to increase RNASEL levels around 10-fold in response to high doses of IFN (Jacobsen, Czarniecki et al. 1983). Rodents are also important viral reservoirs (Olival, Hosseini et al. 2017), but additional studies are needed to determine if IFN-mediated RNASEL induction plays a role in the host-virus interactions in mice. I acknowledge several limitations of this study. First, temporal kinetics analysis was performed between one bat kidney cell line and one human lung cell line. It is possible that some differences observed may be due to intrinsic differences between cell lines and not due to differences in species. Studies in multiple cell backgrounds from both species may help determine whether kinetic differences between bat and human ISGs can be generalized to the whole species. Second, in using Universal IFN in place of black flying fox IFN, I made the assumption that the IFN response would be comparable between both types of IFN. Although I observed a transcriptional profile that is expected for IFN-treated cells, I cannot rule out possible differences in downstream signaling kinetics or magnitude of the response between universal and bat-derived IFN. Nonetheless, a recent transcriptomic study done in PaKi cells using black flying fox IFN showed comparable ISG profiles to those observed in our study (Zhang, Zeng et al. 2017).

Overall, this work lays the foundation for future investigation into the potential unique features of the bat IFN response. While this part of the study focused on ISG induction, it did not address whether bat ISG-encoded effectors possess unique antiviral properties. Uncovering mechanisms of bat ISGs, as explored in the next chapter, may provide insight into the innate immune responses of an important viral reservoir and may inform research and development of antiviral therapies.

CHAPTER THREE
Interferon Regulatory Factor 7 from the Black Flying Fox Provides Antiviral Protection from a Range of RNA Viruses Through a Non-Canonical Pathway

ABSTRACT

Bats as a species are capable of hosting a large number of zoonotic viruses. For reasons that remain unclear, they rarely demonstrate signs of viral disease, even when infected with viruses that are greatly pathogenic to other mammals. Previous work has shown that the pool of interferon-stimulated genes (ISGs) induced by interferon or viral infection is greatly conserved between certain bat species and humans, so it is possible that individual ISG functions have evolved to control viral infection. In this study, I compared the antiviral activity of over 70 ISG human-bat ortholog pairs to identify differences in individual effector function. I identified bat IRF7 as a potent and broad-acting antiviral molecule that, unlike human IRF7, provides antiviral protection without previous activation. I show that bat IRF7 uniquely induces a subset of protective ISGs in a STAT1 and IFN-independent manner, which leads to protection from Alpha-, Flavi-, and Rhabdoviruses. Genetic studies indicate that bat IRF7 may be constitutively active due to additional unique serine residues located in the C-terminal regulatory region. This property of IRF7 constitutes a major difference between bat and human ISG regulation and provides an additional layer of antiviral protection not found in humans.

INTRODUCTION

Bats are asymptomatic carriers of several highly pathogenic viruses, such as Nipah (Chua, Koh et al. 2002), Hendra (Halpin, Young et al. 2000), SARS-like coronavirus (Li, Shi et al. 2005), and Marburg (Towner, Amman et al. 2009). Viruses have been detected in bats from all continents except Antarctica, indicating that bats are a widespread viral host (Hayman 2016). A recent study has identified bats as the mammalian hosts with the greatest viral diversity, hosting a greater number of zoonoses per species than even rodents (Olival, Hosseini et al. 2017). Due to their ability to host such a large number of viruses with no clinical consequences, it is of great interest to study antiviral responses in bat reservoirs.

IFN is the first response to viral pathogens in vertebrate hosts and carries out its antiviral function through the upregulation of hundreds of protective interferon-stimulated genes (ISGs). Upon viral entry, PPRs recognize PAMPS, such as viral nucleic acids, and through various converging pathways induce the phosphorylation of IRF3 and/or IRF7, which translocate into the nucleus to stimulate the secretion of type I IFN. In the canonical JAK-STAT signaling pathway, IFN binds the type I IFN receptor (IFNAR), consisting of IFNAR1 and IFNAR2 subunits, present on the cell surface, leading to activation of the Janus kinases JAK1 and TYK2. Upon activation, these kinases phosphorylate signal transducer and activator of signal proteins STAT1 and STAT2, which then form a trimeric complex with IRF9 to form the transcriptional complex known as ISGF3. ISGF3 moves into the nucleus, where it induces the expression of ISGs by binding ISREs present in ISG promoters (Platanias 2005, Ivashkiv and Donlin 2014). These ISGs, through several different mechanisms of action, can inhibit viral infection.

Although great efforts have been made to expand our knowledge of the transcriptional signatures in response to IFN or viral infection in a number of different bat species (Biesold, Ritz et al. 2011, Wu, Zhou et al. 2013, Wynne, Shiell et al. 2014, Glennon, Jabado et al. 2015, Holzer, Krahling et al. 2016, De La Cruz-Rivera, Kanchwala et al. 2017, Zhang, Zeng et al. 2017), studies examining the function of specific bat antiviral effectors are limited. Previously I found that immortalized cells derived from the black flying fox (*Pteropus alecto)* induced a strong and heavily conserved ISG response (De La Cruz-Rivera, Kanchwala et al. 2017). Because I observed high bat-human homology of the ISG signature induced upon IFNα treatment, I investigated if there were differences in the functions of individual effectors.

In this study, I overexpressed select human ISGs or their bat orthologs individually and compared their ability to inhibit viral infection. I found that compared to human IRF7, bat IRF7 has significantly increased antiviral capacity in cells lacking canonical JAK-STAT signaling. This STAT1-indepdendent antiviral effect is due to induction of ISGs in bat IRF7-expressing cells. I further show that bat IRF7 has IFN-independent, constitutive activity and that it can bypass the canonical IFN pathway and bind regions of ISG promoters directly. This constitutive activity may be in part explained by the presence of additional phosphorylation targets at the C-terminal signal response domain of bat IRF7.

METHODOLOGY

Cell Lines

STAT1$^{-/-}$ human fibroblasts (Dupuis, Jouanguy et al. 2003) were grown at 37°C and 5% CO_2 and passaged in RPMI (Life Technologies #11875-093) supplemented with 10% FBS and 1x nonessential amino acids (NEAA) (Life Technologies #11140076). HEK293 and HeLa cells were grown at 37°C and 5% CO_2 and passaged in DMEM (Life Technologies #11995-065) supplemented with 10% FBS and 1x NEAA. PaKi cells (Crameri, Todd et al. 2009) were grown at 37°C and 5% CO_2 and passaged in DMEM/F12 (Life Technologies #11320-033) supplemented with 10% FBS.

Viruses

YFV-Venus (derived from YF17D-5C25Venus2AUbi) stocks were generated by electroporation of in vitro-transcribed RNA into *STAT1*$^{-/-}$ fibroblasts as previously described (Schoggins, Wilson et al. 2011). VSV-GFP (provided by Jack Rose) was generated by passage in BHK-J cells. VEEV-GFP (provided by I. Frolov) is a double subgenomic enhanced GFP (EGFP) reporter virus derived from the TC83 vaccine strain of VEEV and was generated by passage in BHK-J cells. VSV-GFP, Indiana serotype (provided by Jack Rose) was generated by passage in BHK-J cells. For all viruses, virus-containing supernatant was centrifuged to remove cellular debris and stored at -80C until use.

Viral Infection

Cells were seeded into 24-well plates at a density of $1x10^5$ cells per well, or from a 1:3 split if previously transduced. Viral stocks were diluted into media supplemented with 1% FBS to make infection media. Media was aspirated and replaced with 200 µL of infection media. Infections were carried out at 37°C for 1h, then 800 µL media supplemented with 10% FBS was added back to each well. Cells were harvested for flow cytometry at the following times: CoV: 24h, EAV: 18h, IAV: 8h, ONNV: 18h, SINV: 10h, VEEV: 6h, VSV: 4h, YFV: 24h, ZIKV: 24h.

DNA Constructs and Plasmid Propagation

The human ISG library has been previously described (Schoggins, Wilson et al. 2011). The bat ISG library was created by subcloning codon-optimized ISG ORFs in a pENTR221 backbone into pTRIP. pTRIP.CMV.IVSb.ires.TagRFP-DEST using LR Clonase II (Invitrogen) according to manufacturer's instructions. Correct assembly was verified by Sanger sequencing. pTRIP.CMV.IVSb.ires.TagRFP.FLUC (firefly luciferase) was used as a negative control in the screens.

Plasmids for stable expression pSCRPSY.B-IRF7, pSCRPSY.H-IRF7 were generated by Gateway cloning of pENTR vectors into the lentiviral pSCRPSY backbone using LR Clonase II according to the manufacturer’s instructions. Correct assembly was confirmed by Sanger sequencing. pSCRPSY.Empty was used as a vector control.

Bat and human IRF7 chimera plasmids were generated by subcloning synthesized codon-optimized ORFs containing a GGGGS linker and a 3xFLAG tag at the C-terminus, as well as gateway-compatible *attB* sites (Genewiz) into the PENT221 backbone using BP Clonase II

(Invitrogen). The ORFs were then subcloned into pTRIP. pTRIP.CMV.IVSb.ires.TagRFP for use as expression vectors, and correct was assembly confirmed by Sanger sequencing.

To generate single and double-point IRF7 mutants, pENTR221 vectors containing open reading frames for bat or human full-length IRF7 (pENTR221.H-IRF7.3XFL and pENTR221.B-IRF7.3XFL) were digested with BamHI and EcoRV or BgII and BamHI, respectively. The large fragment was purified using the QIAquick Gel Extraction Kit (Qiagen). Point mutations were added by Gibson (NEB) assembly of the large fragment and a small synthesized (Genewiz) fragment containing the mutation of interest following the manufacturer's directions. Correct assembly was verified using Sanger sequencing. The ORFs were then subcloned into pTRIP. pTRIP.CMV.IVSb.ires.TagRFP for use as expression vectors, and correct assembly was confirmed by Sanger sequencing.

lentiCRISPR v2 was a gift from Feng Zhang (Addgene plasmid # 52961). Targeting guides for knockout of PaKi IRF7 were generated by cloning annealed, complementary 20-bp oligos with *Esp3I*-compatible overhangs (5'- caccgGTCAGCAGCGGCCGCTACG-3' and 5'-aaacTCGTAGCGGCCGCTGCTGAC-3') targeting the *P. alecto IRF7* gene into the lentiCRISPRv2 backbone as described in (Sanjana, Shalem et al. 2014). Targeting guides for endogenous tagging of *IRF7* in PaKi cells are 5'-caccgGCTCGGGGAGGTCTGGGGTC-3' and 5'- aaacGACCCCAGACCTCCCCGAGC. CRISPR guide oligos were designed using CRISPRdirect (Naito, Hino et al. 2015). Proper assembly was confirmed using Sanger sequencing.

Lentiviral Pseudoparticles for ISG Expression

Lentiviral pseudoparticles were generated as described in (Schoggins, Wilson et al. 2011) with minor modifications. In brief, 293T cells were seeded at a density of $1x10^5$ in 6-well plates. The following day, cells were co-transfected with plasmids expressing the pTRIP.CMV.IVSb.ISG.ires.TagRFP proviral DNA, HIV-1 pGag–pol and pCMV-VSVg in a ratio of 1:0.8:0.2, respectively. For each transfection, 6 µl (Roche XTG9-RO) was combined with 2.0 µg total DNA in 100 µl Opti-MEM (Gibco) and added to cells in 1.5 mL of DMEM with 3% FBS. After 4h, media was changed to 2 mL fresh DMEM with 3% FBS. Supernatant was collected 48h post-transfection, filtered through 0.45 µm to remove debris, and stored at -80°C until use.

Transductions

Cells were seeded at a density of $1x10^5$ cells per well on 24-well plates. The following day, lentiviral pseudoparticles diluted in PP media (media supplemented with 3% FBS, 1x NEAA, and 4ug/mL polybrene) were added to cells and cells were spinoculated at 800 x g, 45 min, 37°C. Immediately following spinoculation, media was changed for fresh media containing 10% FBS and 1x NEAA.

Flow Cytometry

Cells were detached using Accumax (Innovative Cell Technologies AM-105), fixed in 1% PFA for 10 min at room temperature**,** and pelleted by centrifugation at 800 x g. Fixed cell pellets were resuspended in 200 µL FACS buffer (1X PBS supplemented with 3% FBS).

Samples were run on a Stratedigm S1000 instrument using CellCapTure software and gated based on live cells, singlets, RFP signal for ISG expression, and finally GFP signal for viral infection. Data analysis was done using FlowJo software (v9.7.6).

ISG Screen

STAT1$^{-/-}$ human fibroblasts were seeded at a density of $1x10^5$ cells per well on 24-well plates. The following day, cells were transduced with pTRIP.CMV.IVSb.ires.TagRFP lentiviral pseudoparticles, leading to expression of an ISG of interest and RFP in a one-well: one-ISG format. After 48h, cells were split 1:3. The following day, cells were infected with a GFP-reporter virus and harvested for flow cytometry as described above.

B19R Treatment

HeLa cells were seeded at a density of $5x10^4$ cells per well of a 24-well tissue culture plate. The following day, they were transduced with pTRIP lentiviral vectors. After 48h, cells were split 1:3 and seeded into fresh 24-well plates with media containing B19R (R&D Systems 8185-BR) and mock (PBS) or IFNα (PBL # 11200) at 100 units/mL. After 24h of pre-treatment with B19R, cells were infected with YFV at an MOI of 0.5. After 24h, cells were collected for flow cytometry analysis. For RNA samples, RNA was isolated using the RNeasy Mini Kit (Qiagen 74106) following the manufacturer's directions.

Microarray

STAT1$^{-/-}$ fibroblasts stably expressing IRF7 or vector control were seeded in 6-well plates at a density of $4x10^6$. The following day, RNA was harvested using the RNeasy Mini Kit (Qiagen)

following the manufacturer's instructions and stored at -80°C until use. The RNA integrity score (RIN) was 10 for all samples. Samples were prepared for and run on an Illumina Human HT 12 v4 chip following Illumina standard protocol.

Real Time Quantitative PCR

Total RNA was prepared as described above. Reactions were prepared with the QuantiFast SYBR Green RT-PCR kit (Qiagen #204154), using 50 ng total RNA per reaction. Samples were run on the Applied Biosystems 7500 Fast Real-Time PCR System using 7500 Software v2.0.6. RPS11 was used as a reference gene. Relative expression was calculated using $2^{-\Delta\Delta CT}$ method. Primers used are listed in Table 2.

Table 2: Primers for RT-qPCR

Gene	**Species**	**Oligonucleotide Sequence 2 (5'→3') or Catalog Number**
OAS1	P. alecto	TGAAGCAGAGACCAGCCAAG
		TTTCCACGTTCCCAAGCGTA
RPS11	P. alecto	ATCCGCCGAGACTATCTCCA
		GGACATCTCTGAAGCAGGGT
USP18	P. alecto	TCGGCAGATCCTGTTGAGAAG
		TGTTGTGTAAACCGACTGGG
IFI44L	H. sapiens	Qiagen QT00051457
IFI6	H. sapiens	GGTCTGCGATCCTGAATGGG
		TCACTATCGAGATACTTGTGGGT
IFNA2	H. sapiens	Qiagen QT00212527
IFNB1	H. sapiens	Qiagen QT00203763
OAS2	H. sapiens	GAACACCATCTGTGACGTCCT
		GAGCCACCTATGGCCACTCC
RPS11	H. sapiens	Qiagen QT00061516
RSAD2	H. sapiens	Qiagen QT00005271

Lentiviral Pseudoparticles for CRISPR-Cas9 Knockout

Lentiviral pseudoparticles were made as described in (Shalem, Sanjana et al. 2014), with some modifications. Briefly, $2x10^6$ HEK293T cells were seeded on a poly-lysine coated 10 cm plate. The following day, cells were co-transfected with 5 µg lentiCRIPSRv2, 2.5 µg pCMV-VSVg and 3.5 µg pGag-pol. For each transfection, 30 µl (Roche XTG9-RO) was combined with 2.0 µg total DNA in 500 µl Opti-MEM (Gibco 7.5mL DMEM with 3% FBS and 1x NEAA. 4h post-transfection, media was changed to 7.5 mL fresh DMEM with 3% FBS and 1x NEAA. Supernatant was collected 48h post-transfection, filtered through 0.45 µm to remove debris, and stored at -80°C until use.

CRISPR KO Bulk STAT1$^{-/-}$ cell lines

Two sgRNA sequences (Table 3) per gene were selected from the sequences contained in the optimized Brunello library (Doench, Fusi et al. 2016) and cloned into lentiCRISPR v2 as described above. 2 x 10^6 *STAT1$^{-/-}$* fibroblasts in 6-well plates were transduced with single sgRNA as described in transductions. 48h after transduction, cells were selected in 4 ug/mL puromycin for 7-10 days before use.

Table 3. Guide RNA Sequences for CRISPR-Cas9-Mediated KO in STAT1$^{-/-}$ Fibroblasts

Targeted Gene	**Oligonucleotide Sequence 1 (5'→3')**	**Oligonucleotide Sequence 2 (5'→3')**
Non-Targeting	CACCGGAACTCAACCAGAGGGCCAA	AAACTTGGCCCTCTGGTTGAGTTCC
IRF3 G1	CACCGAGAAGGGTTGCGTTTAGCAG	AAACCTGCTAAACGCAACCCTTCTC
IRF3 G2	CACCGGTTACTGGGTAACATGGTGT	AAACACACCATGTTACCCAGTAACC
IRAK1 G1	CACCGACACGGTGTATGCTGTGAAG	AAACCTTCACAGCATACACCGTGTC
TBK1 G1	CACCGACAGTGTATAAACTCCCACA	AAACTGTGGGAGTTTATACACTGTC
TBK1 G2	CACCGAGTTGATCTTTGGAGCATTG	AAACCAATGCTCCAAAGATCAACTC
MAVS G1	CACCGAGTACTTCATTGCGGCACTG	AAACCAGTGCCGCAATGAAGTACTC
MAVS G2	CACCGGTGTCTTCCAGGATCGACTG	AAACCAGTCGATCCTGGAAGACACC
STING G1	CACCGGCTGGGACTGCTGTTAAACG	AAACCGTTTAACAGCAGTCCCAGCC
STING G2	CACCGGGTACCGGGGCAGCTACTGG	AAACCCAGTAGCTGCCCCGGTACCC

IRF7 KO in PaKi Cell Line

$3x10^5$ PaKi cells were seeded on 6-well plates. The following day, media was changed to DMEM/F-12 supplemented with 3% FBS, 4 µg/mL polybrene and 20 mM HEPES. LentiCRISPRv2 lentiviral pseudoparticles were added and cells were spinoculated at 800 x g for 45 min at 37°C. Media was changed to DMEM/F-12 with 10% FBS immediately following spinoculation. 48h after transduction, cells were pooled into a 10-cm dish and selected in DMEM/F-12 with 10% FBS and 5 µg/mL puromycin. After 7 days of selection, the surviving bulk population was tested for lack of an IRF7 band by western blot. Single-cell clones were generated by limiting dilution and screened for IRF7 expression by WB. Genetic confirmation of *IRF7* gene modification in the two single cell clones was done Sanger sequencing following genomic PCR (using primers 5'-CAGGCCTAGGGAAGGGGAC-3' and 5'-TCCCACACCTGTGGAAACAC-3') and TOPO cloning.

IRF7-3xFL Endogenous Tagging in PaKi Cell Line

PaKi cells were seeded at a density of $2x10^6$ cells in 10 cm plates. The following day, cells were co-transfected with 1µg lentiCRISPRv2 and 4 µg donor homology plasmid using Lipofectamine 3000 (Thermo L3000008) according to the manufacturer's protocol. The lentiCRISPRv2 plasmid encodes a guide RNA that targets 6 nucleotides upstream of the stop codon. After 4h, media was changed for fresh media containing 0.1uM SCR-7 (Tocris #5342) to promote homology directed-repair. At 48h after transduction, cells were selected with 4µg/mL of puromycin for 72h. The surviving bulk population was tested for an IFN-inducible FLAG signal

by western blot. Single-cell clones were generated by limiting dilution and screened for IRF-3xFL expression by WB. Genetic confirmation of the 3xFL tag was done by genomic PCR, using primers 5'-TGCTCCTCATGTCTGCATGT-3' and 5'-TGGTGTACCTACCCCTGGGA-3', followed by TOPO cloning and Sanger sequencing. All alleles in the cell line were modified.

SDS-PAGE

Unless otherwise indicated, samples for WB were prepared by aspirating media from wells, washing with PBS, and lysing directly in the well with 1X SDS loading buffer (0.04M Tris-HCl pH 6.8, 2% SDS, 2mM BME, 4% glycerol, 0.01% bromophenol blue). The samples were immediately frozen and kept at -20°C until use. Samples were boiled for 5 min, loaded on a 12% polyacrylamide gel (TGX FastCast Acrylamide Kit, Bio-Rad #1610175), and run at 250V for 30 min.

Western Blot

Polyacrylamide gels were transferred to PVDF membranes using either wet transfer (100V, 45 min, 4°C) or semi-dry transfer (3 min, RT). Membranes were blocked with 5% nonfat milk in TBST (50 mM Tris-HCl pH 7.4, 150 mM NaCl, 0.1% Tween-20) for 1h, then incubated with primary antibody 1-2h, washed 3x with TBST for 5 min each, incubated in secondary antibody for 30 min, washed 3x with TBST, and finally developed using ECL Western Blotting Substrate (Thermo Scientific Pierce #32106).

Unless otherwise indicated, all primary antibodies were used at a dilution of 1:1000 in TBST with 1% nonfat milk. The following antibodies were used: bat and human IRF7:

NeoBioLab #A0159, bat and human STAT1: Abcam ab92506, human IFIT1: Abcam ab118062, human TBK1: CST #3504, human IRAK1: CST #4504S, human IRF3: CST #11904, human MAVS: CST #3993T, human STING: CST #50494, bat and human beta actin: Abcam ab6276 (1:40,000), bat and human alpha tubulin: Sigma T6074 (1:20,000), bat and human histone H3: Abcam ab176842 (1:20,000). Anti-mouse (Thermo Scientific 31460) and anti-rabbit (Thermo Scientific 31430) were used at a dilution of 1:5000 in TBST containing 5% nonfat milk.

Dimerization Assays

Lysates from *STAT1*$^{-/-}$ fibroblasts stably expressing bat or human IRF7 were used in dimerization assays as described by (Iwamura, Yoneyama et al. 2001).

ISRE pulldown assays

Lysates from *STAT1*$^{-/-}$ fibroblasts stably expressing vector control or bat or human IRF7 were prepared the same way as for the dimerization assays. 50 μL lysate (~25 μg total protein) was mixed with 2 μg 5'-biotinylated dsDNA probe and 50 μL streptavidin agarose resin (Thermo Scientific #20349) in PBS containing protease inhibitors (Roche) and phosphatase inhibitors (Roche) to a final volume of 250 μL. The mixture was gently rotated at 4°C overnight.

To generate DNA fragments containing ISREs of interest, genomic DNA from human MRC5 (ATCC) cells were used as a template for PCR. Primers 5'-GTTCCCGCGAGGCAAGTG-3' and 5'- GCGCCGCGAAGAAATGAAAC-3' were used to amplify a genomic region containing MX1 ISRE1 and ISRE2. Primers 5'-GAGTCCTGCCAATTTCACTTTCT-3' and 5'- TACAAGTGGCCTCTGGTTCC-3' were used

to amplify a genomic region containing the IFIT2 ISRE. PCR products from these reactions were PCR-purified and used as a template in subsequent PCR reactions. To generate biotinylated DNA probes, ISRE-containing fragments generated previously were amplified via PCR using identical primers with an additional 5'biotin label (IDT). Reactions were PCR-purified, ethanol precipitated, and resuspended to 200 ng/µL before use.

RESULTS

Bat-Human ISG Ortholog Antiviral Screen

To identify differences in antiviral function of ISGs between bat and human orthologs, I designed a high-throughput, FACS-based screening assay (Figure 8A). Lentiviral constructs encoding individual ISGs and a co-expressed RFP reporter were transduced into *STAT1*$^{-/-}$ human fibroblasts. Cells were then infected with a panel of GFP-expressing reporter viruses and harvested for quantification using FACS (Appendix B) (Schoggins, Wilson et al. 2011).

To compare antiviral activities between bat and human ISGs, I calculated the z-score of each ISG and plotted the human ISG z-score versus the bat ISG z-score [Figure 8B]. Many ISGs fell close to the origin, indicating little effect on viral infection. ISGs with similar phenotype fall close to the dotted line, with antiviral ISGs located on the bottom left and ISGs that increased viral infection (pro-viral) found on the top right. I observed broad antiviral activity with both bat and human IRF1, our internal control. Our most frequent observation was that both bat and human genes had similar antiviral activities. For example, both bat and human IFI6 inhibit the Flavivirus yellow fever virus (YFV) and both MAP3K14 orthologs inhibit the Alphaviruses O'nyong'nyong virus (ONNV), Sindbis virus (SINV), and Venezuelan equine encephalitis virus (VEEV). I observed conserved phenotypes with a subset of genes that enhanced viral infection. I saw increased Alphavirus infection with ADAR from both species, an observation which has been reported previously for human ADAR (Gelinas, Clerzius et al. 2011, Schoggins, Wilson et al. 2011). I also observed increased YFV with both orthologs of LY6E, as has been reported for human LY6E during flavivirus or HIV infection (Schoggins, Wilson et al. 2011, Yu, Liang et al.

2017). I observed a few instances of loss-of-function of bat genes, possibly due to expression in a human cell background. These genes included ZBP1 and TMEM140 during ONNV infection (Appendix C). Interestingly, there were a handful of genes in which that bat ortholog had increased antiviral activity. One example of this is IFIT1, for which the bat ortholog alone inhibits ONNV and VEEV. Bat OAS1 is also inhibitory to ONNV (but not SINV or VEEV),

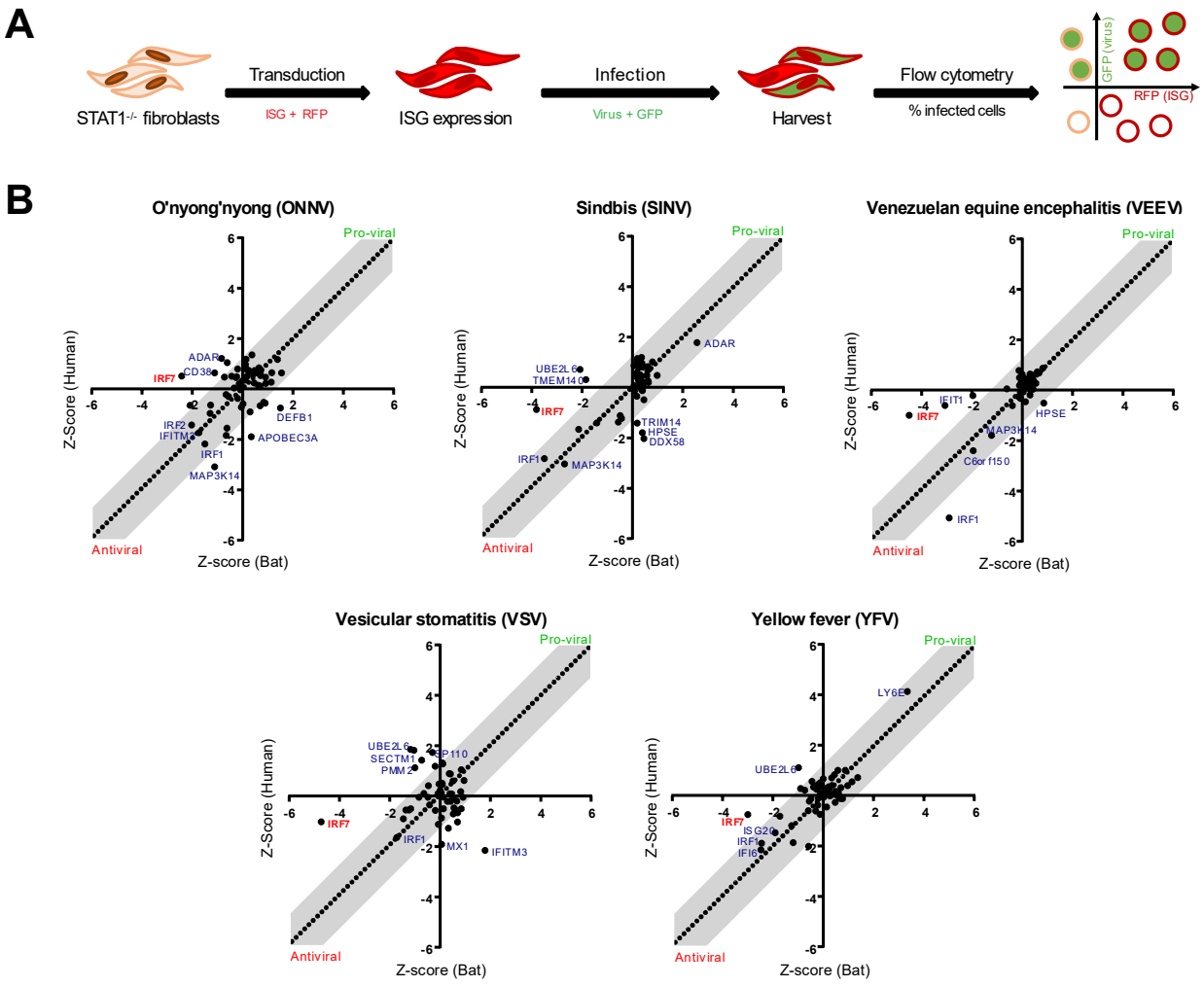

Figure 8: ISG Ortholog Screens.
(A) *Human STAT-/- fibroblasts were transduced with a lentiviral vector encoding a single ISG and RFP reporter. Cells were then infected with a GFP-expressing virus and infection was quantified using flow cytometry.* ***(B)****Z-score plots for all screens. ISGs that inhibit viral infection have negative z-scores and are found on the bottom left. ISGs that promote viral infection have positive z-scores and are in the upper right. Orthologs with similar activity are located inside of the grey bars, indicating ortholog z-scores are within 1.5 of each other.*

while the human ortholog has no effect. However, the gene with the greatest difference in antiviral potential between bat and human orthologs was IRF7 (Figure 8, Appendix B, Appendix C). IRF7 classically exhibits an antiviral effect by inducing the production of IFN, which leads to expression of antiviral ISGs via JAK-STAT signaling. Because the screen was performed in a *STAT1*$^{-/-}$ cellular background that cannot respond to IFN, human IRF7 had little to no effect as expected. Surprisingly, bat IRF7 has broad and potent antiviral activity in a *STAT1*$^{-/-}$ background.

To confirm the results from our screen, I made *STAT1*$^{-/-}$ cell lines that stably express vector control, bat IRF7, or human IRF7 and tested them against a panel of viruses from various viral families (**Figure 9**A). As I observed with transient transduction, bat IRF7 was broadly antiviral while human IRF7 infection did not differ significantly from control. Bat IRF7 was capable of suppressing YFV and Zika virus (ZIKV) from the *Flaviviridae* family, Venezuelan equine encephalitis virus VEEV and ONNV from the *Togaviridae* family, equine arteritis virus (EAV) from the *Ateriviridae* family, vesicular stomatitis virus (VSV) from the *Rhabdoviridae* family, and influenza A virus from the *Orthomyxoviridae* family. The only virus tested for which

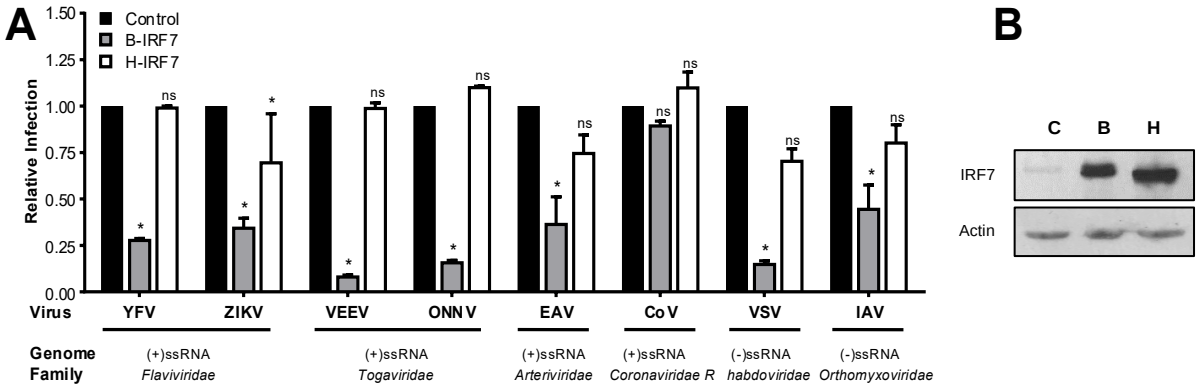

Figure 9: Viral Infections in STAT1$^{-/-}$ Fibroblasts Stably Expressing IRF7
(A) *STAT1$^{-/-}$ fibroblasts were transduced with lentivirus to express IRF7 or vector and then selected with puromycin. Stable cell lines were infected with the indicated viruses at an MOI of 1 and infection was normalized to % infected cells in the control (vector) cell line. For Zika and IAV, n=3. For all others, n=2.*
(B) *Expression levels of IRF7 in STAT1$^{-/-}$ fibroblasts after selection.*

bat IRF7 had no significant antiviral activity was OC43 coronavirus (CoV) from the *Coronaviridae* family. In contrast, human IRF7 in this cellular background exhibited no significant antiviral activity with the exception of ZIKV, for which it was slightly antiviral. This effect was seen despite higher expression levels of human IRF7 in our stable cell lines (Figure 9B).

Bat IRF7 Does Not Require Type I IFN Signaling for Antiviral Activity

Next, I tested IRF7 phenotypes in HeLa cells, which express STAT1 and have an intact canonical JAK-STAT signaling pathway. *STAT1*$^{-/-}$ fibroblasts and HeLa cells were transiently transduced with vector control or IRF7. While only bat IRF7 conferred antiviral protection in *STAT1*$^{-/-}$ fibroblasts, both human and bat IRF7 potently inhibit YFV infection in HeLa (Figure 10A). I observed similar antiviral activity during VEEV and SINV infection (Figure 10B,C).

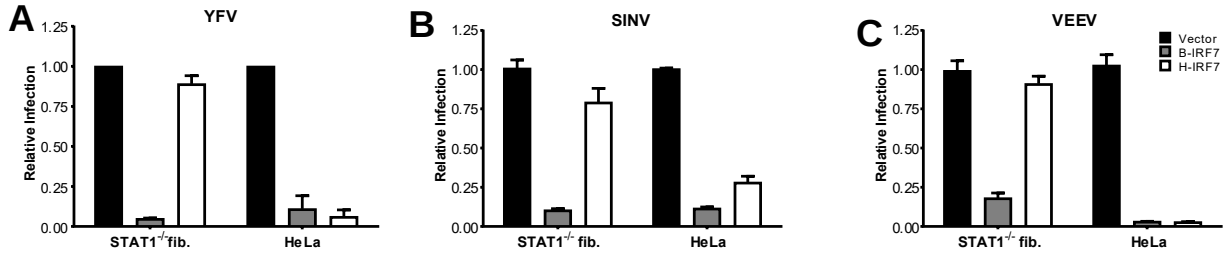

Figure 10: IRF7 Antiviral Activity in STAT1$^{-/-}$ fibroblasts vs HeLa
*STAT1-/- fibroblasts were transduced to express IRF7 or control, then infected with **(A)** YFV, **(B)** SINV or **(C)** VEEV at an MOI of 1. Infection was quantified using flow cytometry and normalized to % infected control cells.*

Western blot analysis of cell lysates indicated that STAT1 was undetectable in *STAT1*$^{-/-}$ fibroblasts but present and inducible by IRF7 in HeLa cells, indicating intact interferon signaling (Figure 11A). In addition, I saw upregulation of the ISG Interferon Induced Protein with Tetratricopeptide Repeats 1 (IFIT1) upon IRF7 overexpression in HeLa cells. Surprisingly,

despite lack of intact IFN signaling in the *STAT1*$^{-/-}$ fibroblasts, bat IRF7 expression resulted in expression of IFIT1.

When I pretreated HeLa cells with recombinant B19R, a soluble decoy IFN receptor that neutralizes the effects of secreted type I IFNs, I saw a dose-dependent loss of human IRF7 and IFN-mediated antiviral activity, while bat IRF7-mediated antiviral activity was maintained (Figure 11B). HeLa cells treated with IFN or expressing IRF7 had significant increases in *IFIT1* mRNA expression as quantified by RT-qPCR (Figure 11C). When treated with B19R, *IFIT1* expression was blunted in cells exposed to IFN or human IRF7, but cells expressing bat IRF7 continued to express *IFIT1* transcripts. These data together indicate that bat IRF7, unlike human IRF7, is capable of inducing a broad and potent antiviral state in a cell lacking the ability to respond to the effects of secreted type I IFNs.

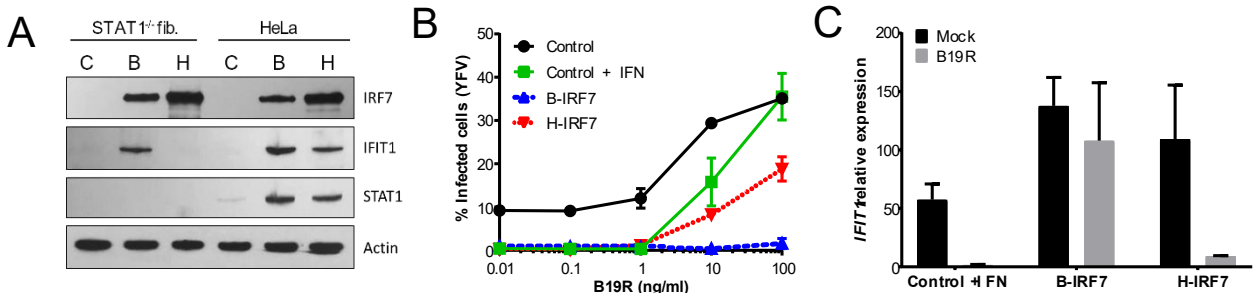

Figure 11: Effect of IFN Inhibition on IRF7 Activity

(A) *Expression levels of ISGs in cells transiently transduced with lentivirus expressing IRF7 or vector control.* ***(B)*** *HeLa cells were transiently transduced with lentivirus expressing IRF7 or vector control. Cells were pre-treated with increasing doses of B19R +/- IFNα for 24h and then infected with YFV in the presence of B19R. Cells were harvested 24h after infection and percent infection was quantified using flow cytometry. Data are represented as mean ± SD for two independent experiments.* ***(C)*** *HeLa cells were transiently transduced to expression vector control or IRF7 for 48h. Cells were then treated with 10ng/mL of B19R +/- 100U/mL IFNα and RNA was isolated at 24h. Levels of IFIT1 were quantified using RT-qPCR and normalized to vector control cells with no IFN or B19R exposure. Data are represented as mean ± SD for two independent experiments.*

Bat IRF7 Induces Increased Tonic ISG Expression

Because bat IRF7 could inhibit a range of RNA viruses, and the fact that it is a transcription factor, I was interested in determining if cells overexpressing bat IRF7 had a unique transcriptional signature. To this end, I collected RNA from *STAT1*$^{-/-}$ fibroblasts stably expressing vector control or IRF7 and performed microarray analysis. Despite lack of immune stimulation, cells expressing bat IRF7 expressed significantly increased levels of over 50 genes, most of which are classified as ISGs (Figure 12A) (Rusinova, Forster et al. 2013). Genes included members of the IFIT, IFITM, MX, OAS, and PARP families, among others. Both bat and human IRF7 expression resulted in downregulation of the genes RETNLB, CACNA1C, and PYY2 (Figure 12B). Interestingly, the expression levels of individual type I, II and III IFNs and their receptors were not significantly different between cells expression vector control or either IRF7 orthologs (Figure 12C). Increased ISG expression levels of *OAS2*, *IFI44L*, *RSAD2*/viperin and *IFI6* in

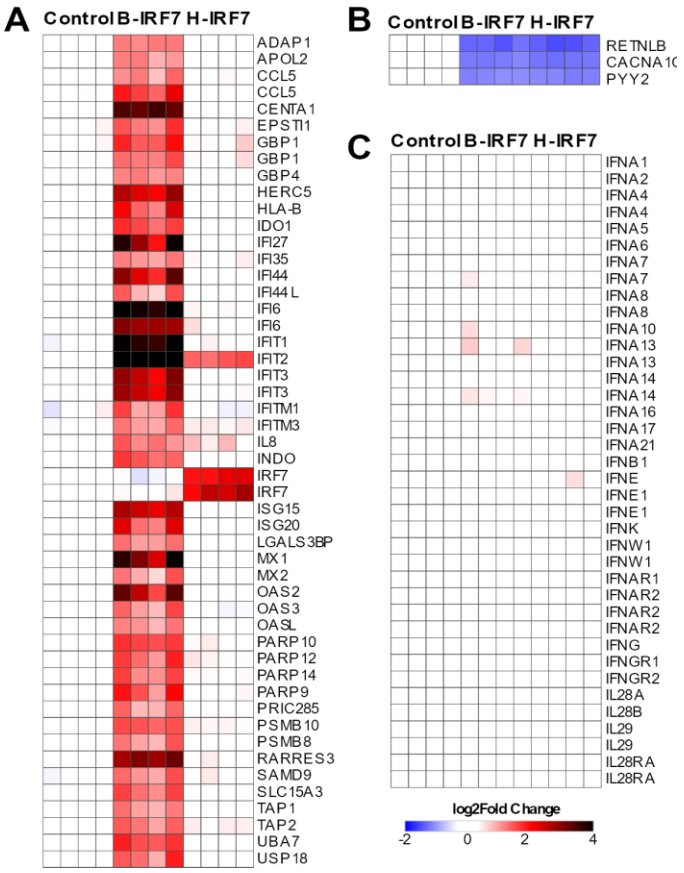

Figure 12: Transcriptional Changes Due to IRF7 Expression
RNA was isolated from unstimulated STAT1$^{-/-}$ *fibroblasts stably expressing vector control or IRF7 and microarray analysis was run on the Illumina Human-HT-12 V4 chip. Each column represents one of four independent experiments per cell line.*

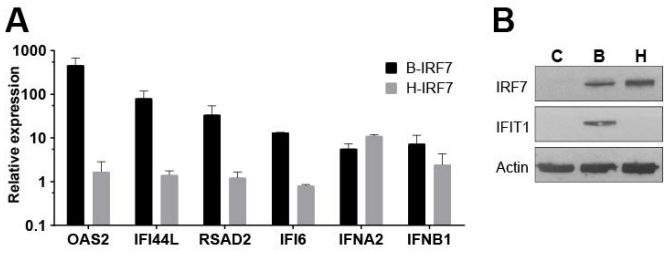

Figure 13: Verification of Microarray
(A) RNA from unstimulated STAT1-/- fibroblasts expressing vector control or IRF7 was isolated and used for RT-qPCR. Relative expression was normalized to vector control cells using RPS11 as a reference gene. For IFI6, n=2. All others, n=6. ***(B)*** *Expression levels of IRF7 and the ISG IFIT1 in lysates from STAT1$^{-/-}$ fibroblasts described above.*

STAT1$^{-/-}$ fibroblasts were confirmed using RT-qPCR (Figure 13A). Two IFN genes, IFNA2 and IFNB1, were modestly (~5-10-fold) induced in both bat and human IRF7-expressing cells to similar levels. As was observed with transiently-transduced cells, cells stably expressing bat IRF7 had increased IFIT1 protein levels compared to cells expressing vector control or human IRF7 (Figure 13B).

IRF7 Loss in Bat Cells Results in Less ISG Induction And Increased Viral Production

To determine if IRF7 was important during the initial immune response in bat-derived cells, I used CRISPR-Cas9 to genetically knock out the *IRF7* gene from PaKi cells. Two single cell clones were isolated in which IRF7 was not detectable by Western blot in either untreated or IFN-treated cells to induce IRF7 (Figure 14A). STAT1 induction was observed in both WT and IRF7 KO cell lines, indicating IFN treatment was successful.

Mutations at the IRF7 locus were detected in both single cell clones (Figure 14B). KO clone 1 (KO1) has a 22 base pair (bp) deletion (Δ116-137) and KO2 has a two bp deletion (Δ125-126). Both changes result in frameshift mutations that lead to a severely truncated protein product.

When WT or KO cell lines were treated with IFN, KO cells exhibited decreased induction of the ISGs *OAS1* and *USP18* at 8h compared to WT, suggesting that IRF7 in bat cell may be promoting ISG expression independently of IFN signaling as is observed in the human cell background (Figure 14C, D).

In addition, I measured the effect of IRF7 loss on virus production. WT and IRF7 KO cells were infected with YFV 17-D at an MOI of 10 and supernatants were harvested at 24h for plaque assay. Compared to WT cells, IRF7 KO cells produce 10-100 times more infectious virus by 24h (Figure 14E). These data suggest that, as expected, IRF7 in PaKi cells plays an antiviral role. In addition, the data support a direct role for IRF7 during ISG induction because IFN treatment in IRF7 KO cell lines only induces ISGs to about 10% of the level in WT Paki.

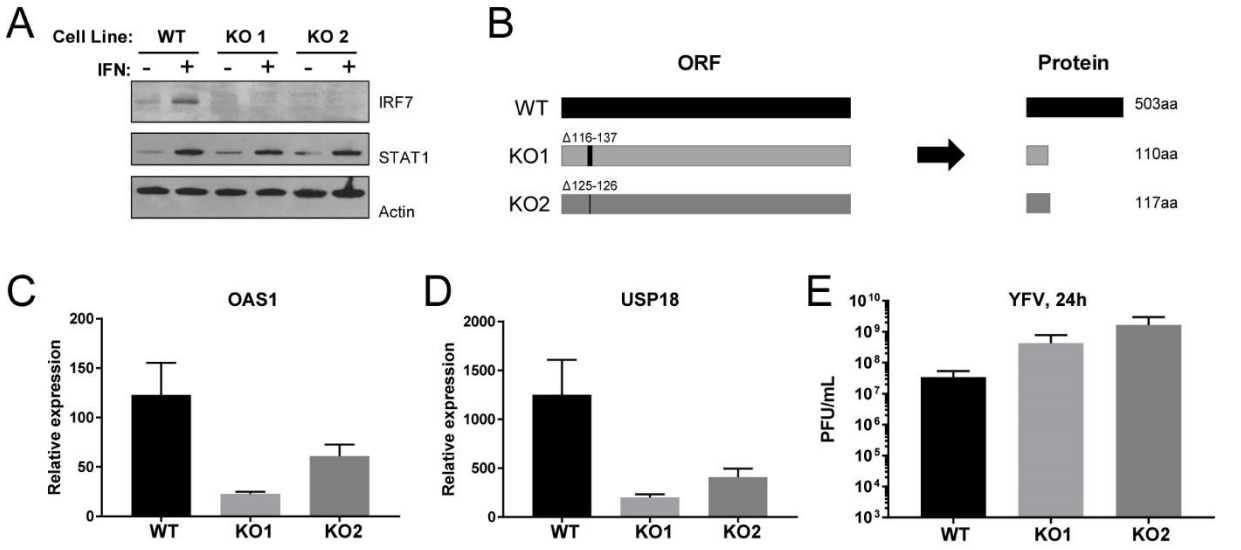

Figure 14: IRF7 KO in Bat Cells

(A) *Lysates from PaKi WT or IRF7 KO single cell clones were assayed by Western blot for IRF7 expression in the absence and presence of 100U/mL universal IFNα for 24h. STAT1 was included as a positive control for IFN treatment. Actin serves as a loading control.* ***(B)*** *Sequencing of genomic DNA from WT or IRF7 KO single cell clones confirmed genetic deletions as indicated. Hypothetical protein products are shown on the right.* ***(C)*** *PaKi WT or IRF7 KO cells were treated with 100U/mL universal IFNα for 8h, and RNA was harvested for RT-qPCR of the ISG OAS1. Expression levels are normalized to untreated time-matched controls. Data is represented as mean ± SD for three independent experiments.* ***(D)*** *Same as (C), for the ISG USP18.* ***(E)*** *WT or IRF7 KO PaKi cells were infected with YFV-17D at an MOI of 10. Unbound virus was removed after 1h and replaced with fresh medium. At 24h, supernatants were taken for plaque assay in BHK cells. Data is represented as mean ± SD for three independent experiments.*

Bat IRF7 is Constitutively Active in Unstimulated Cells

Next, I investigated the cellular properties of bat IRF7 as compared to human IRF7. Inactive human resides in the cytoplasm, but translocates to the nucleus upon activation. I investigated the localization of IRF7 in *STAT1*$^{-/-}$ fibroblasts using cellular fractionation. A fraction of both IRF7 orthologs could be found in the nucleus even in uninfected cells, although the proportion of nuclear bat IRF7 was higher than that of human IRF7 (Figure 15A). To determine the localization of endogenous bat IRF7, I used CRISPR to endogenously tag IRF7 in PaKi cells with a C-terminal 3xFLAG tag (Appendix D). In these cells, IRF7 is detectable even when the cells have not been pretreated with IFN, and some IRF7 is found in the nucleus (Figure 15B). These data indicate that bat IRF7 partially localizes to the nucleus even in uninfected cells, suggesting possible differences between IRF7 activation in bats versus humans.

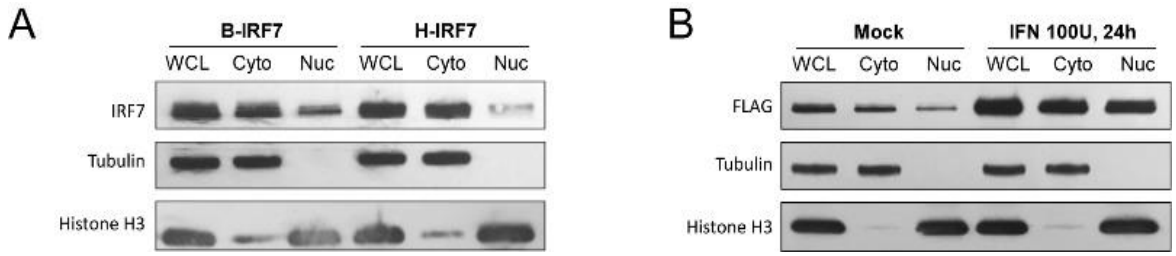

Figure 15: Localization of IRF7
Cells were subjected to cellular fractionation. Tubulin is used as a cytoplasmic control, Histone H3 is used as a nuclear control. ***(A)*** *Lysates are from STAT1*$^{-/-}$ *fibroblasts stably expressing IRF7.* ***(B)*** *Lysates are from PaKi cells with a genomic C-terminal tag on IRF7 with mock or IFN treatment.*

Upon activation, IRF7 forms a dimer that can be detected by native PAGE. To test if bat IRF7 has increased activation at baseline, I assessed dimerization in lysates from *STAT1*$^{-/-}$ fibroblasts stably expressing IRF7 using native protein electrophoresis (Figure 17). Two bands were observed for bat IRF7, while only a single band can be observed for human IRF7, suggesting bat IRF7 may constitutively exist, at least partially, as a dimer.

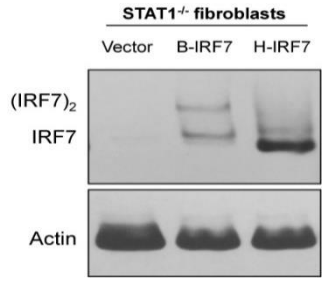

Figure 17: IRF7 Dimerization Assay
Lysates from STAT1$^{-/-}$ fibroblasts stably expressing vector control or IRF7 were resolved by native PAGE.

ISGs are canonically induced by binding of the transcription factor complex ISGF3 (composed of STAT1, STAT2, and IRF9) to ISRE sequences located in the promoters of ISGs. Activated IRF3 has been reported to bind these sequences directly to induce ISGs in an interferon-independent manner (Nakaya, Sato et al. 2001). Murine and human IRF7, if activated by IKKε, have also been shown to directly promote expression of certain ISGs (Schmid, Mordstein et al. 2010). This led me to question whether bat IRF7 was using ISREs to induce ISG expression. I transfected a plasmid encoding a luciferase gene driven by the ISG54 ISRE (encoding IFIT2) in *STAT1$^{-/-}$* fibroblasts stably expressing vector control or IRF7 (Figure 16). Cells expressing bat IRF7 had a significantly higher luminescence signal compared to cells expressing human IRF7 or vector control, indicating that it was likely that bat IRF7 may mediate ISRE-dependent ISG induction. A similar experiment was performed in HEK293 cells, which can produce IFN that can signal to induce ISGs. I transfected cells to express GFP as a control or IRF7, then transfected 48h later with the ISG54 ISRE-luciferase reporter. Although both IRF7 orthologs increased luciferase signal above background, signal was greater in cells expressing bat IRF7, indicating that bat IRF7, through direct or indirect means, causes a stronger ISRE-mediated ISG induction than human IRF7.

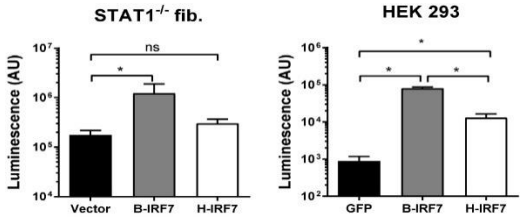

Figure 16: IRF7 Effect on ISRE-Luciferase Reporter
*STAT1-/- fibroblasts (left) or HEK293 expressing IRF7 were transfected with a plasmid that expresses luciferase under control of the hamster ISG54 ISRE and the luciferase signal was measured after 24h. Data represent mean ±SD for three independent experiments. * = p value <0.05 as determined by Dunnett's multiple comparison's test.*

Bat IRF7 Directly Binds ISG Promoters

Next, I investigated whether bat IRF7 was directly binding ISREs to induce ISG expression. I used 5'-biotinylated primers to amplify regions of the human genome containing ISREs from IFIT2 or MX1, two of the genes expressed to higher levels in *STAT1*$^{-/-}$ fibroblasts expressing bat IRF7 over human IRF7 (Figure 12). These DNA probes were incubated with lysates from cells stably expressing vector control or IRF7, and complexes were pulled down using streptavidin beads. Samples were eluted from the beads and Western blot was used to detect IRF7 and actin as a nonspecific control.

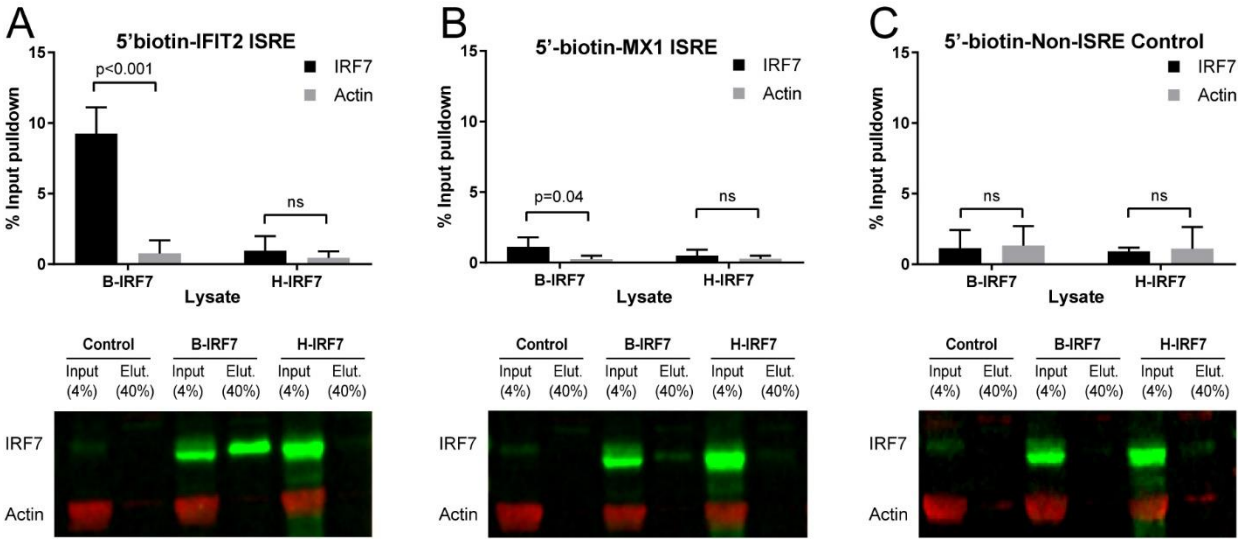

Figure 18: Direct Binding of Bat IRF7 to IFIT2 and MX1 ISREs
*Lysates from STAT1$^{-/-}$ fibroblasts stably expressing IRF7 were incubated with 5'-biotin-labeled DNA probes overnight. The DNA-protein complexes were pulled down using streptavidin beads and the elution was probed for IRF7 and actin as a negative control. Quantification of percent input that was eluted was calculated for both IRF7 and actin for probes **(A)** IFIT2, **(B)** MX1and **(C)** a sequence with no known promoter elements. Data is presented as mean ±SD for three independent experiments. Representative gels are shown under the corresponding graph.*

Using the IFIT2 ISRE probe, approximately 8% of input bat IRF7 was pulled down, indicating direct binding of IRF7 to the IFIT2 promoter (Figure 18A). In contrast, the percent of human IRF7 pulled down was not significantly increased over the percent of actin pulled down.

Using the MX1 probe, approximate 1% of input bat IRF7 was pulled down (Figure 18B). Although less bat IRF7 bound the MX1 promoter, the binding was still significant over nonspecific actin binding. Again, human IRF7 was not pulled down using the MX1 promoter. Neither IRF7 orthologs bound significantly to a non-ISRE negative control (Figure 18C). These results indicate that bat IRF7, even in uninfected, unstimulated *STAT1*$^{-/-}$ fibroblasts, is capable of directly binding ISG ISREs and causing STAT1-independent induction of antiviral ISGs.

Previous studies have shown that activated human IRF7 can induce a STAT1-independent transcriptional signature (Schmid, Mordstein et al. 2010). However, unlike bat IRF7, this transcriptional activity is dependent on IKKε co-expression. A comparison of induced genes from my microarray and the microarray done in (Schmid, Mordstein et al. 2010) can be found on Table 4 .

Table 4: Comparison of Genes Induced in Human Fibroblasts Expressing Bat IRF7 or Human IRF7 Co-Expressed with IKKε

Bat-IRF7			***Both***	**Hum-IRF7 + IKKε**	
ADAP1	IFI6	PARP10	*HERC5*	BCL2A1	IFNA17
APOL2	IFITM1	PARP12	*IFI27*	CCL3	IFNA21
CCL5	IFITM3	PARP14	*IFIT1*	CXCL10	IFNA21
CENTA1	ISG15	PRIC285	*IFIT2*	CXCL11	IFNA4
EPSTI1	ISG20	PSMB10	*IFIT3*	CXCL3	IFNA7
GBP1	LGALS3BP	PSMB8	*IL8*	IFNA1	IFNB1
GBP4	MX1	RARRES3	*INDO*	IFNA10	IL6
HLA-B	MX2	SLC15A3	*RSAD2*	IFNA14	OAS1
IDO1	OAS2	TAP1	*SAMD9*	IFNA16	
IFI35	OAS3	TAP2	*USP18*		
IFI44	OASL	UBA7			
IFI44L	PARP9				

Although there is some overlap of the induced genes, such as IFIT1/2/3 and USP18, overall overlap is poor. Of note, activated human IRF7 induces several IFNα subtypes, as would be expected due to its canonical function, yet these transcriptional changes are not detected by microarray in cells expressing bat IRF7. Additionally, in contrast to bat IRF7, activated human IRF7 does not bind the ISRE nor induce the expression of MX1, an ISG which is believed to be exclusively ISGF3-dependent (Holzinger, Jorns et al. 2007, Schmid, Mordstein et al. 2010). Thus, bat IRF7 seems to contain features that increase affinity for ISG promoters despite lack of immune stimulation.

Bat IRF7 Activity is Not Dependent on Known Activators or Binding Partners of IRF7

To identify genes that may regulate the activation and/or antiviral activity of bat IRF7, I created bulk populations of *STAT1*$^{-/-}$ fibroblasts with genetic deletions of molecules critical for viral sensing and IRF activation. I then measured the antiviral activity of bat and human IRF7 against YFV in each cellular background (Appendix E). Loss of targeted genes and expression of IRF7-3xFL were confirmed via Western blot. I did not notice loss of antiviral activity with the loss of IRF3, indicating IRF3 was most likely not a binding partner or otherwise important to bat IRF7 activity. Loss of IRAK1, a kinase known to phosphorylate human IRF7 in the context of TRIF-mediated signaling (Uematsu, Sato et al. 2005), was also dispensable to antiviral activity. Loss of TBK1 mildly decreased bat IRF7 antiviral activity, suggesting phosphorylation by TBK1 either plays a minor role in activating bat IRF7, or has redundant activity with another kinase, most likely IKKε. The adaptor proteins MAVS and STING, responsible for signaling upon

detection of viral RNA and DNA, respectively, also did not to contribute to the activity of bat IRF7. Together, these data suggest bat IRF7 does not depend on viral sensing for antiviral activity. Together with the data demonstrating an ISG signature and dimerization in uninfected cells, these findings suggest bat IRF7 has constitutive activity in human *STAT1*$^{-/-}$ fibroblasts.

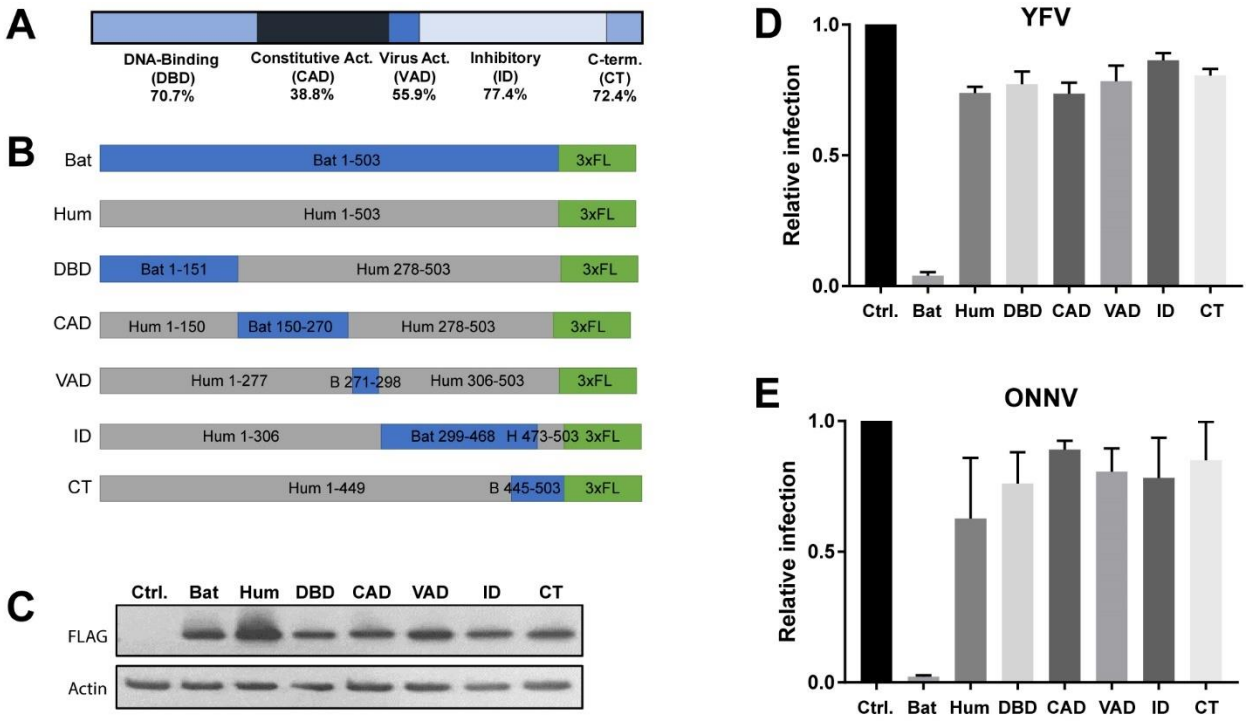

Figure 19: Bat-Human IRF7 Chimeras

(A) *Mapped domains in the human IRF7 protein (Lin, Mamane et al. 2000). Percent identity between bat and human IRF7 orthologs is shown in parenthesis.* ***(B)*** *Assembly of chimeras, with amino acids from each species indicated in each region.* ***(C)*** *Expression levels of each construct. Actin was used as a loading control.* ***(D)*** *STAT1*$^{-/-}$ *fibroblasts were transiently transduced to expressed IRF7 for 48h, then infected with YFV at an MOI of 1 for 24h. Infection was quantified using flow cytometry and normalized to control cells. Data is shown as mean ± SD for three independent experiments.* ***(E)*** *Same as (D), with ONNV infection. Data is shown as mean ± SD for two independent experiments.*

Single Bat IRF7 Domains Cannot Impart IFN-Independent Antiviral Activity to Human IRF7

IRF7 is a modular protein whose regulatory domains have been mapped (Lin, Mamane et al. 2000). The possibility that bat IRF7 could be constitutively active prompted me to investigate whether a single region of bat IRF7 could confer STAT1-independent antiviral activity to human IRF7. To this end, I synthesized chimeras where the DNA-binding domain (DBD), constitutive activation domain (CAD), virus activated domain (VAD), autoinhibitory domain (ID) and C-terminal region (CT) containing both the nuclear localization sequence (NLS) and serine-rich signal response domain (SRD) of human IRF7 was replaced with the bat region (Figure 19A,B). All chimeras were expressed similarly, although human IRF7 expressed better than all other constructs (Figure 19C). I then infected cells with YFV or ONNV to determine if any chimeras could inhibit infection (Figure 19D,E). No single domain conferred STAT1-independent antiviral activity to human IRF7.

Bat IRF7 Contains Two Important Unique Serine Residues in its Regulatory Region

Human and murine IRF7 require phosphorylation for transcriptional activity. The C-terminal regions of IRF7 contains several serines that can serve as potential kinase substrates. Studies examining the role of IRF7 phosphorylation on its transcriptional activity have demonstrated that Ser477 and Ser479 of human IRF7 are necessary for the induction of type I IFN genes upon viral infection. Furthermore, substitution of these residues with the phosphomimetic residue, aspartic acid, increases transcription of IFN genes by inducing nuclear

translocation and direct binding of IRF7 to the IFNβ promoter, both in the context of infected and uninfected cells (Lin, Mamane et al. 2000).

Alignment of bat and human amino acid sequences at the SRD revealed high homology between bat and human IRF7, with conservation of all human serines present in the bat ortholog (Figure 20A). In addition to conserved residues, there are two additional serines that could serve as potential phosphorylation targets in bat IRF7 at positions corresponding to human Leu480 and Ala485. Ser480 is unique to megabat, as all other mammals contain a leucine at this position (Appendix F). The Ala485 is frequently a serine or threonine in other mammals, indicating that a serine in this site is not unique to megabats.

To determine if bat IRF7 required phosphorylation for STAT1-independent antiviral activity, I mutated both the conserved Ser477 and Ser479 to alanines. In addition, the unique Ser480 and Ser485 were mutated to leucine and alanine, respectively, to match the human sequence. I observed loss of antiviral activity with both pairs of modifications, suggesting that phosphorylation of these residues contributed to the activity of bat IRF7 (Figure 20B). Curiously, there was only a partial loss of antiviral activity with single point mutations, suggesting that phosphorylation of neighboring residues may play redundant roles in bat IRF7 activation. When human IRF7 mas mutated to contain both unique bat serines, I observed a mild increase in antiviral activity. However, when L480 and A485 were replaced with phosphomimetic aspartic acids, I observed a full rescue of the antiviral activity observed with bat IRF7.

Expression levels of IFIT1 were assayed as an additional measure of STAT1-independent ISG induction (Figure 20C). As observed previously, bat IRF7 expression results in detectable

IFIT1 protein, while human IRF7 cannot induce IFIT1 in a *STAT1*$^{-/-}$ background. The IFIT1 expression levels observed correlate with the infection data. For example, single mutations to any of the bat IRF7 phosphorylation targets leads to decreased IFIT1 expression. Double mutations to these sites results in further decrease of IFIT1 expression which correlates with

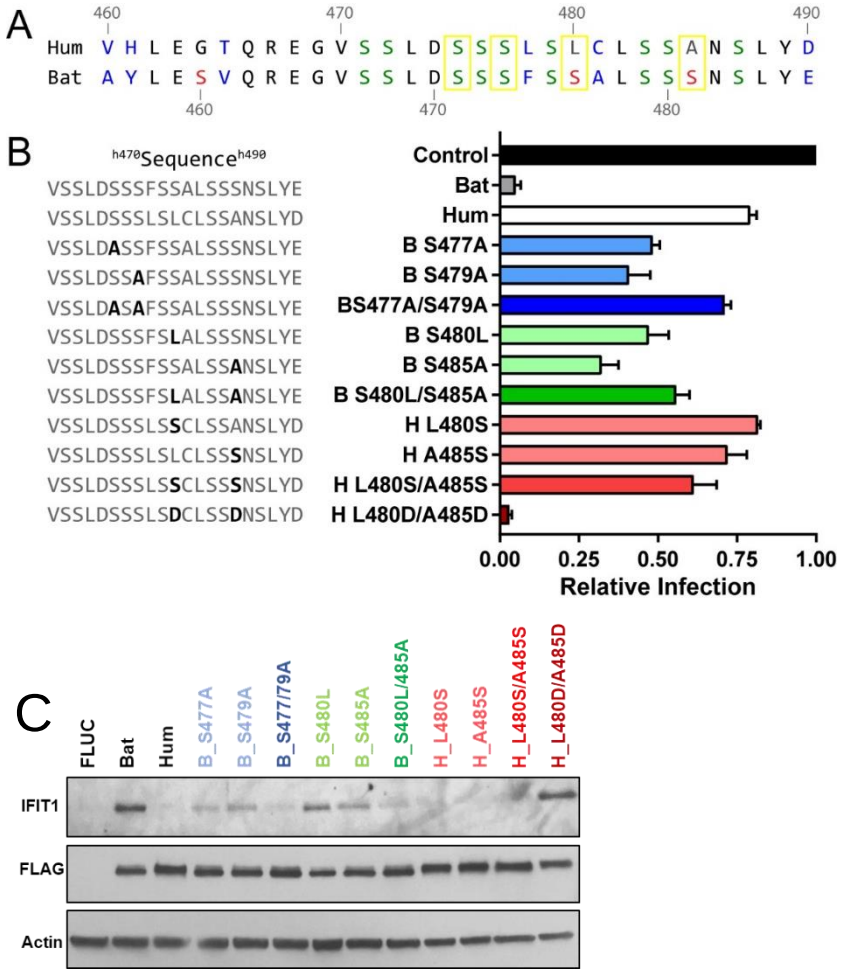

Figure 20: Bat IRF7 contains additional phosphorylation targets at the C-terminus
(A) *Amino acid sequences of the signal response domain of IRF7. Conserved serines are indicated in green. Unique bat serines are indicated in red. Sites that were modified are highlighted in yellow.* ***(B)*** *STAT1*$^{-/-}$ *fibroblasts expressing IRF7 constructs were infected with YFV at an MOI of 1. Cells were harvested for flow cytometry at 24h and infection was normalized to control cells. Data represent mean ± SD for three independent experiments. Modifications to the WT IRF7 protein sequence are indicated in bold on the left.* ***(C)*** *Western blot to assay IFIT1 protein levels and confirm expression of IRF7. Actin serves as a loading control.*

increased infection. Importantly, addition of the phosphomimetic residues Asp480 and Asp485 to human IRF7 leads to robust IFIT1 expression as seen with bat IRF7.

Together, these data suggest bat IRF7 undergoes activation in human *STAT1*$^{-/-}$ fibroblasts which involves both conserved and unique serine residues. Furthermore, modifying human IRF7 to contain phosphomimetic residues at the 480 and 485 sites is sufficient to impart potent STAT1-independent antiviral activity and ISG induction.

DISCUSSION

In this study, I compared the antiviral activity of human and bat ISG orthologs. I identified bat IRF7 as an effector that is capable of potently inhibiting viruses from several viral families. In contrast to human IRF7, which has minor antiviral activity upon loss of IFN signaling, bat IRF7 induces a potent antiviral program in human cells. In addition, unstimulated cells overexpressing bat IRF7, but not human IRF7, have increased levels of certain ISGs which serve to "prime" cells against viral infection. These results suggest a bat IRF7-driven induction of ISGs that serves some functional redundancy but is independent of canonical type I IFN signaling (Figure 21).

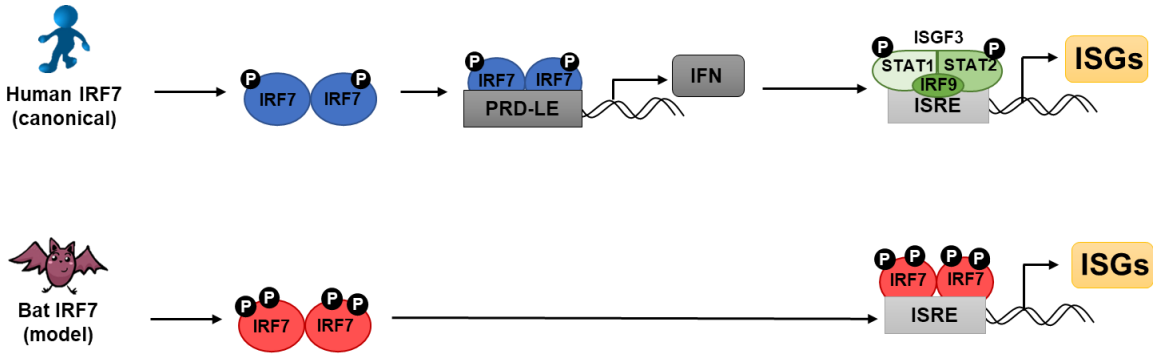

Figure 21: Model of Bat Versus Human IRF7 Function
Human IRF7 mainly functions as a transcriptional activator of type I IFNs. JAK-STAT signaling leads to ISGF3 binding to ISREs and induction of ISGs. Bat IRF7 can bypass canonical signaling and bind ISREs directly, thereby maintaining an antiviral state if type I IFN signaling is not active.

Because bat IRF7 can inhibit viruses belonging to several families and is a transcription factor, it is unlikely that it acts through a virus-specific mechanism. I reasoned it may be inducing a group of ISGs that could cumulatively widen the viral target range. Microarray

analysis revealed that bat IRF7 induces an ISG signature that includes genes that were previously thought to be ISGF3-dependent (Figure 12) (Schmid, Mordstein et al. 2010).

Is it likely that bat IRF7 has a lower threshold for activation, leading to some transcriptional activity in unstimulated cells. Human IRF7 activated by virus or IKKε co-expression does have *in vitro* DNA-binding capability. For example, IRF7 expressed in cells infected with Newcastle Disease Virus (NDV) will bind the ISG15 ISRE (Marie, Smith et al. 2000). However, bat IRF7 induces ISGs that even activated human IRF7 does not induce, indicating bat IRF7 is targeting a unique ISG set. While it is possible that the microarray chip used in (Schmid, Mordstein et al. 2010) study did not contain probes for as many genes as the current study, the stark contrast between induction of interferons and their receptors supports the idea that human and bat IRF7 produce distinct transcriptional signatures.

Perhaps the presence of additional unique residues in bat IRF7 which increase the phosphorylation capacity of the protein can in part explain its baseline activation. However, presence alone is not sufficient, because the additional serines in human are not sufficient to rescue activity. There must be another component of the bat protein structure that allows the kinase, if a kinase is required, to access and modify these residues. One possibility is that human IRF7 is sequestered into an inactive state that masks target residues, analogous to the NFκB RelA-p50 heterodimer by IκB proteins (Kawai and Akira 2007). Bat IRF7, on the other hand, may not interact with these proposed inhibitors in a human background, leading to constitutive activation. However, the fact that bat endogenous bat IRF7 is nuclear in PaKi cell lines supports the idea that bat IRF7 does indeed have constitutive activity in the bat host.

Structural studies and functional done on IRF3 suggest that phosphorylation of specific residues at the C-terminus induce a conformational change in which the inhibitory domain unmasks the transactivation domain, leading to dimerization and activation (Lin, Mamane et al. 1999, Qin, Liu et al. 2003). It is believed that this mechanism of activation holds true for other IRFs such as IRF7. While differences in DNA affinity between IRF3 and IRF7 seem to be due to differences in their N-terminal DNA-binding domains (De Ioannes, Escalante et al. 2011), differences between bat and human IRF7 may be most likely attributed to differences in their thresholds for activation.

Although the current evidence is not sufficient to definitively state why bat IRF7 exists in a constitutively active state, several possibilities can be entertained. The first is that bat IRF7 has an increased potential for phosphorylation due to unique additional serines. These phosphorylated residues may lead to an increased negative charge that may maintain bat IRF7 in a constitutively active state. The relatively high number of phosphorylation targets may serve a redundant role, as ablation of single targets is not sufficient to eliminate antiviral activity. It remains unclear which kinase, if any, is phosphorylating bat IRF7 in a human cell background, as TBK1 and IRAK1 are both dispensable for bat IRF7 activity. Furthermore, ISG induction is seen in cells whose innate immune sensing pathways have not been activated (Figure 13), implying that no canonical IRF7-interacting kinases would be functional. In this case, the possibility of IRF7 phosphorylation by non-canonical cellular kinases cannot be excluded.

Another possibility is that bat IRF7 folds into a conformation that is more permissive interactions with kinases. The CAD, a region that is important for protein-protein interactions, is

poorly conserved compared to the rest of the protein (Figure 19A), which may result in differences in tertiary structure between the two orthologs. Structural differences could make the C-terminus of bat IRF7 more accessible to non-canonical kinases, leading to nonspecific activation.

A third possibility is that bat IRF7 does not require phosphorylation for direct ISRE binding. The protein may be locked into a conformation that permits limited DNA binding, which could explain why ISGs, but not IFNs, are induced with stable bat IRF7 expression. Although this possibility is unlikely, I have not directly disproven it.

Further studies to determine whether bat IRF7 has constitutive activity in cells of its own species are warranted. Currently, two pieces of evidence support that bat IRF7 contributes to ISG induction independently of IFN signaling in bat cells. First, endogenous bat IRF7 is partially nuclear in PaKi cells, indicating some IRF7 is in the correct location to bind ISREs (Figure 15). Second, ISG induction in response to IFN in IRF7 KO Paki cells is diminished compared to WT PaKi cells, even at early time points, suggesting that IRF7 plays a role in ISG induction before it has a chance to induce the "second wave" of IFN signaling.

In an evolutionary race to overcome the effects of the innate immune system, many viruses have developed strategies to shut down the interferon response by interfering with IFN binding to its receptor (Colamonici, Domanski et al. 1995, Yokota, Saito et al. 2003, Jia, Rahbar et al. 2010) and/or inhibiting JAK-STAT signaling (Bode, Ludwig et al. 2003, Jones, Davidson et al. 2005, Senft, Taylor et al. 2010), among other strategies. The constitutive activity of bat IRF7 may confer some baseline protection against viral infection and may provide ongoing

protection against viruses that are known to shut down the IFN response by inhibiting members of the JAK-STAT signaling pathway. This feature of bat IRF7 marks a distinct variation between bat and human IRF7 functions, and is likely one of many characteristics of the bat immune response that is responsible for maintaining viral pathogens under control.

CHAPTER FOUR
Conclusions and Recommendations

OVERVIEW

Through my studies, I have identified two signaling pathways that differ between the bat and human host: induction of RNASEL, and the activation IRF7. Induction of RNASEL concurrently with its signaling partners has implications during the early phases of infection. Specifically, the initial antiviral response is more potent earlier during infection, which may help control infection more effectively. IRF7 is a major regulator of the antiviral response. IRF7 with some constitutive STAT1-independent activity, as I observed for bat IRF7, may provide an additional layer of protection against viral infection that could prevent uncontrolled viral replication in the host, particularly in the case of viruses that interfere with JAK-STAT signaling. These two pathways provide some insight into the host-pathogen interacts that occur in a viral reservoir and will be helpful for further studies investigating antiviral mechanism in new species.

DIFFERENCES BETWEEN BAT AND HUMAN RESPONSES TO IFNα

Overview

In this first project, my goal was to identify unique ISGs in the black flying fox. To do this, I treated black flying fox-derived cells with IFN and used RNA-Seq to examine their transcriptional signature over time. I learned that most ISGs in the black flying fox are strictly transcriptionally regulated, and that the ISG response peaks approximately 8h after IFN exposure. Most of the genes induced were known canonical ISGs, but there were a handful of novel ISGs, including the gene RNASEL. I showed that RNASEL is an important component of the antiviral response in bat cells and hypothesize it may be most important during early phases of infection (Figure 22).

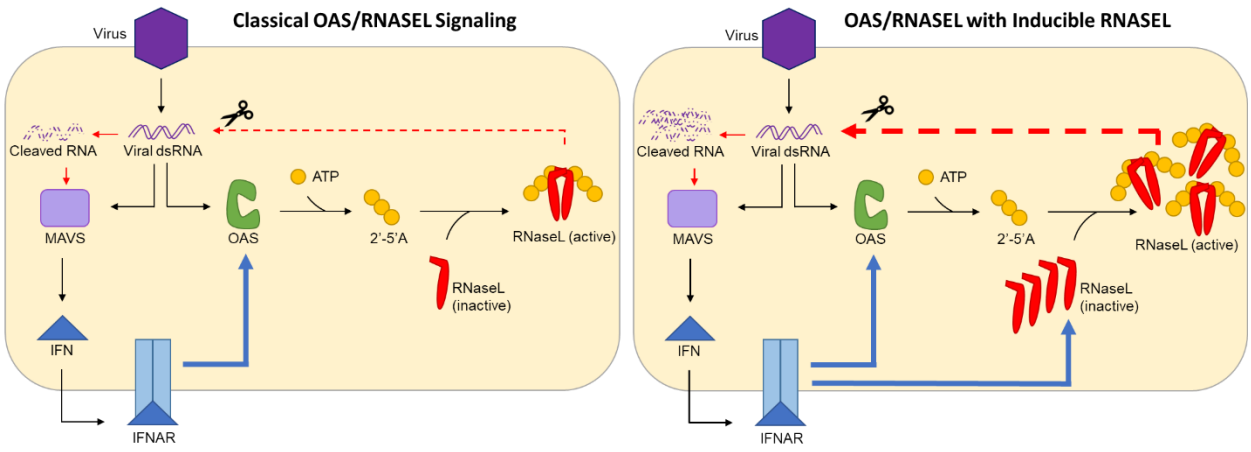

Figure 22: OAS/RNASEL Pathway with RNASEL Induction
The classical OAS/RNASEL pathway is shown on the left. Viral sensing leads to induction of OAS enzymes and activation of RNASEL. RNASEL cleavage products may further activate the IFN response through cytoplasmic RNA sensing pathways. On the right, RNASEL is induced by IFN, leading to increased viral RNA cleavage. Early in infection, increased viral RNA cleavage may significantly inhibit the viral life cycle by eradicating the viral genome or replication intermediates. Additionally, higher RNASEL levels may enhance IFN signaling through accumulation of RNA cleavage products that are sensed by the cell.

The ISG Signature

My characterization of the IFN response in the black flying fox began with defining the transcriptional signature that resulted from IFN treatment. This allowed me to draw several conclusions regarding the IFN response. The first is that most upregulated genes in the black flying fox belong to a core set of ISGs that are also induced in other mammals (Shaw, Hughes et al. 2017). It appears there may not be global differences regarding which specific genes are induced, implying regulatory regions that control ISG induction, such as ISREs and other *cis* regulatory regions have been evolutionarily conserved. In a system that uses a few upstream signaling molecules to induce hundreds of downstream effectors, there is pressure to maintain binding of transcription factors to regulatory regions, leading to the selection of strict consensus sequences. In this case, it may be more efficient for the host to instead modify individual effector functions through natural selection. Maintaining a large repertoire of antiviral effector "templates" that can be modified depending on species-specific pathogen history may be more beneficial to the host than simply turning "off" genes that are not necessary for certain infections.

There were only a few genes upregulated in Paki cells that are not considered canonical ISGs. One is RNASEL, which was characterized and will be described in more detail later in this discussion. The genes from SC1 and SC2, genes that were induced later in the time course, were also not induced in A549 or HEK293. The fact that genes in these SCs were induced later than canonical ISGs suggests they may be products secondary signaling, perhaps from inflammation due to IFN signaling, and they may not represent true IFN-regulated genes.

One of these genes is otogelin-like protein (OTOGL), a protein that is necessary for inner ear development (Yariz, Duman et al. 2012). It is not clear why this gene would be IFN inducible. OTOGL is highly expressed in embryonic tissues, but expression decreases throughout development (Yariz, Duman et al. 2012). Due to the kidney and ear originating from similar embryonic tissues (Torban and Goodyer 2009), OTOGL induction in bat kidney cells may simply be an embryonic remnant.

Another SC1 gene that was induced is *TP53INP*, which plays a role during stress response and may regulate autophagy (Okamura, Arakawa et al. 2001, Sancho, Duran et al. 2012, Seillier, Peuget et al. 2012). *CLEC7A*/Dectin-1 from SC2 can interact with T cells and promote fungicidal activity of neutrophils (Willment, Gordon et al. 2001, Kennedy, Willment et al. 2007). C1QTNF3 and TMEM52B are less well characterized, but based on homology to known family members, may also play roles during inflammatory processes.

Timing of ISG Induction

The second major observation I made from the transcriptional studies in PaKi cells was that the IFN -induced transcriptional signature is tightly regulated. When bat PaKi cells were treated with IFN, transcriptional changes were undetectable for most genes until 4h (Figure 5). This contrasts with human A549 cells, which induced most ISGs by 2h. In addition, although the mRNA response in both cell lines peaked at approximately 8h, there was a greater length of time in which the human genes were upregulated. While most bat ISGs were upregulated for about 8-12h, most human ISGs remain elevated for over 16h, implying differences in transcriptional regulation during an IFN response.

The short-lived ISG signature in bats may serve to avoid unnecessary inflammation caused by chronic exposure to IFN. Using a short but particularly potent antiviral program may be more beneficial to bat hosts than an extended response. In fact, the negative IFN regulator USP18 was the most significantly-induced ISG by both FDR and relative change in IFN-treated PaKi cells at all time points, suggesting there is extraordinary pressure to keep type I IFN signaling under control (Figure 3). It remains unclear whether the IFN response is as short-lived if cells are infected with virus itself instead of being treated directly with interferon. Although there are reports of transcriptional signatures from virus-infected bat cells of a few species (Biesold, Ritz et al. 2011, Wynne, Shiell et al. 2014, Glennon, Jabado et al. 2015), it is difficult to uncouple the signals that contribute to IFN induction and repression during active infection.

There is a possibility that due to the limited number of cell lines I used, the observation may be cell-type specific. I did observe differences between my two human cell lines A549 and HEK 293. Specifically, HEK 293 cells responded poorly to IFN and only induced a small number of ISGs (Appendix A). In addition, the few ISGs that were induced in HEK293 (IRF7, IRF9, TDRD7, DTX3L and PARP9) were induced with delayed kinetics compared to A549 and PaKi cells. More studies comparing several human and bat cell lines should be done to determine if differences in length of the IFN response can be generalized to most human and bat cell lines.

ISG Expression Levels

When comparing ISG mRNA levels between bat and human cell lines, I observed that many ISGs were expressed to higher baseline levels in bat cells compared to human cells (Figure 5). Upon IFN treatment, I also noticed that many ISGs were expressed to greater maximum

levels in bat cells compared to human cells. Combined with the temporal kinetics, this data provides some evidence that the ISG response in bats may be more potent, but more tightly regulated. This indicates that it may be most important to control viruses during initial infection. Again, more studies are needed to determine if differences in baseline or induced ISG levels between bat and human can be generalized to the species.

RNASEL as a Unique ISG in the Black Flying Fox

I identified RNASEL as an ISG in three black flying fox-derived cell lines (Figure 7A). I then demonstrated that RNASEL was important for the antiviral response, as cells with less RNASEL were more susceptible to viral infection. One common problem during my studies was lack of appropriate antibodies for detecting bat proteins. In the case of RNASEL, its ribosomal RNA-degrading function has been extensively described (Silverman 2007, Li, Banerjee et al. 2016), and I was able to demonstrate knockout of RNASEL using a functional readout (Figure 7C). Finally, as RNASEL cleavage products have been shown to potentiate IFN signaling through RIG-I sensing, I tested the IFN sensitivity of WT and RNASEL KO cells and found that in RNASEL KO cells, IFN had less of an antiviral effect than in WT cells.

Curiously, I was not able to isolate single cell clones containing homozygous deleterious mutations of *RNASEL*. Although I detected modifications to the *RNASEL* genes at the bulk population level in approximately half of all alleles, every surviving single cell clone tested had a WT genotype. The reason for this is unclear. It is possible that *RNASEL* could be an essential gene in bats but not humans, as human *RNASEL*$^{-/-}$ cell lines have been made previously (Li, Banerjee et al. 2016).

IRF7 FUNCTION AND ACTIVATION

Overview

I have demonstrated that bat IRF7 has constitutive activity in human cells that protects them from viral infection (Figure 23). Bat IRF7, in contrast to human IRF7, can bind ISG promoter sequences in uninfected cells, promoting an antiviral state. However, there are still numerous questions that remain unanswered about IRF7. In the case of bat IRF7, what is the activator? Is the mechanism of activation the same in bat cells and *in vivo*? In this discussion, I will address lingering questions regarding IRF7 function and activation, and provide suggestions as to how they might be answered with future experiments.

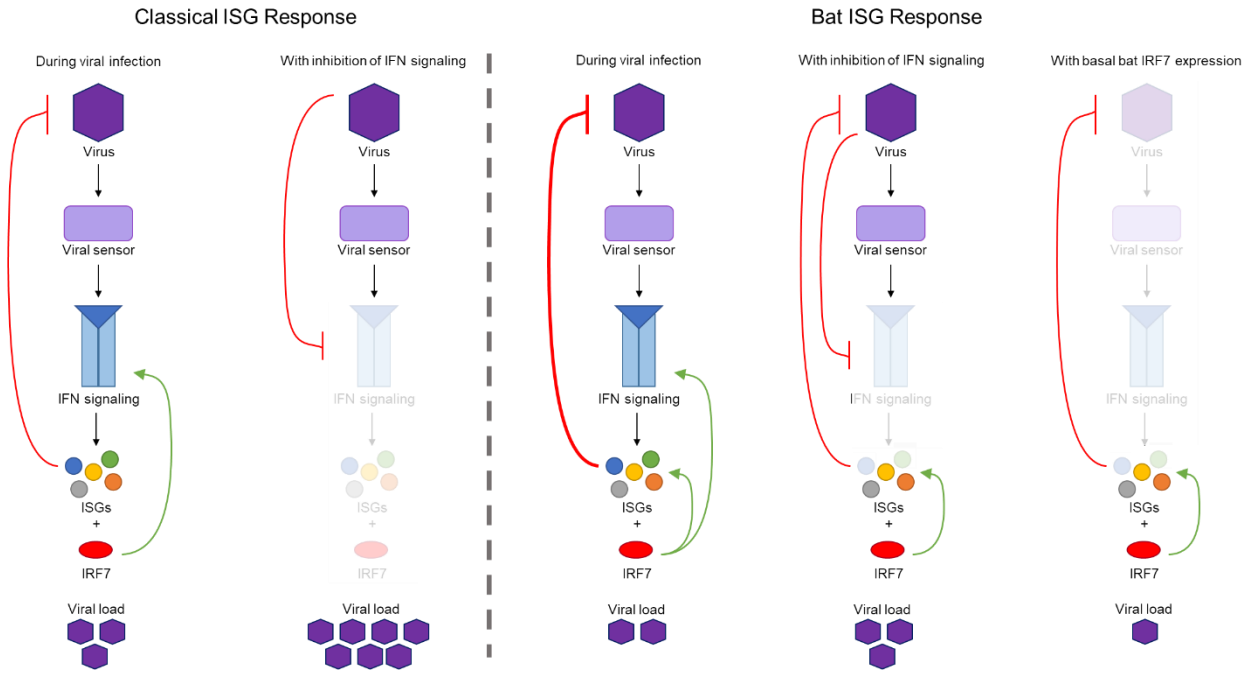

Figure 23: ISG Response in The Presence or Absence of bat IRF7

During the classical ISG response, sensing of viral components leads to IFN production and ISG expression. IRF7 induction leads to further IFN production through a positive feedback loop. A virus that inhibits IFN signaling will prevent ISG expression, leading to higher viral load. If cells are expressing bat IRF7, a group of antiviral ISGs will be induced independently of IFN signaling. If IFN signaling is targeted by a virus, IRF7-mediated ISG expression will provide some antiviral protection. If bat IRF7 is expressed in uninfected cells, it will result in ISG upregulation that will prevent viral infection.

IRF7 Binding Specificity

One of the major differences between bat and human IRF7 that I observed involves binding affinity to ISREs. Bat IRF7, if expressed stably in unstimulated cells, will bind to DNA regions containing ISRE sequences belonging to human genes IFIT2 and MX1 (Figure 18). Human IRF7, even if activated, does not bind the MX1 ISRE (Schmid, Mordstein et al. 2010). Thus, it is likely that the consensus binding sequence for human IRF7 differs from that of bat IRF7.

In addition, it is possible that the bat ISG ISRE sequences are different in bat cells compared to human cells, and that the IRF7-driven signature in bat cells contains a different set of ISGs. One unbiased approach to uncover the bat IRF7 consensus binding sequence would be to perform chromatin immunoprecipitation-sequencing (ChIP-Seq). The PaKi cells with endogenously-tagged IRF7 would serve as good starting material for these experiments, as all interactions would be determined using endogenous protein.

One curious issue I ran into while designing tagged IRF7 constructs was that bat IRF7 cannot tolerate an N-terminal tag. Despite adequate expression, bat IRF7 with an HA tag on the N-terminus could not inhibit viral infection in *STAT1*$^{-/-}$ fibroblasts. Because I did not test the function of this construct in HeLa cells, I cannot definitively state whether N-terminal tags only affect binding to ISG promoter or to both ISG and IFN promoters, but his observation may be a clue that the N-terminus of bat IRF7, which contains the DNA-binding region, is particularly sensitive to changes.

IRF7 Binding Partners

The interacting partners of IRF7 are not well-understood, as experiments looking at global binding partners to IRF7 have not been reported. Apart from known activators such as TBK1 and IKKε, several examples of IRF7-interacting proteins that modulate IRF7 activity have been described. TRIM28 is believed to be an IRF7-specific SUMO E3 ligase that acts as a negative regulator of IRF7 (Liang, Deng et al. 2011). Another ubiquitin E3 ligase, RAUL, has also been shown to negatively regulate IRF7 as well as IRF3 (Yu and Hayward 2010). NFATC3 was recently identified as an IRF7 transcriptional co-activator in pDCs (Bao, Wang et al. 2016).

The question remains: Does bat IRF7 require interactions with other proteins for activity? My studies determined that the kinase TBK1 is not essential to bat IRF7 activity, although IRF7 could have been activated by another kinase, such as IKKα or IKKε. The adaptor proteins MAVS and STING are also not required, which is not surprising considering that ISG induction by bat IRF7 was observed in uninfected cells that presumably were not signaling through nucleic acid sensing pathways.

Bat IRF7 may not rely on activators, but rather on lack of inhibitors. One speculation is that human IRF7 is maintained in an inactive state by interactions with inhibitors. Human IRF7 may be sequestered into an inactive state in uninfected cells and then released to dimerize and act as a transcriptional activator of IFN during infection. Bat IRF7, on the other hand, may not interact with the inhibitor on a human cell background, leading to constitutive activity. Because bat IRF7 constitutive activity in unstimulated bat cells has not been tested, this question cannot yet be answered.

Currently, the lab is working on determining conditions in which bat cells can express exogenous genes without activation of nucleic acid sensors. Transfection and electroporation cause significant cell death and activate nucleic acid-sensing pathways that would activate IRF7, rendering this method unsuitable for studying constitutive IRF7 activity in isolation. Transduction with lentiviral constructs which are designed to integrate protein-coding genes directly into the recipient cell genome and circumvent sensing pathways is not successful in the bat cell lines we currently possess. The use a selectable lentiviral system results in such low expression that detection of exogenous genes is difficult, and the low expression levels are not sufficient to promote a measurable phenotype. Further work will need to be done regarding optimizing gene expression in cell culture before the use of common genetic and biochemical techniques can be applied to our bat cells.

Co-immunoprecipitation coupled with mass spectrometry (Co-IP/MS) might provide additional insight regarding protein-protein interactions. Depending on the conditions of the experiment, it may reveal interactions between IRF7 and transcriptional coactivators, differences between bat IRF7 and human IRF7 binding partners, or even IRF7 interactions with inhibitory proteins if this is one of the many post-translational controls of IRF7 activity. These experiments can be done using overexpression in human cell lines or using endogenous bat IRF7 if the endogenously-tagged IRF7 PaKi cells are used.

Requirements for Bat IRF7 Activation

Experiments done with bat-human IRF7 chimeras allowed me to conclude that a single region of bat IRF7 does not control its activation. There are many reasons why these proteins

may not have the full activity of bat IRF7. The first reason is tertiary structure. Replacing portions of a protein with those of an ortholog, especially in regions with low homology, carries the risk that the chimeric protein will not fold correctly. To rule out improper folding as a cause of lack of antiviral activity, the purified chimeric proteins could be analyzed using circular dichroism (CD) spectroscopy. The antiviral activity of the chimeras could also be tested in cells that respond to type I IFNs, such as HeLa cells (Figure 10). Only properly-folded IRF7 chimeras should have antiviral activity in HeLa or any cell with intact IFN signaling.

The second reason none of the chimeras had activity in *STAT1*$^{-/-}$ fibroblasts could be that bat IRF7 relies on more than one component of the protein for activation. The combination of my mutagenesis and chimera data support this hypothesis. It is possible that bat IRF7 is more likely to be targeted for phosphorylation due to increased number of target residues at its C-terminus. However, the presence of the residues is not enough, as I saw when adding serine residues to the human IRF7 protein. If bat IRF7 is indeed more likely to be a kinase target, I predict there are two major contributions to its availability as a substrate. First, the presence of available targets for phosphorylation, and second, a tertiary structure with a configuration that permits interactions with its activator and/or promotes dimerization. These requirements may be fulfilled individually by two or more separate regions of the protein, as is suggested by the chimera assays, or can be achieved using a "shortcut", as was observed by bypassing kinase activation and adding phosphomimetic sites directly to human IRF7.

The constitutive activity I observed with stably expressed IRF7 leads to some ISG production but no IFN production. Considering the canonical function of IRF7 is to produce

interferons, I reason that bat IRF7 has two activated configurations. The first (IFN-independent) semi-active conformation can be achieved by simple induction or expression, with no viral infection or other immune stimulation is required. This configuration of bat IRF7 can form dimers, bind ISREs and induce a specific, limited, ISG response independently of IFN. The second activated configuration (IFN-dependent) depends on pathogen sensing and is activated through canonical pathways. In this configuration, IRF7 is a transcriptional activator of type I IFN and may additionally activate ISGs directly. Experiments done with IRF7 in Paki cells previously show that bat IRF7, when activated with Sendai infection, does indeed increase type I IFN expression (Zhou, Cowled et al. 2014).

IRF7 Phosphorylation

Another question that remains unanswered is the identity of the kinase, if any, that is phosphorylating bat IRF7. Although phosphorylation was not demonstrated directly, there is evidence supporting that phosphorylation is required for bat IRF7 activity. First, replacing serines in the C-terminus with phosphodeficient residues results in cumulative loss of antiviral activity. Second, inserting unique bat serine residues into human IRF7 does not increase antiviral activity, but inserting the phosphomimic aspartic acid at the same site makes human IRF7 more antiviral. Although the second example may be artificial, it nevertheless suggests that the unique serines must be modified for full functionality. Together, these data support the idea that the charge added during phosphorylation is essential for bat IRF7 activity. Nonetheless, because phosphorylation of bat IRF7 has not been directly demonstrated, it is formally possible that bat

IRF7 induces ISGs independently of phosphorylation, although this would be highly unusual for an IRF protein.

Preliminary experiments done with IRF7 transfection into 293T provide clues as to the phosphorylation status of IRF7. When bat IRF7 is transfected by itself, it provides antiviral protection to the cell. When it is co-transfected with IKKε, there is a shift of bat IRF7 by Western blot, suggesting phosphorylation. Considering bat IRF7 is antiviral in the absence of IKKε activation, there is likely another kinase that phosphorylates IRF7 immediately following its translation. In some Western blots done using lysates from *STAT1*$^{-/-}$ stably expressing IRF7, a second, heavier bat IRF7 band can be appreciated (Figure 15A, Figure 18A). In fact, in the ISRE-binding assays, it is this higher molecular weight band that is pulled down with the ISRE (Figure 18A). However, the higher molecular weight band can be found in both cytoplasmic and nuclear fractions (Figure 15). It remains unclear exactly what this heavier minor product of IRF7 is. With purified protein, phosphorylation mapping can be achieved using mass spectroscopy. If done in the absence and present of virus, it may help differentiate between the serines that become phosphorylated during constitutive activity and those that are only phosphorylated during infection, providing valuable insight regarding the activation of bat IRF7.

IRF7 Folding

Although phosphorylation of bat IRF7 is likely important for its constitutive activation, there must be a reason that the activating kinase can interact better with bat IRF7 than human IRF7. One reason for this could be differences in folding that make the phosphorylation sites more accessible to other proteins. Interestingly, the highly conserved cysteine at position 486 is

an alanine in bats (Appendix F). Whether this cysteine participates in disulfide bonds remains unclear, as the available crystal structures of IRF7 are constructed from N-terminal truncation mutants and do not contain this residue. However, disulfide bond prediction software suggests that Cys481 in humans is likely to form disulfide bonds with Cys494 (Ferre and Clote 2005). Cys494 is a conserved cysteine residue in hominids. A disulfide bond between Cys481 and Cys494 may cause a fold that causes steric hindrance and therefore provides specificity for IRF7-kinase interactions. If this fold is absent in bat IRF7, the site may participate in promiscuous binding to cellular kinases regardless of viral sensing, leading to constitutive activity. This cysteine residue does not seem to be present at a similar position in IRF3 or any of the other IRF family members, making predictions from existing crystal structures difficult (Qin, Liu et al. 2003).

The CAD and ID of bat and human IRF7 share little homology compared to other regions of the protein (Figure 19). It is possible that residues in these regions cumulatively affect folding in a way that makes bat IRF7 less likely to remain in a condensed, inactive conformation. Without full crystal structures of both orthologs, we can only make predictions as to how particular residues will affect IRF7 folding and activation. Solving and comparing the tertiary structures of full length bat and human IRF7 will provide insight regarding function.

CONCLUSION

These studies were done to discover unique antiviral pathways in the black flying fox, a reservoir of several viral pathogens. Through this work I uncovered two different antiviral strategies employed by this species to control viral infection. The first is the induction of RNASEL by IFN, which has the effect of amplifying the antiviral response during early phases of infection. The second is the induction of ISGs directly by IRF7, which provides additional antiviral protection in the case the primary antiviral program directed by IFN is blocked. These two pathways likely work with others to contribute to the unique immune system in bats. It is my hope that further work on this topic will eventually lead to novel antiviral therapies and greater understanding of immunology, host-pathogen interactions, and bat biology.

APPENDIX A

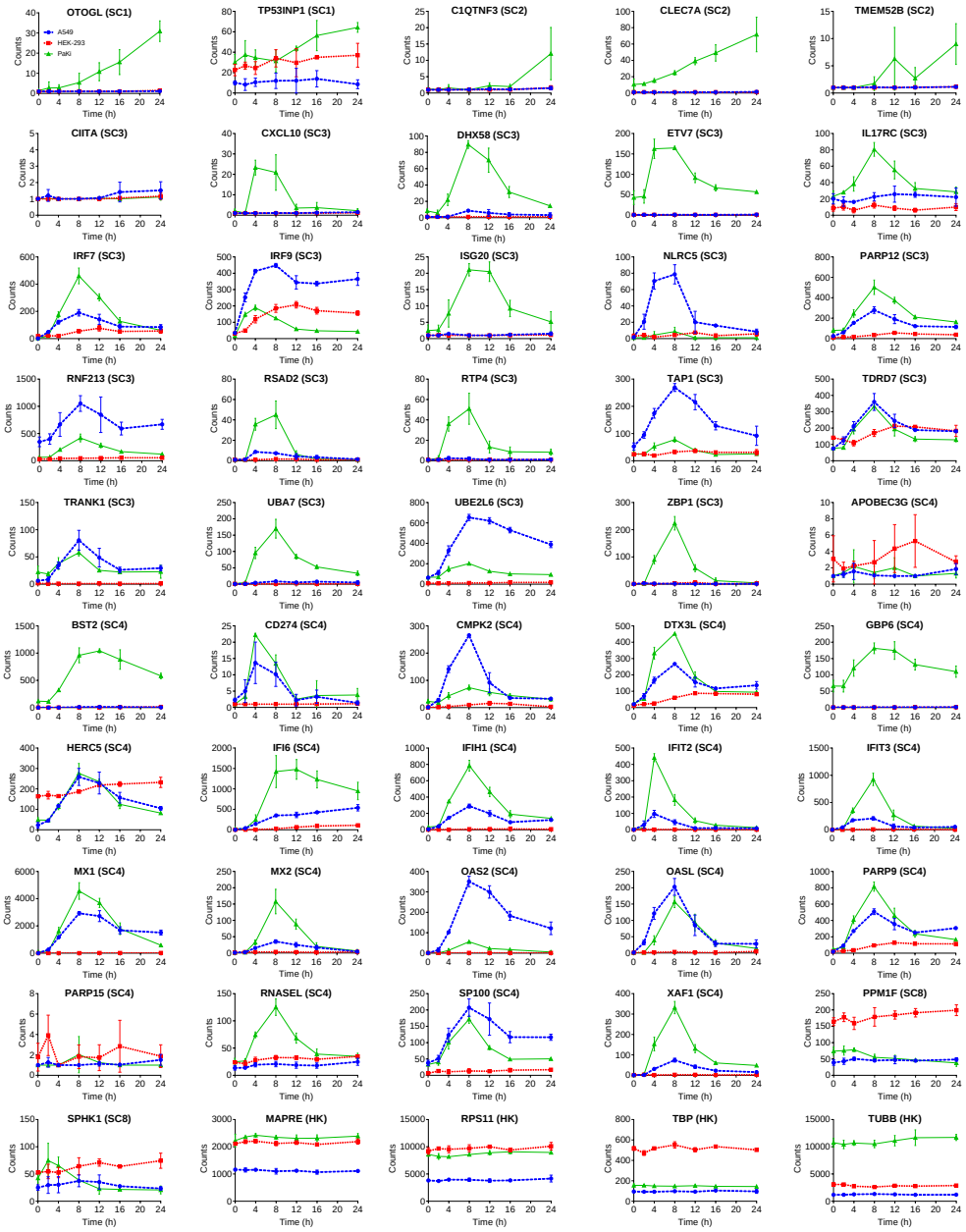

Appendix A: Normalized Nanostring mRNA counts over time in bat and human cells. *A549 (blue), HEK293 (red), or Paki (green) cells were treated with IFNa (50U/mL) and RNA was harvested at the indicated time points. A customized Nanostring nCounter library was used to detect mRNA counts of 50 genes. Data are represented as mean ± SD for three independent experiments.*

APPENDIX B

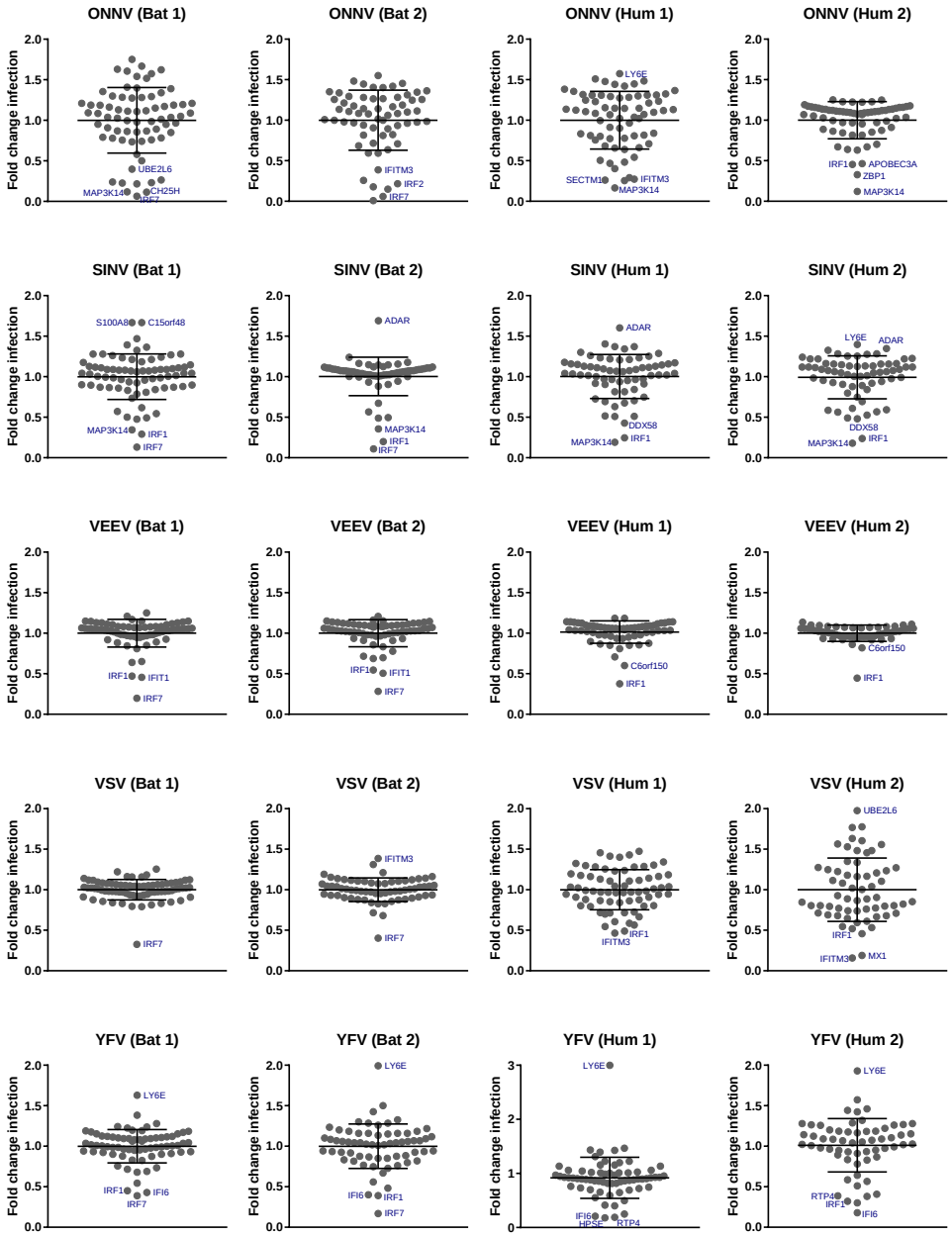

Appendix B: ISG Ortholog Screen Summary.
Each dot represents one ISG. Infections are normalized to average % infected cells in each experiment. Each virus was tested in two independent screens.

APPENDIX C

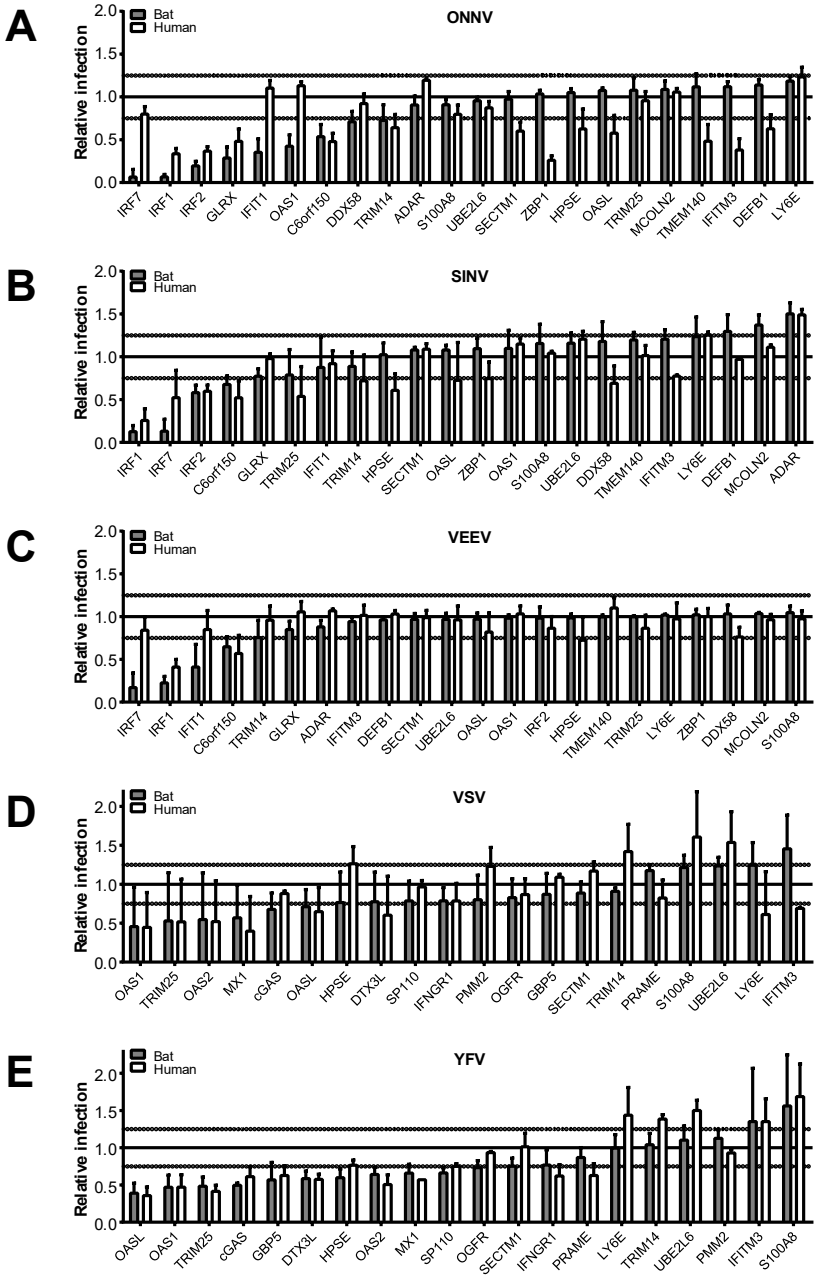

Appendix C: Verification ISG screens.
Select ISGs were chosen for re-screening to verify phenotype. Infection are normalized to % infected cells in each experiment. Each ISG was tested in two independent experiments.

APPENDIX D

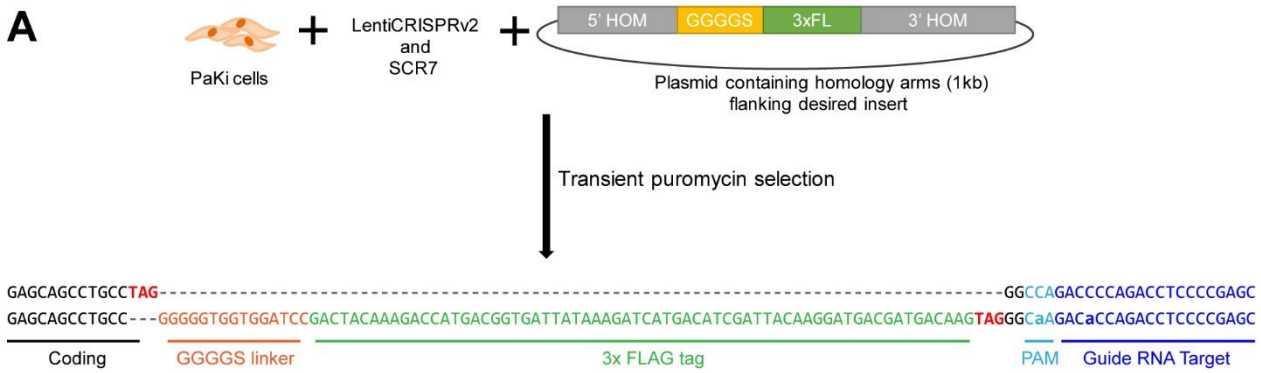

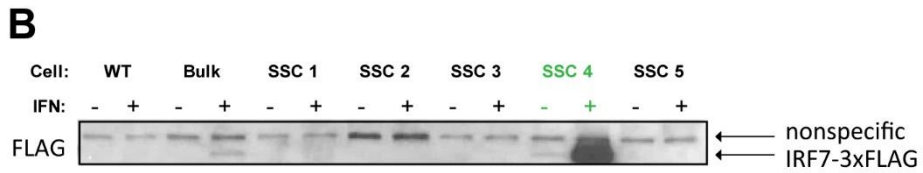

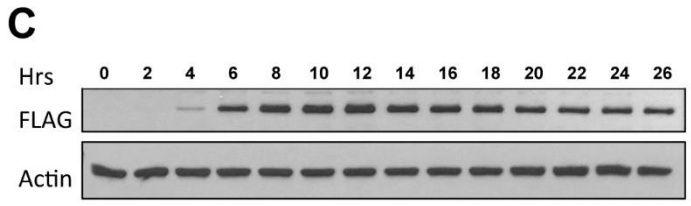

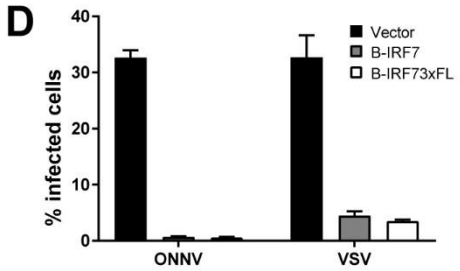

Appendix D: Endogenous Tagging of PaKi IRF7

(A) *Tagging strategy. PaKi cells were transfected with lentiCRISPRv2 with gRNAs targeting the C-terminal region of IRF7 along with a donor plasmid containing a linker and 3xFLAG tag flanked by ~500bp upstream and downstream of the CRISPR target site. SCR7 was added to promote homology-directed repair. Cells were selected with puromycin for 3 days and then expanded for analysis.* ***(B)*** *Western blot of untagged (WT) PaKi cells, bulk transfected cells, and single cell clones. Bulk and clone 4 have an IFN-inducible FLAG signal.* ***(C)*** *Timecourse of IRF7 induction. PaKi IRF7-3xFLAG cells were treated with 50U/mL of universal IFNα and lysates were probed for FLAG expression.* ***(D)*** *STAT1$^{-/-}$ fibroblasts were transduced with bat IRF7 or bat IRF7 with a C-terminal 3xFLAG tag identical to that used in endogenously-tagged PaKi cells. Cells were then infected with ONNV or VSV at an MOI of 1 and infection was quantified via flow cytometry. N=2.*

APPENDIX E

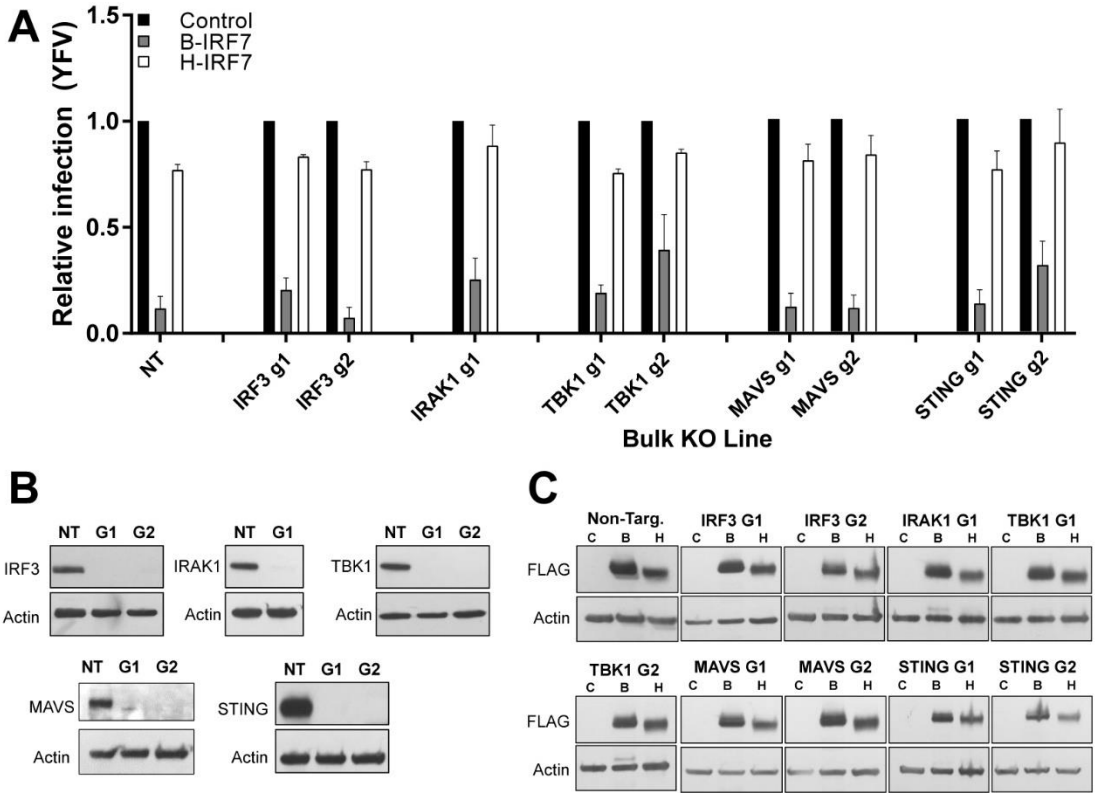

Appendix E: CRISPR Mini-Screen to Identify Essential Factors for Bat IRF7 Activity
(A) *Individual effectors were knocked out of STAT1$^{-/-}$ fibroblasts using CRISPR-Cas9. Cells were transduced with a lentivirus expressing IRF7-3xFLAG or control for 48h. Cells were then infected with YFV at an MOI of 1 and harvested for flow cytometry at 24h. Infection was normalized to percent infection in control cells.* ***(B)*** *Western blots demonstrating knockout of individual innate immune molecules in bulk cell lines.* ***(C)*** *Western blots demonstrating IRF7 expression in bulk cell lines 48h after transduction with IRF7-3xFLAG or control.*

APPENDIX F

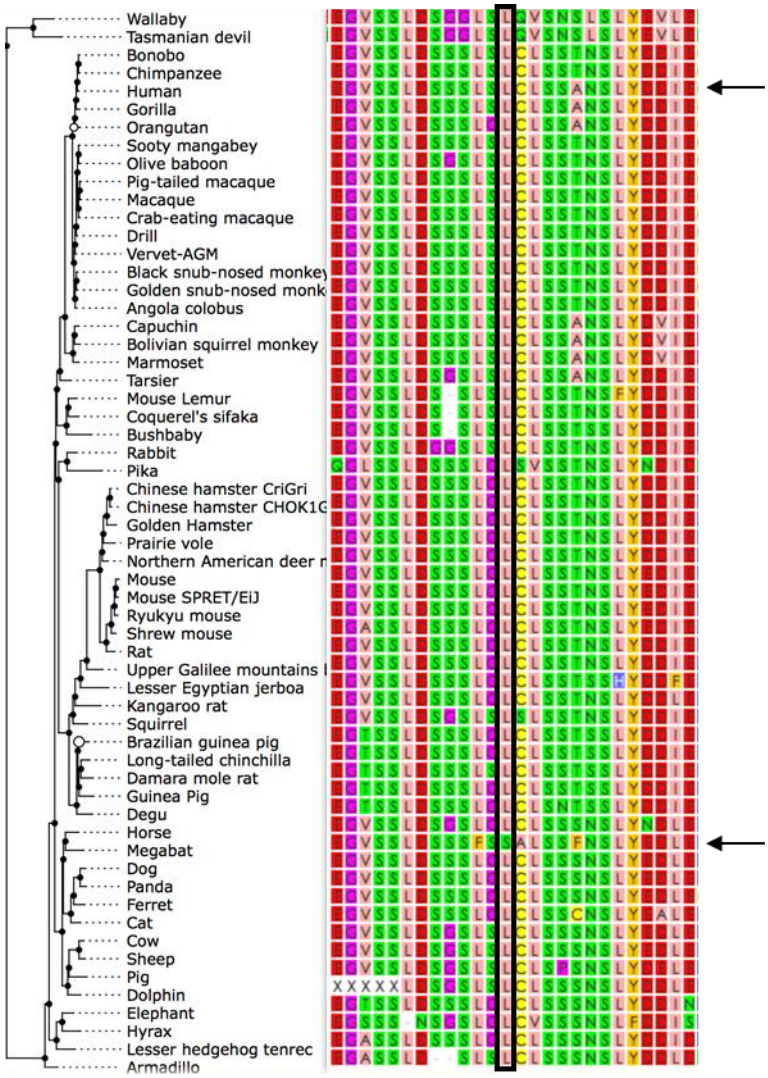

Appendix F: Alignment of IRF7 amino acid sequences

Human and megabat sequences are indicated with arrows. Megabats have an evolutionarily unique serine residue at the position corresponding to human IRF7 L480 (black box). Loss of the cysteine residue at the next position is also rare in evolutionary history. Of note, the phenylalanine at position 485 is a serine residue in the black flying fox.

BIBLIOGRAPHY

Aguet, M., M. Grobke and P. Dreiding (1984). "Various human interferon alpha subclasses cross-react with common receptors: their binding affinities correlate with their specific biological activities." Virology **132**(1): 211-216.

Ahn, M., J. Cui, A. T. Irving and L. F. Wang (2016). "Unique Loss of the PYHIN Gene Family in Bats Amongst Mammals: Implications for Inflammasome Sensing." Sci Rep **6**: 21722.

Akira, S., S. Uematsu and O. Takeuchi (2006). "Pathogen recognition and innate immunity." Cell **124**(4): 783-801.

Altschul, S. F., T. L. Madden, A. A. Schaffer, J. Zhang, Z. Zhang, W. Miller and D. J. Lipman (1997). "Gapped BLAST and PSI-BLAST: a new generation of protein database search programs." Nucleic Acids Res **25**(17): 3389-3402.

Andrilenas, K. K., V. Ramlall, J. Kurland, B. Leung, A. G. Harbaugh and T. Siggers (2018). "DNA-binding landscape of IRF3, IRF5 and IRF7 dimers: implications for dimer-specific gene regulation." Nucleic Acids Res.

Arimoto, K. I., S. Lochte, S. A. Stoner, C. Burkart, Y. Zhang, S. Miyauchi, S. Wilmes, J. B. Fan, J. J. Heinisch, Z. Li, M. Yan, S. Pellegrini, F. Colland, J. Piehler and D. E. Zhang (2017). "STAT2 is an essential adaptor in USP18-mediated suppression of type I interferon signaling." Nat Struct Mol Biol **24**(3): 279-289.

Bach, E. A., M. Aguet and R. D. Schreiber (1997). "The IFN gamma receptor: a paradigm for cytokine receptor signaling." Annu Rev Immunol **15**: 563-591.

Bao, M., Y. Wang, Y. Liu, P. Shi, H. Lu, W. Sha, L. Weng, S. Hanabuchi, J. Qin, J. Plumas, L. Chaperot, Z. Zhang and Y. J. Liu (2016). "NFATC3 promotes IRF7 transcriptional activity in plasmacy--toid dendritic cells." J Exp Med **213**(11): 2383-2398.

Best, S. M., K. L. Morris, J. G. Shannon, S. J. Robertson, D. N. Mitzel, G. S. Park, E. Boer, J. B. Wolfinbarger and M. E. Bloom (2005). "Inhibition of interferon-stimulated JAK-STAT signaling by a tick-borne flavivirus and identification of NS5 as an interferon antagonist." J Virol **79**(20): 12828-12839.

Biesold, S. E., D. Ritz, F. Gloza-Rausch, R. Wollny, J. F. Drexler, V. M. Corman, E. K. Kalko, S. Oppong, C. Drosten and M. A. Muller (2011). "Type I interferon reaction to viral infection in interferon-competent, immortalized cell lines from the African fruit bat Eidolon helvum." PLoS One **6**(11): e28131.

Bode, J. G., S. Ludwig, C. Ehrhardt, U. Albrecht, A. Erhardt, F. Schaper, P. C. Heinrich and D. Haussinger (2003). "IFN-alpha antagonistic activity of HCV core protein involves induction of suppressor of cytokine signaling-3." FASEB J **17**(3): 488-490.

Brook, C. E. and A. P. Dobson (2015). "Bats as 'special' reservoirs for emerging zoonotic pathogens." Trends Microbiol **23**(3): 172-180.

Brunette, R. L., J. M. Young, D. G. Whitley, I. E. Brodsky, H. S. Malik and D. B. Stetson (2012). "Extensive evolutionary and functional diversity among mammalian AIM2-like receptors." J Exp Med **209**(11): 1969-1983.

Calisher, C. H., J. E. Childs, H. E. Field, K. V. Holmes and T. Schountz (2006). "Bats: important reservoir hosts of emerging viruses." Clin Microbiol Rev **19**(3): 531-545.

Choi, E. J., C. H. Lee and O. S. Shin (2015). "Suppressor of Cytokine Signaling 3 Expression Induced by Varicella-Zoster Virus Infection Results in the Modulation of Virus Replication." Scand J Immunol **82**(4): 337-344.

Chua, K. B., C. L. Koh, P. S. Hooi, K. F. Wee, J. H. Khong, B. H. Chua, Y. P. Chan, M. E. Lim and S. K. Lam (2002). "Isolation of Nipah virus from Malaysian Island flying-foxes." Microbes Infect **4**(2): 145-151.

Cochet, M., D. Vaiman and F. Lefevre (2009). "Novel interferon delta genes in mammals: cloning of one gene from the sheep, two genes expressed by the horse conceptus and discovery of related sequences in several taxa by genomic database screening." Gene **433**(1-2): 88-99.

Colamonici, O. R., P. Domanski, S. M. Sweitzer, A. Larner and R. M. Buller (1995). "Vaccinia virus B18R gene encodes a type I interferon-binding protein that blocks interferon alpha transmembrane signaling." J Biol Chem **270**(27): 15974-15978.

Cowled, C., M. Baker, M. Tachedjian, P. Zhou, D. Bulach and L. F. Wang (2011). "Molecular characterisation of Toll-like receptors in the black flying fox Pteropus alecto." Dev Comp Immunol **35**(1): 7-18.

Crameri, G., S. Todd, S. Grimley, J. A. McEachern, G. A. Marsh, C. Smith, M. Tachedjian, C. De Jong, E. R. Virtue, M. Yu, D. Bulach, J. P. Liu, W. P. Michalski, D. Middleton, H. E. Field and L. F. Wang (2009). "Establishment, immortalisation and characterisation of pteropid bat cell lines." PLoS One **4**(12): e8266.

Darnell, J. E., Jr., I. M. Kerr and G. R. Stark (1994). "Jak-STAT pathways and transcriptional activation in response to IFNs and other extracellular signaling proteins." Science **264**(5164): 1415-1421.

Davis, A. D., R. J. Rudd and R. A. Bowen (2007). "Effects of aerosolized rabies virus exposure on bats and mice." J Infect Dis **195**(8): 1144-1150.

De Ioannes, P., C. R. Escalante and A. K. Aggarwal (2011). "Structures of apo IRF-3 and IRF-7 DNA binding domains: effect of loop L1 on DNA binding." Nucleic Acids Res **39**(16): 7300-7307.

De La Cruz-Rivera, P. C., M. Kanchwala, H. Liang, A. Kumar, L. F. Wang, C. Xing and J. W. Schoggins (2017). "The IFN Response in Bats Displays Distinctive IFN-Stimulated Gene Expression Kinetics with Atypical RNASEL Induction." J Immunol.

Deguine, J. and G. M. Barton (2014). "MyD88: a central player in innate immune signaling." F1000Prime Rep **6**: 97.

Doench, J. G., N. Fusi, M. Sullender, M. Hegde, E. W. Vaimberg, K. F. Donovan, I. Smith, Z. Tothova, C. Wilen, R. Orchard, H. W. Virgin, J. Listgarten and D. E. Root (2016). "Optimized sgRNA design to maximize activity and minimize off-target effects of CRISPR-Cas9." Nat Biotechnol **34**(2): 184-191.

Dupuis, S., E. Jouanguy, S. Al-Hajjar, C. Fieschi, I. Z. Al-Mohsen, S. Al-Jumaah, K. Yang, A. Chapgier, C. Eidenschenk, P. Eid, A. Al Ghonaium, H. Tufenkeji, H. Frayha, S. Al-Gazlan, H. Al-Rayes, R. D. Schreiber, I. Gresser and J. L. Casanova (2003). "Impaired response to interferon-alpha/beta and lethal viral disease in human STAT1 deficiency." Nat Genet **33**(3): 388-391.

Endo, T. A., M. Masuhara, M. Yokouchi, R. Suzuki, H. Sakamoto, K. Mitsui, A. Matsumoto, S. Tanimura, M. Ohtsubo, H. Misawa, T. Miyazaki, N. Leonor, T. Taniguchi, T. Fujita, Y. Kanakura, S. Komiya and A. Yoshimura (1997). "A new protein containing an SH2 domain that inhibits JAK kinases." Nature **387**(6636): 921-924.

Essers, M. A., S. Offner, W. E. Blanco-Bose, Z. Waibler, U. Kalinke, M. A. Duchosal and A. Trumpp (2009). "IFNalpha activates dormant haematopoietic stem cells in vivo." Nature **458**(7240): 904-908.

Ferre, F. and P. Clote (2005). "DiANNA: a web server for disulfide connectivity prediction." Nucleic Acids Res **33**(Web Server issue): W230-232.

Field, H., P. Young, J. M. Yob, J. Mills, L. Hall and J. Mackenzie (2001). "The natural history of Hendra and Nipah viruses." Microbes Infect **3**(4): 307-314.

Fleming, S. B. (2016). "Viral Inhibition of the IFN-Induced JAK/STAT Signalling Pathway: Development of Live Attenuated Vaccines by Mutation of Viral-Encoded IFN-Antagonists." Vaccines (Basel) **4**(3).

Frey, K. G., C. M. Ahmed, R. Dabelic, L. D. Jager, E. N. Noon-Song, S. M. Haider, H. M. Johnson and N. J. Bigley (2009). "HSV-1-induced SOCS-1 expression in keratinocytes: use of a SOCS-1 antagonist to block a novel mechanism of viral immune evasion." J Immunol **183**(2): 1253-1262.

Gelinas, J. F., G. Clerzius, E. Shaw and A. Gatignol (2011). "Enhancement of replication of RNA viruses by ADAR1 via RNA editing and inhibition of RNA-activated protein kinase." J Virol **85**(17): 8460-8466.

Glennon, N. B., O. Jabado, M. K. Lo and M. L. Shaw (2015). "Transcriptome Profiling of the Virus-Induced Innate Immune Response in Pteropus vampyrus and Its Attenuation by Nipah Virus Interferon Antagonist Functions." J Virol **89**(15): 7550-7566.

Guo, C. J., L. S. Yang, Y. F. Zhang, Y. Y. Wu, S. P. Weng, X. Q. Yu and J. G. He (2012). "A novel viral SOCS from infectious spleen and kidney necrosis virus: interacts with Jak1 and inhibits IFN-alpha induced Stat1/3 activation." PLoS One **7**(7): e41092.

Guo, J. T., J. Hayashi and C. Seeger (2005). "West Nile virus inhibits the signal transduction pathway of alpha interferon." J Virol **79**(3): 1343-1350.

Halpin, K., P. L. Young, H. E. Field and J. S. Mackenzie (2000). "Isolation of Hendra virus from pteropid bats: a natural reservoir of Hendra virus." J Gen Virol **81**(Pt 8): 1927-1932.

Hayman, D. T. (2016). "Bats as Viral Reservoirs." Annu Rev Virol **3**(1): 77-99.

Hiscott, J., P. Pitha, P. Genin, H. Nguyen, C. Heylbroeck, Y. Mamane, M. Algarte and R. Lin (1999). "Triggering the interferon response: the role of IRF-3 transcription factor." J Interferon Cytokine Res **19**(1): 1-13.

Holzer, M., V. Krahling, F. Amman, E. Barth, S. H. Bernhart, V. A. Carmelo, M. Collatz, G. Doose, F. Eggenhofer, J. Ewald, J. Fallmann, L. M. Feldhahn, M. Fricke, J. Gebauer, A. J. Gruber, F. Hufsky, H. Indrischek, S. Kanton, J. Linde, N. Mostajo, R. Ochsenreiter, K. Riege, L. Rivarola-Duarte, A. H. Sahyoun, S. J. Saunders, S. E. Seemann, A. Tanzer, B. Vogel, S. Wehner, M. T. Wolfinger, R. Backofen, J. Gorodkin, I. Grosse, I. Hofacker, S. Hoffmann, C. Kaleta, P. F. Stadler, S. Becker and M. Marz (2016). "Differential transcriptional responses to Ebola and Marburg virus infection in bat and human cells." Sci Rep **6**: 34589.

Holzinger, D., C. Jorns, S. Stertz, S. Boisson-Dupuis, R. Thimme, M. Weidmann, J. L. Casanova, O. Haller and G. Kochs (2007). "Induction of MxA gene expression by influenza A virus requires type I or type III interferon signaling." J Virol **81**(14): 7776-7785.

Honda, K., A. Takaoka and T. Taniguchi (2006). "Type I interferon [corrected] gene induction by the interferon regulatory factor family of transcription factors." Immunity **25**(3): 349-360.

Hou, F., L. Sun, H. Zheng, B. Skaug, Q. X. Jiang and Z. J. Chen (2011). "MAVS forms functional prion-like aggregates to activate and propagate antiviral innate immune response." Cell **146**(3): 448-461.

Isaacs, A. and J. Lindenmann (1957). "Virus interference. I. The interferon." Proc R Soc Lond B Biol Sci **147**(927): 258-267.

Ivashkiv, L. B. and L. T. Donlin (2014). "Regulation of type I interferon responses." Nat Rev Immunol **14**(1): 36-49.

Iwamura, T., M. Yoneyama, K. Yamaguchi, W. Suhara, W. Mori, K. Shiota, Y. Okabe, H. Namiki and T. Fujita (2001). "Induction of IRF-3/-7 kinase and NF-kappaB in response to double-stranded RNA and virus infection: common and unique pathways." Genes Cells **6**(4): 375-388.

Jacobsen, H., C. W. Czarniecki, D. Krause, R. M. Friedman and R. H. Silverman (1983). "Interferon-induced synthesis of 2-5A-dependent RNase in mouse JLS-V9R cells." Virology **125**(2): 496-501.

Janardhana, V., M. Tachedjian, G. Crameri, C. Cowled, L. F. Wang and M. L. Baker (2012). "Cloning, expression and antiviral activity of IFNgamma from the Australian fruit bat, Pteropus alecto." Dev Comp Immunol **36**(3): 610-618.

Jensen, S. and A. R. Thomsen (2012). "Sensing of RNA viruses: a review of innate immune receptors involved in recognizing RNA virus invasion." J Virol **86**(6): 2900-2910.

Jia, D., R. Rahbar, R. W. Chan, S. M. Lee, M. C. Chan, B. X. Wang, D. P. Baker, B. Sun, J. S. Peiris, J. M. Nicholls and E. N. Fish (2010). "Influenza virus non-structural protein 1 (NS1) disrupts interferon signaling." PLoS One **5**(11): e13927.

Johnson, K. E., B. Song and D. M. Knipe (2008). "Role for herpes simplex virus 1 ICP27 in the inhibition of type I interferon signaling." Virology **374**(2): 487-494.

Jones, M., A. Davidson, L. Hibbert, P. Gruenwald, J. Schlaak, S. Ball, G. R. Foster and M. Jacobs (2005). "Dengue virus inhibits alpha interferon signaling by reducing STAT2 expression." J Virol **79**(9): 5414-5420.

Kamizono, S., T. Hanada, H. Yasukawa, S. Minoguchi, R. Kato, M. Minoguchi, K. Hattori, S. Hatakeyama, M. Yada, S. Morita, T. Kitamura, H. Kato, K. Nakayama and A. Yoshimura

(2001). "The SOCS box of SOCS-1 accelerates ubiquitin-dependent proteolysis of TEL-JAK2." J Biol Chem **276**(16): 12530-12538.

Kennedy, A. D., J. A. Willment, D. W. Dorward, D. L. Williams, G. D. Brown and F. R. DeLeo (2007). "Dectin-1 promotes fungicidal activity of human neutrophils." Eur J Immunol **37**(2): 467-478.

Kepler, T. B., C. Sample, K. Hudak, J. Roach, A. Haines, A. Walsh and E. A. Ramsburg (2010). "Chiropteran types I and II interferon genes inferred from genome sequencing traces by a statistical gene-family assembler." BMC Genomics **11**: 444.

Ketscher, L., R. Hannss, D. J. Morales, A. Basters, S. Guerra, T. Goldmann, A. Hausmann, M. Prinz, R. Naumann, A. Pekosz, O. Utermohlen, D. J. Lenschow and K. P. Knobeloch (2015). "Selective inactivation of USP18 isopeptidase activity in vivo enhances ISG15 conjugation and viral resistance." Proc Natl Acad Sci U S A **112**(5): 1577-1582.

Kim, D., G. Pertea, C. Trapnell, H. Pimentel, R. Kelley and S. L. Salzberg (2013). "TopHat2: accurate alignment of transcriptomes in the presence of insertions, deletions and gene fusions." Genome Biol **14**(4): R36.

Kotenko, S. V., G. Gallagher, V. V. Baurin, A. Lewis-Antes, M. Shen, N. K. Shah, J. A. Langer, F. Sheikh, H. Dickensheets and R. P. Donnelly (2003). "IFN-lambdas mediate antiviral protection through a distinct class II cytokine receptor complex." Nat Immunol **4**(1): 69-77.

Kurt-Jones, E. A., L. Popova, L. Kwinn, L. M. Haynes, L. P. Jones, R. A. Tripp, E. E. Walsh, M. W. Freeman, D. T. Golenbock, L. J. Anderson and R. W. Finberg (2000). "Pattern recognition receptors TLR4 and CD14 mediate response to respiratory syncytial virus." Nat Immunol **1**(5): 398-401.

Lau, S. K., K. S. Li, Y. Huang, C. T. Shek, H. Tse, M. Wang, G. K. Choi, H. Xu, C. S. Lam, R. Guo, K. H. Chan, B. J. Zheng, P. C. Woo and K. Y. Yuen (2010). "Ecoepidemiology and complete genome comparison of different strains of severe acute respiratory syndrome-related Rhinolophus bat coronavirus in China reveal bats as a reservoir for acute, self-limiting infection that allows recombination events." J Virol **84**(6): 2808-2819.

Law, C. W., Y. Chen, W. Shi and G. K. Smyth (2014). "voom: Precision weights unlock linear model analysis tools for RNA-seq read counts." Genome Biol **15**(2): R29.

Lee, H. R., M. H. Kim, J. S. Lee, C. Liang and J. U. Jung (2009). "Viral interferon regulatory factors." J Interferon Cytokine Res **29**(9): 621-627.

Lefevre, F., M. Guillomot, S. D'Andrea, S. Battegay and C. La Bonnardiere (1998). "Interferon-delta: the first member of a novel type I interferon family." Biochimie **80**(8-9): 779-788.

Leroy, E. M., B. Kumulungui, X. Pourrut, P. Rouquet, A. Hassanin, P. Yaba, A. Delicat, J. T. Paweska, J. P. Gonzalez and R. Swanepoel (2005). "Fruit bats as reservoirs of Ebola virus." Nature **438**(7068): 575-576.

Li, G., Y. Xiang, K. Sabapathy and R. H. Silverman (2004). "An apoptotic signaling pathway in the interferon antiviral response mediated by RNase L and c-Jun NH2-terminal kinase." J Biol Chem **279**(2): 1123-1131.

Li, W., Z. Shi, M. Yu, W. Ren, C. Smith, J. H. Epstein, H. Wang, G. Crameri, Z. Hu, H. Zhang, J. Zhang, J. McEachern, H. Field, P. Daszak, B. T. Eaton, S. Zhang and L. F. Wang (2005). "Bats are natural reservoirs of SARS-like coronaviruses." Science **310**(5748): 676-679.

Li, Y., S. Banerjee, Y. Wang, S. A. Goldstein, B. Dong, C. Gaughan, R. H. Silverman and S. R. Weiss (2016). "Activation of RNase L is dependent on OAS3 expression during infection with diverse human viruses." Proc Natl Acad Sci U S A **113**(8): 2241-2246.

Liang, Q., H. Deng, X. Li, X. Wu, Q. Tang, T. H. Chang, H. Peng, F. J. Rauscher, 3rd, K. Ozato and F. Zhu (2011). "Tripartite motif-containing protein 28 is a small ubiquitin-related modifier E3 ligase and negative regulator of IFN regulatory factor 7." J Immunol **187**(9): 4754-4763.

Liao, Y., G. K. Smyth and W. Shi (2014). "featureCounts: an efficient general purpose program for assigning sequence reads to genomic features." Bioinformatics **30**(7): 923-930.

Lin, R., C. Heylbroeck, P. M. Pitha and J. Hiscott (1998). "Virus-dependent phosphorylation of the IRF-3 transcription factor regulates nuclear translocation, transactivation potential, and proteasome-mediated degradation." Mol Cell Biol **18**(5): 2986-2996.

Lin, R., Y. Mamane and J. Hiscott (2000). "Multiple regulatory domains control IRF-7 activity in response to virus infection." J Biol Chem **275**(44): 34320-34327.

Lin, R. J., C. L. Liao, E. Lin and Y. L. Lin (2004). "Blocking of the alpha interferon-induced Jak-Stat signaling pathway by Japanese encephalitis virus infection." J Virol **78**(17): 9285-9294.

Lu, G., J. T. Reinert, I. Pitha-Rowe, A. Okumura, M. Kellum, K. P. Knobeloch, B. Hassel and P. M. Pitha (2006). "ISG15 enhances the innate antiviral response by inhibition of IRF-3 degradation." Cell Mol Biol (Noisy-le-grand) **52**(1): 29-41.

Malakhova, O. A., K. I. Kim, J. K. Luo, W. Zou, K. G. Kumar, S. Y. Fuchs, K. Shuai and D. E. Zhang (2006). "UBP43 is a novel regulator of interferon signaling independent of its ISG15 isopeptidase activity." EMBO J **25**(11): 2358-2367.

Malathi, K., B. Dong, M. Gale, Jr. and R. H. Silverman (2007). "Small self-RNA generated by RNase L amplifies antiviral innate immunity." Nature **448**(7155): 816-819.

Mali, P., L. Yang, K. M. Esvelt, J. Aach, M. Guell, J. E. DiCarlo, J. E. Norville and G. M. Church (2013). "RNA-guided human genome engineering via Cas9." Science **339**(6121): 823-826.

Marie, I., J. E. Durbin and D. E. Levy (1998). "Differential viral induction of distinct interferon-alpha genes by positive feedback through interferon regulatory factor-7." EMBO J **17**(22): 6660-6669.

Marie, I., E. Smith, A. Prakash and D. E. Levy (2000). "Phosphorylation-induced dimerization of interferon regulatory factor 7 unmasks DNA binding and a bipartite transactivation domain." Mol Cell Biol **20**(23): 8803-8814.

Martinand, C., C. Montavon, T. Salehzada, M. Silhol, B. Lebleu and C. Bisbal (1999). "RNase L inhibitor is induced during human immunodeficiency virus type 1 infection and down regulates the 2-5A/RNase L pathway in human T cells." J Virol **73**(1): 290-296.

Martinand, C., T. Salehzada, M. Silhol, B. Lebleu and C. Bisbal (1998). "RNase L inhibitor (RLI) antisense constructions block partially the down regulation of the 2-5A/RNase L pathway in encephalomyocarditis-virus-(EMCV)-infected cells." Eur J Biochem **254**(2): 248-255.

McCandliss, R., A. Sloma and S. Pestka (1981). "Isolation and cell-free translation of human interferon mRNA from fibroblasts and leukocytes." Methods Enzymol **79**(Pt B): 51-59.

Meuwissen, M. E., R. Schot, S. Buta, G. Oudesluijs, S. Tinschert, S. D. Speer, Z. Li, L. van Unen, D. Heijsman, T. Goldmann, M. H. Lequin, J. M. Kros, W. Stam, M. Hermann, R. Willemsen, R. W. Brouwer, I. W. F. Van, M. Martin-Fernandez, I. de Coo, J. Dudink, F. A. de Vries, A. Bertoli Avella, M. Prinz, Y. J. Crow, F. W. Verheijen, S. Pellegrini, D. Bogunovic and G. M. Mancini (2016). "Human USP18 deficiency underlies type 1 interferonopathy leading to severe pseudo-TORCH syndrome." J Exp Med **213**(7): 1163-1174.

Mi, H., S. Poudel, A. Muruganujan, J. T. Casagrande and P. D. Thomas (2016). "PANTHER version 10: expanded protein families and functions, and analysis tools." Nucleic Acids Res **44**(D1): D336-342.

Morin, P., J. Braganca, M. T. Bandu, R. Lin, J. Hiscott, J. Doly and A. Civas (2002). "Preferential binding sites for interferon regulatory factors 3 and 7 involved in interferon-A gene transcription." J Mol Biol **316**(5): 1009-1022.

Mostafavi, S., H. Yoshida, D. Moodley, H. LeBoite, K. Rothamel, T. Raj, C. J. Ye, N. Chevrier, S. Y. Zhang, T. Feng, M. Lee, J. L. Casanova, J. D. Clark, M. Hegen, J. B. Telliez, N. Hacohen, P. L. De Jager, A. Regev, D. Mathis, C. Benoist and C. Immunological Genome Project (2016). "Parsing the Interferon Transcriptional Network and Its Disease Associations." Cell **164**(3): 564-578.

Muller, B., S. M. Goodman and L. Peichl (2007). "Cone photoreceptor diversity in the retinas of fruit bats (megachiroptera)." Brain Behav Evol **70**(2): 90-104.

Naito, Y., K. Hino, H. Bono and K. Ui-Tei (2015). "CRISPRdirect: software for designing CRISPR/Cas guide RNA with reduced off-target sites." Bioinformatics **31**(7): 1120-1123.

Nakaya, T., M. Sato, N. Hata, M. Asagiri, H. Suemori, S. Noguchi, N. Tanaka and T. Taniguchi (2001). "Gene induction pathways mediated by distinct IRFs during viral infection." Biochem Biophys Res Commun **283**(5): 1150-1156.

Nel, L. H. and C. E. Rupprecht (2007). "Emergence of lyssaviruses in the Old World: the case of Africa." Curr Top Microbiol Immunol **315**: 161-193.

Okamura, S., H. Arakawa, T. Tanaka, H. Nakanishi, C. C. Ng, Y. Taya, M. Monden and Y. Nakamura (2001). "p53DINP1, a p53-inducible gene, regulates p53-dependent apoptosis." Mol Cell **8**(1): 85-94.

Olival, K. J., P. R. Hosseini, C. Zambrana-Torrelio, N. Ross, T. L. Bogich and P. Daszak (2017). "Host and viral traits predict zoonotic spillover from mammals." Nature.

Olival, K. J., P. R. Hosseini, C. Zambrana-Torrelio, N. Ross, T. L. Bogich and P. Daszak (2017). "Host and viral traits predict zoonotic spillover from mammals." Nature **546**(7660): 646-650.

Oritani, K., K. L. Medina, Y. Tomiyama, J. Ishikawa, Y. Okajima, M. Ogawa, T. Yokota, K. Aoyama, I. Takahashi, P. W. Kincade and Y. Matsuzawa (2000). "Limitin: An interferon-like cytokine that preferentially influences B-lymphocyte precursors." Nat Med **6**(6): 659-666.

Oshiumi, H., M. Matsumoto, K. Funami, T. Akazawa and T. Seya (2003). "TICAM-1, an adaptor molecule that participates in Toll-like receptor 3-mediated interferon-beta induction." Nat Immunol **4**(2): 161-167.

Papenfuss, A. T., M. L. Baker, Z. P. Feng, M. Tachedjian, G. Crameri, C. Cowled, J. Ng, V. Janardhana, H. E. Field and L. F. Wang (2012). "The immune gene repertoire of an important viral reservoir, the Australian black flying fox." BMC Genomics **13**: 261.

Parker, J., G. Tsagkogeorga, J. A. Cotton, Y. Liu, P. Provero, E. Stupka and S. J. Rossiter (2013). "Genome-wide signatures of convergent evolution in echolocating mammals." Nature **502**(7470): 228-231.

Pauli, E. K., M. Schmolke, T. Wolff, D. Viemann, J. Roth, J. G. Bode and S. Ludwig (2008). "Influenza A virus inhibits type I IFN signaling via NF-kappaB-dependent induction of SOCS-3 expression." PLoS Pathog **4**(11): e1000196.

Pestka, S. (2007). "The interferons: 50 years after their discovery, there is much more to learn." J Biol Chem **282**(28): 20047-20051.

Pestka, S., C. D. Krause and M. R. Walter (2004). "Interferons, interferon-like cytokines, and their receptors." Immunol Rev **202**: 8-32.

Pestka, S., J. A. Langer, K. C. Zoon and C. E. Samuel (1987). "Interferons and their actions." Annu Rev Biochem **56**: 727-777.

Pine, R. (1992). "Constitutive expression of an ISGF2/IRF1 transgene leads to interferon-independent activation of interferon-inducible genes and resistance to virus infection." J Virol **66**(7): 4470-4478.

Platanias, L. C. (2005). "Mechanisms of type-I- and type-II-interferon-mediated signalling." Nat Rev Immunol **5**(5): 375-386.

Qin, B. Y., C. Liu, S. S. Lam, H. Srinath, R. Delston, J. J. Correia, R. Derynck and K. Lin (2003). "Crystal structure of IRF-3 reveals mechanism of autoinhibition and virus-induced phosphoactivation." Nat Struct Biol **10**(11): 913-921.

Rani, M. R., E. Croze, T. Wei, J. Shrock, A. Josyula, D. V. Kalvakolanu and R. M. Ransohoff (2010). "STAT-phosphorylation-independent induction of interferon regulatory factor-9 by interferon-beta." J Interferon Cytokine Res **30**(3): 163-170.

Roberts, A., H. Pimentel, C. Trapnell and L. Pachter (2011). "Identification of novel transcripts in annotated genomes using RNA-Seq." Bioinformatics **27**(17): 2325-2329.

Roberts, R. M., L. Liu and A. Alexenko (1997). "New and atypical families of type I interferons in mammals: comparative functions, structures, and evolutionary relationships." Prog Nucleic Acid Res Mol Biol **56**: 287-325.

Robinson, M. D., D. J. McCarthy and G. K. Smyth (2010). "edgeR: a Bioconductor package for differential expression analysis of digital gene expression data." Bioinformatics **26**(1): 139-140.

Rusinova, I., S. Forster, S. Yu, A. Kannan, M. Masse, H. Cumming, R. Chapman and P. J. Hertzog (2013). "Interferome v2.0: an updated database of annotated interferon-regulated genes." Nucleic Acids Res **41**(Database issue): D1040-1046.

Saito, T. and M. Gale, Jr. (2007). "Principles of intracellular viral recognition." Curr Opin Immunol **19**(1): 17-23.

Sancho, A., J. Duran, A. Garcia-Espana, C. Mauvezin, E. A. Alemu, T. Lamark, M. J. Macias, R. DeSalle, M. Royo, D. Sala, J. U. Chicote, M. Palacin, T. Johansen and A. Zorzano (2012). "DOR/Tp53inp2 and Tp53inp1 constitute a metazoan gene family encoding dual regulators of autophagy and transcription." PLoS One **7**(3): e34034.

Sanjana, N. E., O. Shalem and F. Zhang (2014). "Improved vectors and genome-wide libraries for CRISPR screening." Nat Methods **11**(8): 783-784.

Sato, M., H. Suemori, N. Hata, M. Asagiri, K. Ogasawara, K. Nakao, T. Nakaya, M. Katsuki, S. Noguchi, N. Tanaka and T. Taniguchi (2000). "Distinct and essential roles of transcription factors IRF-3 and IRF-7 in response to viruses for IFN-alpha/beta gene induction." Immunity **13**(4): 539-548.

Schafer, S. L., R. Lin, P. A. Moore, J. Hiscott and P. M. Pitha (1998). "Regulation of type I interferon gene expression by interferon regulatory factor-3." J Biol Chem **273**(5): 2714-2720.

Schmid, S., M. Mordstein, G. Kochs, A. Garcia-Sastre and B. R. Tenoever (2010). "Transcription factor redundancy ensures induction of the antiviral state." J Biol Chem **285**(53): 42013-42022.

Schoggins, J. W., S. J. Wilson, M. Panis, M. Y. Murphy, C. T. Jones, P. Bieniasz and C. M. Rice (2011). "A diverse range of gene products are effectors of the type I interferon antiviral response." Nature **472**(7344): 481-485.

Seif, F., M. Khoshmirsafa, H. Aazami, M. Mohsenzadegan, G. Sedighi and M. Bahar (2017). "The role of JAK-STAT signaling pathway and its regulators in the fate of T helper cells." Cell Commun Signal **15**(1): 23.

Seillier, M., S. Peuget, O. Gayet, C. Gauthier, P. N'Guessan, M. Monte, A. Carrier, J. L. Iovanna and N. J. Dusetti (2012). "TP53INP1, a tumor suppressor, interacts with LC3 and ATG8-family proteins through the LC3-interacting region (LIR) and promotes autophagy-dependent cell death." Cell Death Differ **19**(9): 1525-1535.

Seim, I., X. Fang, Z. Xiong, A. V. Lobanov, Z. Huang, S. Ma, Y. Feng, A. A. Turanov, Y. Zhu, T. L. Lenz, M. V. Gerashchenko, D. Fan, S. Hee Yim, X. Yao, D. Jordan, Y. Xiong, Y. Ma, A. N. Lyapunov, G. Chen, O. I. Kulakova, Y. Sun, S. G. Lee, R. T. Bronson, A. A.

Moskalev, S. R. Sunyaev, G. Zhang, A. Krogh, J. Wang and V. N. Gladyshev (2013). "Genome analysis reveals insights into physiology and longevity of the Brandt's bat Myotis brandtii." Nat Commun **4**: 2212.

Senft, A. P., R. H. Taylor, W. Lei, S. A. Campbell, J. L. Tipper, M. J. Martinez, T. L. Witt, C. C. Clay and K. S. Harrod (2010). "Respiratory syncytial virus impairs macrophage IFN-alpha/beta- and IFN-gamma-stimulated transcription by distinct mechanisms." Am J Respir Cell Mol Biol **42**(4): 404-414.

Shalem, O., N. E. Sanjana, E. Hartenian, X. Shi, D. A. Scott, T. S. Mikkelsen, D. Heckl, B. L. Ebert, D. E. Root, J. G. Doench and F. Zhang (2014). "Genome-scale CRISPR-Cas9 knockout screening in human cells." Science **343**(6166): 84-87.

Shaw, A. E., J. Hughes, Q. Gu, A. Behdenna, J. B. Singer, T. Dennis, R. J. Orton, M. Varela, R. J. Gifford, S. J. Wilson and M. Palmarini (2017). "Fundamental properties of the mammalian innate immune system revealed by multispecies comparison of type I interferon responses." PLoS Biol **15**(12): e2004086.

Sheppard, P., W. Kindsvogel, W. Xu, K. Henderson, S. Schlutsmeyer, T. E. Whitmore, R. Kuestner, U. Garrigues, C. Birks, J. Roraback, C. Ostrander, D. Dong, J. Shin, S. Presnell, B. Fox, B. Haldeman, E. Cooper, D. Taft, T. Gilbert, F. J. Grant, M. Tackett, W. Krivan, G. McKnight, C. Clegg, D. Foster and K. M. Klucher (2003). "IL-28, IL-29 and their class II cytokine receptor IL-28R." Nat Immunol **4**(1): 63-68.

Shuai, K. and B. Liu (2003). "Regulation of JAK-STAT signalling in the immune system." Nat Rev Immunol **3**(11): 900-911.

Silverman, R. H. (2007). "Viral encounters with 2',5'-oligoadenylate synthetase and RNase L during the interferon antiviral response." J Virol **81**(23): 12720-12729.

Sleijfer, S., M. Bannink, A. R. Van Gool, W. H. Kruit and G. Stoter (2005). "Side effects of interferon-alpha therapy." Pharm World Sci **27**(6): 423-431.

Sorgeloos, F., B. K. Jha, R. H. Silverman and T. Michiels (2013). "Evasion of antiviral innate immunity by Theiler's virus L* protein through direct inhibition of RNase L." PLoS Pathog **9**(6): e1003474.

Starr, R., T. A. Willson, E. M. Viney, L. J. Murray, J. R. Rayner, B. J. Jenkins, T. J. Gonda, W. S. Alexander, D. Metcalf, N. A. Nicola and D. J. Hilton (1997). "A family of cytokine-inducible inhibitors of signalling." Nature **387**(6636): 917-921.

Suhara, W., M. Yoneyama, I. Kitabayashi and T. Fujita (2002). "Direct involvement of CREB-binding protein/p300 in sequence-specific DNA binding of virus-activated interferon regulatory factor-3 holocomplex." J Biol Chem **277**(25): 22304-22313.

Sun, L., J. Wu, F. Du, X. Chen and Z. J. Chen (2013). "Cyclic GMP-AMP synthase is a cytosolic DNA sensor that activates the type I interferon pathway." Science **339**(6121): 786-791.

Tai, Y. C. a. S., Terrence P. (2006). "A multivariate empirical Bayes statistic for replicated microarray time course data." The Annals of Statistics **34**(5): 2387-2412.

Taniguchi, T., K. Ogasawara, A. Takaoka and N. Tanaka (2001). "IRF family of transcription factors as regulators of host defense." Annu Rev Immunol **19**: 623-655.

Tao, J., X. Zhou and Z. Jiang (2016). "cGAS-cGAMP-STING: The three musketeers of cytosolic DNA sensing and signaling." IUBMB Life **68**(11): 858-870.

Teeling, E. C., M. S. Springer, O. Madsen, P. Bates, J. O'Brien S and W. J. Murphy (2005). "A molecular phylogeny for bats illuminates biogeography and the fossil record." Science **307**(5709): 580-584.

Torban, E. and P. Goodyer (2009). "The kidney and ear: emerging parallel functions." Annu Rev Med **60**: 339-353.

Towner, J. S., B. R. Amman, T. K. Sealy, S. A. Carroll, J. A. Comer, A. Kemp, R. Swanepoel, C. D. Paddock, S. Balinandi, M. L. Khristova, P. B. Formenty, C. G. Albarino, D. M. Miller, Z. D. Reed, J. T. Kayiwa, J. N. Mills, D. L. Cannon, P. W. Greer, E. Byaruhanga, E. C. Farnon, P. Atimnedi, S. Okware, E. Katongole-Mbidde, R. Downing, J. W. Tappero, S. R. Zaki, T. G. Ksiazek, S. T. Nichol and P. E. Rollin (2009). "Isolation of genetically diverse Marburg viruses from Egyptian fruit bats." PLoS Pathog **5**(7): e1000536.

Towner, J. S., X. Pourrut, C. G. Albarino, C. N. Nkogue, B. H. Bird, G. Grard, T. G. Ksiazek, J. P. Gonzalez, S. T. Nichol and E. M. Leroy (2007). "Marburg virus infection detected in a common African bat." PLoS One **2**(8): e764.

Uematsu, S., S. Sato, M. Yamamoto, T. Hirotani, H. Kato, F. Takeshita, M. Matsuda, C. Coban, K. J. Ishii, T. Kawai, O. Takeuchi and S. Akira (2005). "Interleukin-1 receptor-associated kinase-1 plays an essential role for Toll-like receptor (TLR)7- and TLR9-mediated interferon-{alpha} induction." J Exp Med **201**(6): 915-923.

Upton, C., K. Mossman and G. McFadden (1992). "Encoding of a homolog of the IFN-gamma receptor by myxoma virus." Science **258**(5086): 1369-1372.

Vilcek, J. (2003). "Novel interferons." Nat Immunol **4**(1): 8-9.

Wang, L.-F., J. S. Mackenzie and C. C. Broder (2013). Henipaviruses. Fields Virology. D. M. Knipe and P. M. Howley. Philadelphia, Lippincott Williams & Wilkins. **2:** 268-313.

Williamson, M. M., P. T. Hooper, P. W. Selleck, H. A. Westbury and R. F. Slocombe (2000). "Experimental hendra virus infectionin pregnant guinea-pigs and fruit Bats (Pteropus poliocephalus)." J Comp Pathol **122**(2-3): 201-207.

Willment, J. A., S. Gordon and G. D. Brown (2001). "Characterization of the human beta -glucan receptor and its alternatively spliced isoforms." J Biol Chem **276**(47): 43818-43823.

Winthrop, K. L. (2017). "The emerging safety profile of JAK inhibitors in rheumatic disease." Nat Rev Rheumatol **13**(4): 234-243.

Wreschner, D. H., T. C. James, R. H. Silverman and I. M. Kerr (1981). "Ribosomal RNA cleavage, nuclease activation and 2-5A(ppp(A2'p)nA) in interferon-treated cells." Nucleic Acids Res **9**(7): 1571-1581.

Wu, J., L. Sun, X. Chen, F. Du, H. Shi, C. Chen and Z. J. Chen (2013). "Cyclic GMP-AMP is an endogenous second messenger in innate immune signaling by cytosolic DNA." Science **339**(6121): 826-830.

Wu, L., P. Zhou, X. Ge, L. F. Wang, M. L. Baker and Z. Shi (2013). "Deep RNA sequencing reveals complex transcriptional landscape of a bat adenovirus." J Virol **87**(1): 503-511.

Wynne, J. W., B. J. Shiell, G. A. Marsh, V. Boyd, J. A. Harper, K. Heesom, P. Monaghan, P. Zhou, J. Payne, R. Klein, S. Todd, L. Mok, D. Green, J. Bingham, M. Tachedjian, M. L. Baker, D. Matthews and L. F. Wang (2014). "Proteomics informed by transcriptomics reveals Hendra virus sensitizes bat cells to TRAIL-mediated apoptosis." Genome Biol **15**(11): 532.

Yariz, K. O., D. Duman, C. Zazo Seco, J. Dallman, M. Huang, T. A. Peters, A. Sirmaci, N. Lu, M. Schraders, I. Skromne, J. Oostrik, O. Diaz-Horta, J. I. Young, S. Tokgoz-Yilmaz, O. Konukseven, H. Shahin, L. Hetterschijt, M. Kanaan, A. M. Oonk, Y. J. Edwards, H. Li, S. Atalay, S. Blanton, A. A. Desmidt, X. Z. Liu, R. J. Pennings, Z. Lu, Z. Y. Chen, H. Kremer and M. Tekin (2012). "Mutations in OTOGL, encoding the inner ear protein otogelin-like, cause moderate sensorineural hearing loss." Am J Hum Genet **91**(5): 872-882.

Yokota, S., H. Saito, T. Kubota, N. Yokosawa, K. Amano and N. Fujii (2003). "Measles virus suppresses interferon-alpha signaling pathway: suppression of Jak1 phosphorylation and association of viral accessory proteins, C and V, with interferon-alpha receptor complex." Virology **306**(1): 135-146.

Yokota, S., N. Yokosawa, T. Okabayashi, T. Suzutani and N. Fujii (2005). "Induction of suppressor of cytokine signaling-3 by herpes simplex virus type 1 confers efficient viral replication." Virology **338**(1): 173-181.

Yu, J., C. Liang and S. L. Liu (2017). "Interferon-inducible LY6E Protein Promotes HIV-1 Infection." J Biol Chem **292**(11): 4674-4685.

Yu, Y. and G. S. Hayward (2010). "The ubiquitin E3 ligase RAUL negatively regulates type i interferon through ubiquitination of the transcription factors IRF7 and IRF3." Immunity **33**(6): 863-877.

Zhang, G., C. Cowled, Z. Shi, Z. Huang, K. A. Bishop-Lilly, X. Fang, J. W. Wynne, Z. Xiong, M. L. Baker, W. Zhao, M. Tachedjian, Y. Zhu, P. Zhou, X. Jiang, J. Ng, L. Yang, L. Wu, J. Xiao, Y. Feng, Y. Chen, X. Sun, Y. Zhang, G. A. Marsh, G. Crameri, C. C. Broder, K. G. Frey, L. F. Wang and J. Wang (2013). "Comparative analysis of bat genomes provides insight into the evolution of flight and immunity." Science **339**(6118): 456-460.

Zhang, M., M. X. Zhang, Q. Zhang, G. F. Zhu, L. Yuan, D. E. Zhang, Q. Zhu, J. Yao, H. B. Shu and B. Zhong (2016). "USP18 recruits USP20 to promote innate antiviral response through deubiquitinating STING/MITA." Cell Res **26**(12): 1302-1319.

Zhang, Q., L. P. Zeng, P. Zhou, A. T. Irving, S. Li, Z. L. Shi and L. F. Wang (2017). "IFNAR2-dependent gene expression profile induced by IFN-alpha in Pteropus alecto bat cells and impact of IFNAR2 knockout on virus infection." PLoS One **12**(8): e0182866.

Zhou, A., R. J. Molinaro, K. Malathi and R. H. Silverman (2005). "Mapping of the human RNASEL promoter and expression in cancer and normal cells." J Interferon Cytokine Res **25**(10): 595-603.

Zhou, P., C. Cowled, A. Mansell, P. Monaghan, D. Green, L. Wu, Z. Shi, L. F. Wang and M. L. Baker (2014). "IRF7 in the Australian black flying fox, Pteropus alecto: evidence for a unique expression pattern and functional conservation." PLoS One **9**(8): e103875.

Zhou, P., C. Cowled, L. F. Wang and M. L. Baker (2013). "Bat Mx1 and Oas1, but not Pkr are highly induced by bat interferon and viral infection." Dev Comp Immunol **40**(3-4): 240-247.

Zhou, P., M. Tachedjian, J. W. Wynne, V. Boyd, J. Cui, I. Smith, C. Cowled, J. H. Ng, L. Mok, W. P. Michalski, I. H. Mendenhall, G. Tachedjian, L. F. Wang and M. L. Baker (2016). "Contraction of the type I IFN locus and unusual constitutive expression of IFN-alpha in bats." Proc Natl Acad Sci U S A **113**(10): 2696-2701.